

Cloning of cDNAs Encoding Neurotoxic Peptides from the Spider *Phoneutria nigriventer*. E. Kalapothakis, C.L. Penaforte, P.S.L. Beirão, M.A. Romano-Silva, J.S. Cruz, **M.A.M. Prado**, P.E.M. Guimarães, M.V. Gomez, V.F. Prado. **Toxicon 36: 1843-1850 (1998).**

Phoneutria nigriventer Toxins Block Tityustoxin-Induced Calcium Influx in Synaptosomes. D.M. Miranda, M.A. Romano-Silva, E. Kalapothakis, C.R. Diniz, M.N. Cordeiro, T. Moraes-Santos, **M.A.M. Prado**, M.V. Gomez. **Neuroreport 9: 1371-1373 (1998).**

Use of Fluorescent Probes to Follow Membrane Traffic in Nerve Terminals. C. Guatimosim, M.A. Romano-Silva, M.V. Gomez, **M.A.M. Prado**. **Brazilian Journal of Medical and Biological Research, Volume 31(11): 1491-1500 (1998).**

Cloning , cDNA Sequence Analysis and Patch Clamp Studies of a Toxin from the Venom of the Spider *Phoneutria nigriventer*. E. Kalapothakis, C.L. Penaforte, R.M. Leão, J.S. Cruz, V.F. Prado, M.N. Cordeiro, C.R. Diniz, M.A. Romano-Silva, **M.A.M. Prado**, M.V. Gomez, P.S.L. Beirão. **Toxicon 36: 1971-1980 (1998).**

The effect of calcium channels blockers on the K⁺-evoked release of [³H] adenine nucleotides from rat brain cortical synaptosomes. F. Mesquita Jr., **M.A.M. Prado**, R.S. Gomez, M.A. Romano-Silva and M.V. Gomez. **Neuroscience Letters 258: 57-9 (1998).**

Phoneutria nigriventer toxin Tx3-1 blocks A-type K⁺ currents controlling Ca⁺⁺ oscillation frequency in GH₃ cells. C. Kushmerick, E. Kalapothakis, P.S.L. Beirão, C.L. Penaforte , V.F. Prado, , J.S. Cruz, C.R. Diniz, M.N. Cordeiro, M.V. Gomez, M.A. Romano-Silva, **M.A.M. Prado**. **J. Neurochem 72: 1472-81 (1999)**

Halothane enhances exocytosis of [³H]-acetylcholine withouth increasing calcium influx in rat brain cortical slices. R.S. Gomez, **M.A.M. Prado**, F. Carazza, M.V. Gomez. **British Journal of Pharmacology 127: 679-684 (1999).**

Expression of the vesicular acetylcholine transporter, proteins involved in exocytosis and functional calcium signaling in varicosities and soma of a murine septal cell line. J. Barbosa Jr., A.R. Massensini, M.S. Santos, S.I. Meireles, R.S. Gomez, M.V. Gomez, M.A. Romano-Silva, V.F. Prado, **M.A.M. Prado. J. Neurochem. 73: 1881-1893 (1999).**

Control of the binding of a vesamicol-analogue to the vesicular acetylcholine transporter. A.D. Clarizia, M.V. Gomez, M.A. Romano-Silva, S.M. Parsons, V.F. Prado, **M.A.M. Prado. NeuroReport 10: 2783-2787 (1999).**

Inhibition of glutamate uptake by a polypeptide toxin from the spider *Phoneutria nigriventer*. H.J. Reis, **M.A.M. Prado**, E. Kalapothakis, M.N. Cordeiro, C.R. Diniz, L.A. de Marco, M.V. Gomez, M.A. Romano-Silva. **Biochem. J. 343: 413-418 (1999).**

Muscarinic regulation of Ca^{++} oscillation frequency in GH₃ cells. C. Kushmerick, M.A. Romano-Silva, M.V. Gomez, **M.A.M. Prado. Brain Research 18: 39-45 (1999).**

Molecular cloning of cDNAs encoding insecticidal neurotoxic peptides from the spider *Phoneutria nigriventer*. C.L. Penaforte, V.F. Prado, M.A.M. Prado, M.A. Romano-Silva, P.M. Guimarães, L. de Marco, M.V. Gomez, E. Kalapothakis. **Toxicon (in press)**

The effect of isoflurane on the release of [3H]acetylcholine from rat brain cortical slices R.S. Gomez, M.V. Gomez, M.A.M. Prado (**in press, Brain Research Bulletin**).

Inhibition of glutamate uptake by Tx3-4 is dependent on the redox state of cysteine residues Helton J. Reis, Marcus V. Gomez, Evanguedes Kalapothakis, Carlos R. Diniz, Marta N. CordeiroW, Marco A.M. Prado and Marco A. Romano-Silva (**in press, Neuroreport**)

Participação em congressos

1998 Society for Neuroscience (oral presentation)

1999 International Society for Neurochemistry (poster presentation)

Alunos orientados

Caracterização molecular do transportador vesicular de acetilcolina de camundongos- José Barbosa Jr., Mestrado, UFMG-1998.

Dependência de cálcio para exocitose e endocitose de vesículas sinápticas- Cristina Guatimosim Fonseca, Doutorado, UFMG- Defesa em Novembro de 1999 (Classificadao entre os cinco melhores candidatos para o prêmio Jovem Talento oferecido pela Sociedade Brasileira de Bioquímica e Biologia Molecular em 1998).

Efeito de anestésicos gerais na liberação de neurotransmissores- Renato Santiago Gomez, Doutorado, UFMG- Defesa em abril de 2000 (Classificado entre os cinco melhores candidatos para o prêmio Jovem Talento oferecido pela Sociedade Brasileira de Bioquímica e Biologia Molecular em 1999).

Expressão localização e fosforilação do transportador vesicular de acetilcolina- José Barbosa Junior, Doutorado, UFMG-término 2001.

Tráfego “in vivo” do transportador vesicular de acetilcolina-*green fluorescent protein* em células SN56, Magda da Silva Santos, Doutorado (Co-orientação), UFMG, término 2001.

“Screening” de toxinas e venenos com ação em canais iônicos – Christopher Kushmerick, Pós-Doutor término 2000.

Cristina Guatimosim Fonseca- Pós-Doutor, CNPq, Controle da endocitose em células bipolares pela fosforilação de proteínas, término 2001.

Alessandra Duarte Clarizia- Mestranda, Regulação do transportador vesicular de acetilcolina por proteína quinase C (defesa prevista para Setembro de 1999).

Lucimar Teodoro Ferreira- Mestranda, Interação do Transportador vesicular de acetilcolina com proteínas envolvidas com o tráfego de organelas (Início Maio de 2000).

Guilherme Soares Velloso- Iniciação científica (1999-)

Estágio no exterior

Fiz no ano de 1999 um estágio de 3 semanas no Laboratório do Prof. Marc G. Caron, da Duke University and Howard Hughes Medical Institute para iniciar colaborações em projetos envolvendo o tráfego do transportador vesicular de acetilcolina e geração de animais knock out para essa proteína.

Phoneutria nigriventer Toxin Tx3-1 Blocks A-Type K⁺ Currents Controlling Ca²⁺ Oscillation Frequency in GH₃ Cells

C. Kushmerick, E. Kalapothakis, *P. S. L. Beirão, *C. L. Penaforte, *V. F. Prado, *J. S. Cruz, †C. R. Diniz, †M. N. Cordeiro, M. V. Gomez, M. A. Romano-Silva, and M. A. M. Prado

Laboratório de Neurofarmacologia, Departamento de Farmacologia, and *Departamento de Bioquímica e Imunologia, Instituto de Ciências Biológicas, Universidade Federal de Minas Gerais, and †Fundação Ezequiel Dias, Belo Horizonte, Minas Gerais, Brasil

Abstract: GH₃ cells present spontaneous Ca²⁺ action potentials and oscillations of intracellular Ca²⁺, which can be modified by altering the activity of K⁺ or Ca²⁺ channels. We took advantage of this spontaneous activity to screen for effects of a purified toxin (Tx3-1) from the venom of *Phoneutria nigriventer* on ion channels. We report that Tx3-1 increases the frequency of Ca²⁺ oscillations, as do two blockers of potassium channels, 4-aminopyridine and charybdotoxin. Whole-cell patch clamp experiments show that Tx3-1 reversibly inhibits the A-type K⁺ current (I_A) but does not block other K⁺ currents (delayed-rectifying, inward-rectifying, and large-conductance Ca²⁺-sensitive) or Ca²⁺ channels (T and L type) in these cells. In addition, we describe the sequence of a full cDNA clone of Tx3-1, which shows that Tx3-1 has no homology to other known blockers of K⁺ channels and gives insights into the processing of this neurotoxin. We conclude that Tx3-1 is a selective inhibitor of I_A, which can be used to probe the role of this channel in the control of cellular function. Based on the effect of Tx3-1, we suggest that I_A is an important determinant of the frequency of Ca²⁺ oscillations in unstimulated GH₃ cells. **Key Words:** GH₃ cells—Ca²⁺ oscillations—K⁺ channels—*Phoneutria*—Tx3-1—Confocal microscopy—Patch clamp.

J. Neurochem. **72**, 1472–1481 (1999).

Voltage-sensitive ion channels are of fundamental importance for controlling the membrane potential and the electrical activity of excitable cells. Recently, there has been increased interest in the biochemical and pharmacological characterization of neurotoxins from the venom of the spider *Phoneutria nigriventer* as tools to investigate the functions of ion channels at the molecular and cellular levels (Diniz et al., 1990; Araújo et al., 1993; Romano-Silva et al., 1993; Cassola et al., 1998; Kalapothakis et al., 1998a,b; Miranda et al., 1998). One of the three toxic fractions of *Phoneutria* venom, PhTx3 (containing peptide toxins Tx3-1 through Tx3-6), has received considerable attention in the last few years, as one of its toxins (Tx3-3) is a potent blocker of ω -agatoxin-

IVA-sensitive Ca²⁺ channels, most likely of the P/Q type, in synaptosomes (Prado et al., 1996; Guatimosim et al., 1997) and granular cells of the cerebellum (R. M. Leão and P. S. L. Beirão, unpublished observations).

Although we are starting to understand the pharmacological action of some of the *Phoneutria* toxins, the targets of most of them remain unknown. The absence of significant sequence homology of *Phoneutria* toxins with other toxins having known mechanisms of action poses a challenge for understanding their actions based on structural comparisons (Cordeiro et al., 1992, 1993). It would thus be helpful to develop screening methods at the cellular level to provide clues as to how these toxins act.

The GH₃ cell line possesses a number of characteristics that make it suitable for studying the action of toxins against ion channels. This neuroendocrine cell line presents spontaneous Ca²⁺ action potentials (APs) that cause oscillations of intracellular Ca²⁺ due to influx of Ca²⁺ through L-type channels (Kidokoro, 1975; Schlegel et al., 1987). Normally, these APs do not require tetrodotoxin-sensitive Na⁺ channels (Kidokoro, 1975); however, toxins that open Na⁺ channels may change the form of the resultant Ca²⁺ oscillations (C. Kushmerick, unpublished observation). The excitability of GH₃ cells is controlled by K⁺ channels (Ozawa and Sand, 1986). These cells respond to thyrotropin-releasing hormone (TRH) by increasing the frequency of APs (Kidokoro, 1975) and associated Ca²⁺ oscillations (for review, see Hinkle et al., 1996), and evidence suggests a role for an inward-rectifying K⁺ current (IK_{1,R}) in mediating part of

Received October 5, 1998; revised manuscript received November 26, 1998; accepted November 27, 1998.

Address correspondence and reprint requests to Dr. C. Kushmerick at Departamento de Farmacologia, Instituto de Ciências Biológicas, Universidade Federal de Minas Gerais, Av. Antonio Carlos 6627, Pampulha, 31270-901 Belo Horizonte, MG, Brasil.

Abbreviations used: AP, action potential; 4-AP, 4-aminopyridine; BK, large-conductance, Ca²⁺-sensitive K⁺ channel; ChyTx, charybdotoxin; I_A, A-type K⁺ current; IK_{1,R}, inward-rectifying K⁺ current; Kv, voltage-gated K⁺ channel; SK, small-conductance, Ca²⁺-sensitive K⁺ channel; TRH, thyrotropin-releasing hormone.

this effect (Bauer et al., 1990; Barros et al., 1996, 1997; Weinsberg et al., 1997). Aside from IK_{L-R} channels, however, these cells also express at least three voltage-gated K^+ channel (K_v) isoforms (Takimoto et al., 1995) and two types of Ca^{2+} -activated K^+ channels (Ritchie, 1987), and the role of these channels in determining excitability is incompletely understood. Toxins that alter the activity of Ca^{2+} , Na^+ , or K^+ channels may change the pattern of Ca^{2+} oscillations, and this information can guide the design of voltage clamp experiments to characterize their molecular targets. Specific toxins thus characterized should be useful to probe the role of distinct channels in cell physiology and in the control of Ca^{2+} oscillations in this anterior pituitary-derived cell line.

MATERIALS AND METHODS

Materials

Chemicals were from Sigma (St. Louis, MO, U.S.A.), unless otherwise specified. PhTx-3 and Tx3-1 were purified from the venom of *P. nigriventer* by gel filtration and reverse-phase HPLC as described (Rezende et al., 1991). Fluo-3 AM (Molecular Probes) and nifedipine were dissolved in dimethyl sulfoxide at a concentration of 1 mM and stored at -20°C . 4-Aminopyridine (4-AP) was diluted in water and stored at -20°C .

Cell culture

GH₃ cells were purchased from American Type Culture Collection (Rockville, MD, U.S.A.). The cells were kept in Ham's F-10 medium supplemented with 15% horse serum, 2.5% fetal bovine serum, 50 U/ml penicillin, and 50 $\mu\text{g}/\text{ml}$ streptomycin. Culture medium was changed three times per week, and the cells were maintained in a 5% CO_2 atmosphere at 37°C . For confocal microscopy, cells were plated onto 22-mm-diameter glass coverslips treated with poly-L-lysine (50 $\mu\text{g}/\text{ml}$, 30 min) and used 3–10 days later. For electrophysiology experiments, cells were plated onto sterile plastic dishes and used 1–10 days later.

Confocal microscopy

Experiments were performed at room temperature (20 – 25°C). Cells on coverslips were incubated in Ringer's solution (in mM: 140 NaCl, 5.4 KCl, 1.8 CaCl_2 , 0.5 MgCl_2 , 10 glucose, 5 HEPES, pH 7.4, adjusted with NaOH) containing 10 μM fluo-3 AM for 1 h. The coverslips were washed in dye-free Ringer's solution and then transferred to a custom holder in which the coverslip formed the bottom of a 400- μl bath. A gravity-fed perfusion system and a peristaltic pump drain allowed solution exchange with a time constant for solution turnover of ~ 10 s. Imaging was performed with a Bio-Rad MRC 1024 UV laser scanning confocal system running the software TimeCourse 1.0 coupled to a Zeiss microscope (Axiovert 100) with a water immersion objective ($40\times$, 1.2 NA). Excitation was by the 488-nm line of an argon laser (Coherent), and emitted light passed through a 522/32-nm bandpass filter. Laser power was 0.3–1%, and the detector iris was set to 8 (i.e., maximal open). In all of the experiments, each cell was analyzed individually and served as its own control; thus, there was no need to calibrate the amount of fluo-3 present. Nonetheless, in a few experiments, we used indo-1 and UV illumination instead of fluo-3 and quantified $[Ca^{2+}]_i$ according to Grynkiewicz et al. (1985), using ionomycin with 10 mM Ca^{2+} , 5 mM EGTA, and 5 mM Mn^{2+} to measure F_{max} ,

F_{min} , and background fluorescence, respectively. Resting Ca^{2+} in these GH₃ cells was ~ 50 nM. The amplitude of Ca^{2+} oscillations varied from cell to cell, but most were between 200 and 400 nm at the peak of oscillation.

To measure Ca^{2+} oscillations at high temporal resolution, the confocal system was operated in line scan mode. An individual cell loaded with fluo-3 was selected, and the average fluorescent intensity along a line through its center was measured as a function of time (sampling at 167 Hz) by the TimeCourse software.

To collect data from individual cells in a population, a field of cells was selected and fluo-3 images recorded at 1–3 Hz (usually 1.7 Hz) for the duration of the experimental protocols. This frequency of scanning was chosen to maximize temporal resolution without incurring significant photobleaching. At the end of the experiment, cell perimeters were drawn, and the average fluorescent intensity in each cell per time point was calculated using the TimeCourse software.

Statistical analysis of Ca^{2+} oscillations

Analysis of the frequency of oscillations was carried out in several steps. Each cell was analyzed individually. First, positions of the oscillations in the experimental record were determined using a software peak detection algorithm written by one of the authors (C.K.). Then, the number of oscillations that occurred before treatment (i.e., control) and during treatment was counted. The mean frequency of oscillations for each cell was calculated as the number of oscillations divided by the period of observation. To calculate the probability that the observed changes in oscillation frequency occurred by chance, we constructed cumulative frequency distributions from the data and calculated the Kolmogorov–Smirnov statistic (D_{K-S}) as the maximum difference between the curves (Press et al., 1986). The probability (p) that the observed value of D_{K-S} was due to chance for N cells was determined using the equation

$$p = \sum_{j=1}^{\infty} (-1)^{j-1} \exp[-(jD_{K-S})^2 N]$$

To observe the distribution of responses in the population of cells, the frequency of oscillations before and during treatment was measured, and the ratio was calculated for each cell individually. A value for this ratio of >1.0 indicates an increase in oscillation frequency. To analyze what percentage of cells responded to a given treatment, the data were plotted as cumulative frequency distributions. Each treatment was investigated in at least three independent experiments.

Electrophysiology

An EPC-9 patch clamp amplifier and Pulse software (HEKA) were used at room temperature (20 – 25°C) to measure whole-cell ion currents (Hamill et al., 1981). Capacitive currents were electronically compensated, and except where noted, a P/4 protocol (Armstrong and Benzanilla, 1974) was used for linear leak subtraction. The A-type K^+ current (I_A) was low-pass filtered at 4 kHz and sampled at 20 kHz. The IK_{L-R} was low-pass filtered at 667 Hz and sampled at 2 kHz. Other currents were low-pass filtered at 2 kHz and sampled at 10 kHz. Pipettes were pulled from glass capillaries and had a resistance of 1–3 M Ω when filled with pipette solution.

Pipette solution to measure K_v currents contained the following (in mM): 10 NaCl, 130 KCl, 5 EGTA, 5 HEPES, pH 7.4, adjusted with KOH. To measure large-conductance, Ca^{2+} -sensitive K^+ channel (BK) currents, the pipette solution was the same as for K_v currents, except that intracellular free Ca^{2+}

was adjusted to 12 μM by the addition of 5 mM CaCl_2 , as determined by software written by one of the authors (P.S.L.B.). Extracellular solution used to measure Kv and BK currents contained the following (in mM): 140 NaCl, 5.4 KCl, 1.8 CaCl_2 , 0.5 MgCl_2 , 10 glucose, 5 HEPES, pH 7.4, adjusted with NaOH.

$\text{IK}_{\text{L-R}}$ values were measured in isotonic K^+ , as described (Bauer et al., 1990). Pipette solution contained the following (in mM): 130 KCl, 2 MgCl_2 , 10 HEPES, 20 EGTA, pH 7.4, adjusted with KOH. Extracellular solution contained the following (in mM): 130 KCl, 4 MgCl_2 , 5 glucose, 5 HEPES, 20 EGTA, pH 7.4, adjusted with KOH.

To measure current through Ca^{2+} channels, K^+ currents were blocked by Cs^+ , and Ba^{2+} was used as the charge carrier. Pipette solution contained the following (in mM): 10 NaCl, 140 CsCl, 5 HEPES, 5 EGTA, 4 Mg-ATP, 0.3 Li-GTP, 20 creatine phosphate, pH 7.3, adjusted with CsOH. Extracellular solution contained the following (in mM): 126 NaCl, 5 KCl, 25 BaCl_2 , 19 glucose, 5 HEPES, pH 7.4, adjusted with NaOH.

Perfusion during electrophysiology experiments was accomplished using a micropipette (inner diameter 500 μm) positioned within 100 μm of the cell under study. The solution was gravity fed at a rate of ≈ 0.1 ml/s, and a solenoid valve was used to choose between two solutions with a dead time of < 5 s.

Molecular biology

Standard recombinant DNA techniques were carried out as described by Sambrook et al. (1989). Restriction endonucleases were used according to the manufacturer's instruction (New England BioLabs).

Isolation of Tx3-1 cDNA

Construction of the venom gland cDNA library has been described elsewhere (Kalapothakis et al., 1998a). Approximately 1.25×10^6 independent recombinants were generated and screened (Kalapothakis et al., 1998a). Clones containing cDNA longer than 300 bp were selected and sequenced in forward and reverse direction using an Automated ALF DNA Sequencer (Pharmacia). Nucleic acid sequences were analyzed using BLASTX (Altschul et al., 1990).

Northern blots

Preparation of total RNA was performed as described by Chomczynski and Sacchi (1987). RNA was resolved by formaldehyde electrophoresis (Sambrook et al., 1989), and northern blotting was performed essentially as described by Kalapothakis et al. (1998a). Filters were hybridized overnight and then washed at high-stringency conditions ($0.1 \times$ saline sodium citrate and 0.1% sodium dodecyl sulfate at 60°C) before exposure at -80°C to Hyperfilm-MP (Amersham) in a cassette containing an intensifying screen.

RESULTS

Confocal images of Ca^{2+} oscillations in individual GH_3 cells

Figure 1A shows images of GH_3 cells loaded with the Ca^{2+} indicator fluo-3 undergoing spontaneous (i.e., unstimulated) Ca^{2+} oscillations. The images are positioned sequentially from left to right and top to bottom and are separated by an interval of 1 s. Ca^{2+} oscillations appear as changes in the fluorescent intensity of a given cell between frames. Figure 1B shows the time course of two Ca^{2+} oscillations at high time resolution achieved using

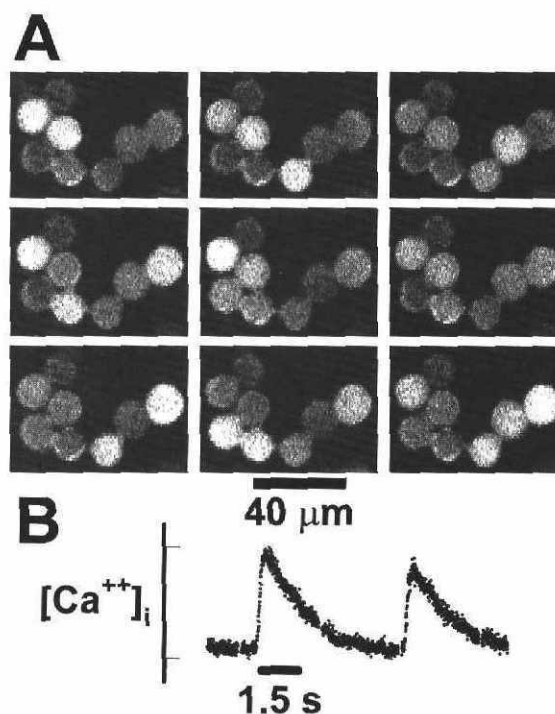


FIG. 1. A: Ca^{2+} oscillations in GH_3 cells loaded with 10 μM fluo-3 AM for 1 h and then observed by confocal fluorescent microscopy. Images were taken at 3 Hz. Every third image is shown, positioned sequentially from left to right and top to bottom. **B:** Intracellular Ca^{2+} from the center of a single cell, recorded at high temporal resolution (167 Hz) using line scan mode.

the line scan mode of the microscope through the center of a single cell. A Ca^{2+} AP in the plasma membrane (Kidokoro, 1975) results in a rapid increase in intracellular Ca^{2+} (10–90% rise time of 200 ms), followed by an exponential decline to basal levels ($\tau \sim 2$ s). Some time later (6 s in the example, but the period is highly variable), another Ca^{2+} oscillation occurs and the process repeats.

Pharmacology of Ca^{2+} oscillations

Figure 2 shows how the Ca^{2+} oscillations respond to various pharmacological treatments. Each trace in Fig. 2 represents intracellular calcium in an individual representative cell. Ca^{2+} oscillations in GH_3 cells are dependent on Ca^{2+} entry through L-type Ca^{2+} channels (Schlegel et al., 1987). Removal of extracellular Ca^{2+} (Fig. 2, trace 1) or perfusion with 2 μM nifedipine (Fig. 2, trace 2) both reversibly abolished Ca^{2+} oscillations. During treatment with nifedipine, we stimulated the cells with 60 mM K^+ (substituted isosmotically for Na^+ ; indicated by the arrow in Fig. 2, trace 2). The resultant increase in fluorescence demonstrates that the dye functions in the presence of nifedipine and the increase in Ca^{2+} may be due to incomplete block of L-type channels by nifedipine or to the T-type channels present in these cells (Simasko et al., 1988).

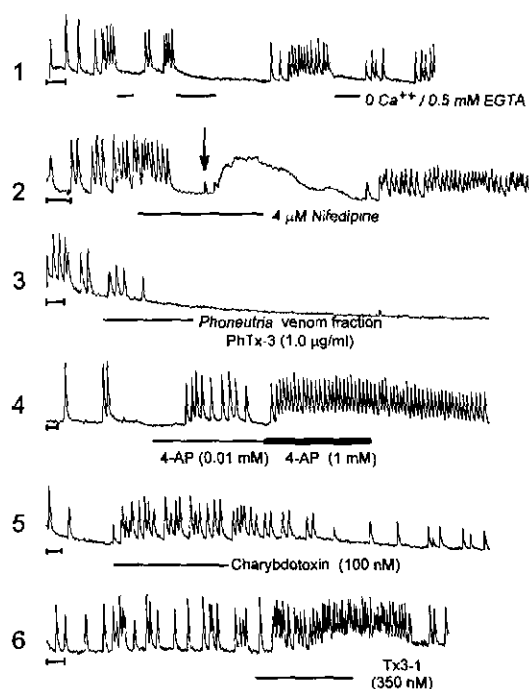


FIG. 2. Pharmacology of Ca^{2+} oscillations. GH₃ cells were loaded with fluo-3, and average fluorescent intensity was followed with time. Each trace shows the response of an individual representative cell (the number of cells tested for each treatment is given in the text). The cells were perfused continuously with Ringer's solution or, at the times indicated by the bars, with Ringer's solution modified as follows: trace 1, Ca^{2+} -free solution obtained by omitting $CaCl_2$ from the Ringer's solution and including 0.5 mM EGTA; trace 2, nifedipine (4 μ M) and stimulation for 30 s with 60 mM KCl (substituted equimolar for NaCl; indicated by the arrow); trace 3, fraction 3 of the venom of *P. nigriventer*; trace 4, 0.01 and 1 mM 4-AP; trace 5, 100 nM ChyTx; trace 6, purified *Phoneutria* toxin Tx3-1 (350 nM). Bars at the origin of each trace are 20 s.

The fraction of *Phoneutria* venom named PhTx3 contains peptides that block L-type Ca^{2+} channels (Kalapothakis et al., 1998b). Consistent with the idea that L-type Ca^{2+} channels are essential for oscillations, perfusion with PhTx3 rapidly abolished Ca^{2+} oscillations (Fig. 2, trace 3). The effects of these treatments were observed in all cells tested ($n = 20$ for removal of Ca^{2+} , $n = 15$ for nifedipine, $n = 33$ for PhTx3).

The I_A in GH₃ cells is inhibited by 4-AP (Rogawski, 1988; results shown below), and in these cells, 4-AP causes an increase in AP frequency (Sand et al., 1980). As shown in Fig. 2 (trace 4), 4-AP increased Ca^{2+} oscillation frequency in a dose-dependent manner and was effective at concentrations as low as 10 μ M. Charybdotoxin (ChyTx), a potent inhibitor of BK, has been reported to prolong the duration of APs and thereby decrease their frequency (Lang and Ritchie, 1990). We tested the effect of ChyTx on Ca^{2+} oscillations and observed that the toxin actually increased Ca^{2+} oscillation frequency when used at 100 nM (Fig. 2, trace 5). At 10 nM, however, ChyTx did not affect Ca^{2+} oscillation frequency (not shown). Apamin, a selective inhibitor of

small-conductance, Ca^{2+} -sensitive K^+ channel (SK) current, was also tested for an effect on Ca^{2+} oscillations. At 1 or 5 μ M, we were unable to detect any effect of apamin on oscillation frequency (not shown).

Tx3-1, a peptide of 4,500 Da purified from *Phoneutria* venom, is toxic to mammals (Cordeiro et al., 1993). To date, there is no information regarding its molecular mechanism of action. We applied Tx3-1 to GH₃ cells, reasoning that if it blocked Ca^{2+} or K^+ channels, it would have an effect on Ca^{2+} oscillations similar to the Ca^{2+} or K^+ channel blockers described above. We observed, as shown in Fig. 2 (trace 6), that Tx3-1 increases oscillation frequency, indicating that it blocks a K^+ channel involved in the regulation of spike frequency. In general, the increase in oscillation frequency induced by 4-AP, ChyTx, and Tx3-1 reversed only slowly upon washout of the drug or toxin.

Quantification and statistical evaluation of changes in Ca^{2+} oscillation frequency

The frequency of Ca^{2+} oscillations in GH₃ cells varied greatly from cell to cell. Figure 3 shows the statistical treatment used to judge the significance of the effects of 4-AP, ChyTx, and Tx3-1 on oscillation frequency. In Fig. 3 A–C, we show the cumulative frequency distribution of oscillation frequencies before and during treatment (i.e., the ordinate represents the percentage of cells with oscillation frequency less than or equal to the corresponding value on the abscissa). For the three treatments, the Kolmogorov–Smirnov statistic (see Materials and Methods) was determined, and the statistical significance was calculated (values of p are given in the figure legend). Figure 3D–F shows the distribution of responses

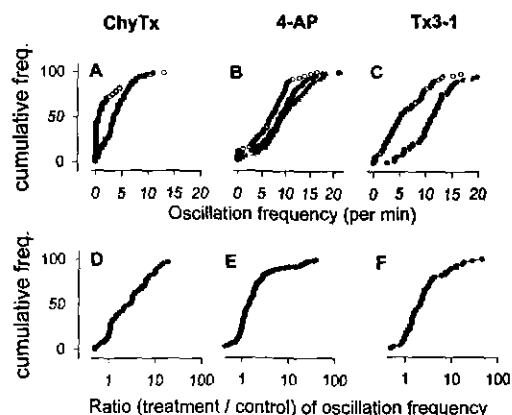


FIG. 3. Statistical analysis of oscillation frequency. Intracellular Ca^{2+} was recorded in a population of cells before and during treatment with ChyTx, 4-AP, or Tx3-1. Upper panels (A–C) show cumulative plots of the distribution of oscillation frequency. Statistical significance (p values) was calculated using the Kolmogorov–Smirnov test. **A:** \circ , control; \bullet , 100 nM ChyTx ($p = 1 \times 10^{-6}$). **B:** \circ , control; \bullet , 0.01 mM 4-AP ($p = 0.01$); \blacktriangle , 1.0 mM 4-AP ($p = 3.6 \times 10^{-6}$). **C:** \circ , control; \bullet , 350 nM Tx3-1 ($p = 2 \times 10^{-7}$). Lower panels (D–F) show cumulative plots of the distribution of ratios of oscillation frequencies during treatment to control. **D:** \bullet , 100 nM ChyTx. **E:** \bullet , 1.0 mM 4-AP. **F:** \bullet , 350 nM Tx3-1.

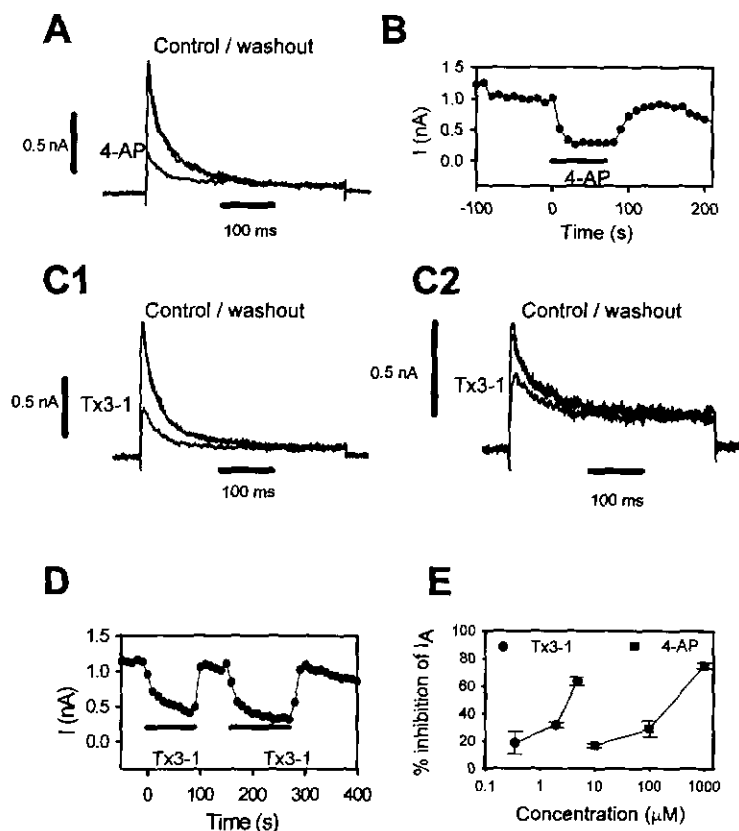


FIG. 4. Inhibition of I_A by Tx3-1. Whole-cell voltage clamp was used to hold the cells at -80 mV. At intervals of 10 s, the cells were stepped to -100 mV for 200 ms to remove inactivation, followed by a step to $+30$ mV for 400 ms during which currents were recorded. **A:** Identification of the 4-AP-sensitive inactivating A current in GH₃ cells. **B:** Time course of inhibition and recovery of I_A by 4-AP. **C:** Inhibition of I_A by Tx3-1 ($4.8 \mu\text{M}$) in two cells with different amounts of noninactivating current. **D:** Time course of inhibition and recovery of I_A by Tx3-1. **E:** Dose-response of inhibition of I_A by Tx3-1 (●) and 4-AP (■). Error bars are standard deviations. Numbers of cells tested were as follows: 4-AP ($n = 2$ at all concentrations); Tx3-1, $4.8 \mu\text{M}$ ($n = 3$), $1.75 \mu\text{M}$ ($n = 2$), 350 nM ($n = 6$).

to each treatment, plotted as a cumulative frequency distribution. The value on the abscissa is the ratio of oscillation frequency during treatment over control; values >1.0 indicate that the frequency of oscillations increased. In each case, most of the cells responded by increasing their frequency of oscillations. The mean \pm 95% confidence limit -fold increase in oscillation frequency was 4.0 ± 1.0 for ChyTx ($n = 60$), 3.5 ± 0.46 for 4-AP ($n = 180$), and 4.5 ± 1.8 for *Phoneutria* Tx3-1 ($n = 60$).

Effects of Tx3-1 on whole-cell currents

The results presented above suggest that Tx3-1 may augment Ca^{2+} oscillation frequency by blocking a K^+ channel. To test this hypothesis, the whole-cell voltage clamp technique was used to look for effects of Tx3-1 on ion channels. To avoid artifacts due to "rundown" (i.e., spontaneous changes in currents due to dialysis of cellular components) in the experiments described, the data were analyzed only when inhibition was reversible upon washout of drug or toxin (currents labeled "washout").

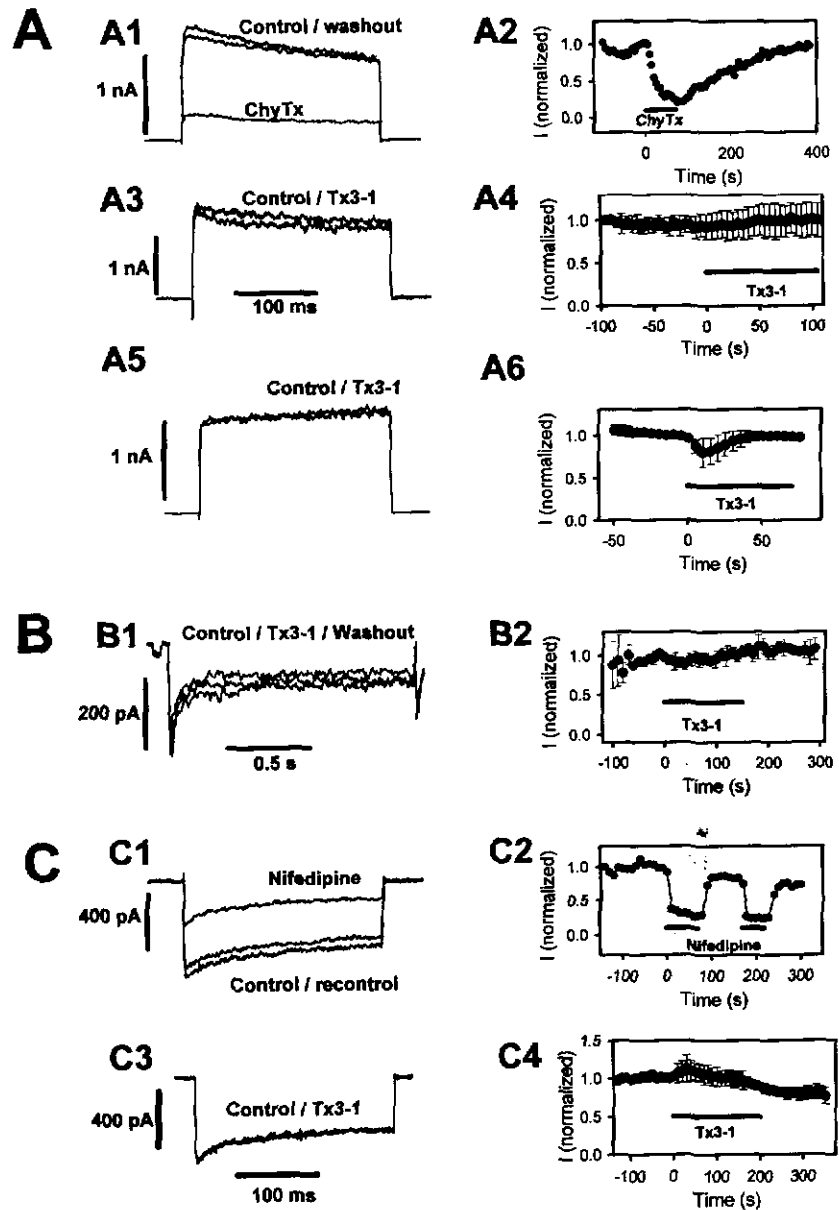
Voltage-dependent K^+ currents were generated by stepping cells from a holding of -80 mV to a prepulse potential of -100 mV for 200 ms, followed by a step to $+30$ mV for 400 ms. The current measured during the step to $+30$ mV had two components: one that activated with a time constant (τ) of ≈ 3 ms and became inactivated with $\tau \approx 30$ ms (i.e., the A current) and another that became inactivated little if at all during the 400-ms

pulse (i.e., a delayed rectifier). With use of this voltage protocol, the A current we observed was often significantly larger than the delayed-rectifying current, which facilitated observing its inhibition by drugs and toxins. Figure 4A and B shows the identification of I_A . This identification is based on its kinetics and its inhibition by 1 mM 4-AP. Many of the cells tested exhibited 1–2 nA of I_A using this protocol, although in some cells, the magnitude of I_A was less (300–600 pA). In general, cells with less I_A had greater quantities of noninactivating current.

Figure 4C shows the inhibition by Tx3-1 of Kv currents in two different cells: one in which the A current is much larger than the delayed rectifier and the other in which the delayed rectifier is an appreciable fraction of the total current. In both cases, Tx3-1 inhibits only the A current. Figure 4D shows the time course of the reversible and repeatable inhibition of I_A by Tx3-1. The dose dependence of inhibition of I_A by 4-AP and Tx3-1 is shown in Fig. 4E. Note that at the concentration in which both of these inhibitors increase oscillation frequency (350 nM Tx3-1 or 10 μM 4-AP), they significantly inhibit I_A .

Data from the Ca^{2+} oscillation experiments suggested that 100 nM ChyTx, a BK inhibitor, increases the frequency of Ca^{2+} oscillations (Figs. 2 and 3), raising the possibility that the response to Tx3-1 could be mediated by BK. To test this, we looked for an effect of Tx3-1

FIG. 5. Effects of Tx3-1 on other whole-cell currents. **A:** Effect of Tx3-1 on ChyTx-sensitive BK currents. Free Ca^{2+} in the pipette solution was raised to $12 \mu M$, and cells were stepped from a holding potential of -80 mV to 0 mV for 250 ms. **A1:** Representative current, showing inhibition by 50 nM ChyTx. **A2:** Time course of BK current during application of 50 nM ChyTx (indicated by the bar) and after washout. **A3:** Representative current in control conditions and in the presence of Tx3-1 (350 nM). **A4:** Time course of BK current before and during application of 350 nM Tx3-1 (indicated by the bar). $n = 3$ cells. **A5:** Representative current in control conditions and in the presence of Tx3-1 ($2 \mu M$). **A6:** Time course of BK current before and during application of $2 \mu M$ Tx3-1 (indicated by the bar). $n = 3$ cells. Error bars are standard deviations. **B:** Effect of Tx3-1 on $IK_{L,R}$ channels. Currents were measured in isotonic K^+ during voltage steps (1.5 s) from -40 to -120 mV and are shown without leak subtraction. **B1:** Representative $IK_{L,R}$ in control conditions, in the presence of $3 \mu M$ Tx3-1, and after washout. **B2:** Time course of $IK_{L,R}$ in control extracellular solution, in the presence of Tx3-1 (indicated by the bar), and during washout. $n = 6$ cells, 2 each at 1 , 2 , and $3 \mu M$. Error bars are standard deviations. **C:** Effect of Tx3-1 on L- and T-type Ca^{2+} channels. K^+ channels were blocked with Cs^+ , and Ba^{2+} was used as the charge carrier. Cells were held at -80 mV, and currents were measured during steps to 0 mV. **C1:** Representative Ca^{2+} current showing reversible inhibition by nifedipine. **C2:** Time course of Ca^{2+} current during inhibition by nifedipine (indicated by the bars) and recovery. **C3:** Representative current in control conditions and in the presence of 350 nM Tx3-1 (indicated by the bar). **C4:** Time course of peak Ca^{2+} current in control extracellular solution, in the presence of Tx3-1 (indicated by the bar), and during washout. $n = 3$ cells. Error bars are standard deviations.



under conditions designed to isolate BK currents. Inclusion of $12 \mu M$ free Ca^{2+} in the pipette solution results in the appearance of large ChyTx-sensitive currents at 0 mV several minutes after establishing whole-cell mode (Fig. 5, A1 and A2). In these conditions, we do not see A currents, even when the BK currents are blocked by ChyTx. The reason for this might be a combination of the difference in voltage protocols used to generate these currents versus those in Fig. 4 and rundown during the waiting time after establishing whole-cell mode. It is also possible that high intracellular Ca^{2+} inhibits A currents. Under these same conditions, we tested 350 nM Tx3-1, a concentration that, as shown above, increased the frequency of Ca^{2+} oscillations. As shown in Fig. 5A (A3 and A4), 350 nM Tx3-1 had no effect on this current (n

$= 4$ cells). We also tested $2 \mu M$ Tx3-1 and observed that at this higher concentration, the toxin also does not inhibit BK currents (Fig. 5, A5 and A6; $n = 3$ cells).

Inhibition of the $IK_{L,R}$ in GH₃ cells increases the frequency of APs and may be involved in the response of GH₃ cells to TRH (Barros et al., 1997; Weinsberg et al., 1997). To determine if the increase in Ca^{2+} oscillation frequency elicited by Tx3-1 was mediated through effects on these channels, we measured $IK_{L,R}$ before, during, and after treatment with Tx3-1. Figure 5B (B1) shows one such experiment using $3.0 \mu M$ Tx3-1. No leak subtraction was applied to these currents. Figure 5B (B2) shows the time course of $IK_{L,R}$ during application of Tx3-1. In six cells tested, no effect on $IK_{L,R}$ was seen.

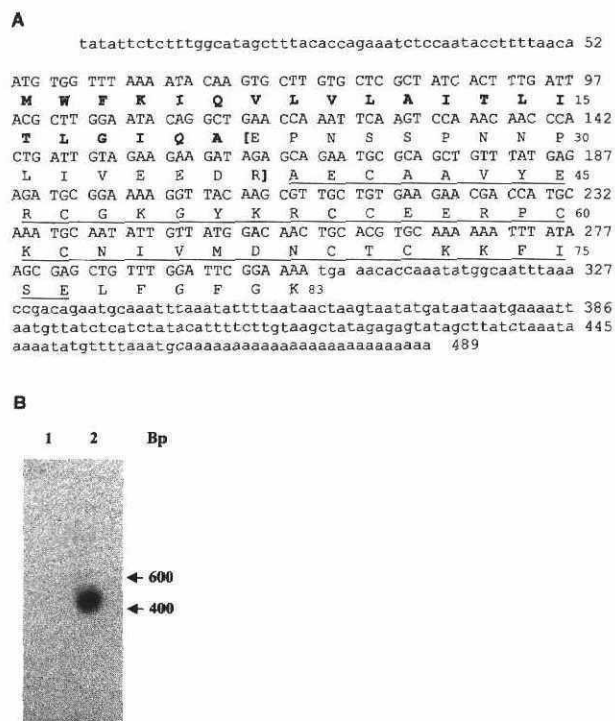


FIG. 6. Molecular analysis of Tx3-1. **A:** Nucleotide sequence of DNA encoding Tx3-1. The coding region is shown in uppercase with the 5' and 3' untranslated regions in lowercase. The segment that corresponds to the previously determined amino acid sequence of Tx3-1 is underlined. The signal peptide (in bold) and the propeptide (in brackets) are also indicated. **B:** Northern blotting analysis. Lane 1, total RNA (20 μ g) from the whole body of *P. nigriventer* minus the venom gland, used as a negative control. Lane 2, *P. nigriventer* venom gland total RNA (20 μ g). The filter was hybridized with a probe for the isolated cDNA of Tx3-1.

Finally, we were unable to detect any inhibition or activation of Ca^{2+} channels by Tx3-1 under patch clamp conditions that yielded nifedipine-sensitive L-type and inactivating T-type currents (Ba^{2+} used as the charge carrier; $n = 4$ cells; Fig. 5C).

Sequence analysis of Tx3-1 cDNA

To gain more insight into Tx3-1, we isolated a cDNA clone from a venom gland library (Fig. 6). The cDNA encoding Tx3-1 contained 489 bp, including a 5' untranslated region (nucleotides 1–52), an open reading frame of 252 bp encoding a precursor polypeptide of 83 amino acids, and a large 3' untranslated region composed of 185 bp (Fig. 6A). The cDNA sequence obtained in this study confirmed the reported amino acid sequence of Tx3-1 determined by automatic peptide sequencing (Cordeiro et al., 1993) and revealed the presence of six extra amino acid residues (LFGFGK) at the C terminus. The deduced signal peptide of Tx3-1 with 21 amino acids is followed by an intervening propeptide region composed of 16 amino acid residues. Northern blot analysis of venom gland total RNA using the isolated clone as a probe shows a band of ~450–500 bp, suggesting that we have isolated a full-length cDNA (Fig. 6B).

DISCUSSION

Several poisonous animals use neurotoxins to paralyze or kill their prey or predators (Olivera et al., 1990). As some of these toxins interact selectively with ionic channels, they are potentially useful as tools to study the physiological role of particular channels or to determine structural features of channels that are important for their function. Characterization of such toxins is often performed using whole-cell patch clamp under conditions designed to isolate a single channel type. Given the diversity of channels characterized thus far and their overlapping pharmacology, it is useful to have an idea of how a toxin can act in order to design proper voltage clamp experiments.

The venom of the spider *P. nigriventer* appears to be a rich source of channel-blocking toxins. A number of neurotoxic peptides have been purified from the venom of this spider (Rezende et al., 1991; Cordeiro et al., 1992, 1993). Furthermore, sequences obtained from *P. nigriventer* venom gland cDNAs suggest the existence of at least 30 toxic peptides (Kalapothakis et al., 1998a,b; our unpublished observations). Although some of these peptides have homology among each other, the *Phoneutria* toxins are mostly unrelated to other known neurotoxins. This lack of homology precludes predictions of toxin action based on amino acid sequence and makes necessary the development of new strategies to obtain knowledge of toxin effects.

Effects of *Phoneutria* toxin Tx3-1 on Ca^{2+} oscillations and I_A

We have used confocal fluorescent microscopy and the Ca^{2+} indicator fluo-3 to follow intracellular Ca^{2+} in individual GH_3 cells and investigate the cellular action of a novel *Phoneutria* toxin, Tx3-1. Ca^{2+} oscillations in GH_3 cells respond to pharmacological agents that modify ion channels in an expected way. Thus, preventing influx of Ca^{2+} through L-type channels by nifedipine abolished oscillations, underscoring the importance of these channels to the process (Schlegel et al., 1987). In addition, the fact that KCl can increase intracellular Ca^{2+} in the presence of nifedipine suggests that other calcium channels (presumably T type) may allow calcium influx but alone are not capable of generating oscillations. An alternative explanation is that nifedipine does not block completely L-type currents, and upon KCl depolarization, some calcium influx occurs. This last proposal is supported by the experiment in Fig. 5 (C1), showing that 4 μM nifedipine does not eliminate L-type currents. Nonetheless, it is clear that calcium oscillations depend on calcium influx through nifedipine-sensitive channels.

Treatment with 4-AP or ChyTx increased frequency as expected because K^+ channels appear to regulate excitability in these cells (Ozawa and Sand, 1986). Application of the *Phoneutria* venom fraction PhTx3 abolished oscillations, presumably by the action of the L-type channel blockers present in this fraction (Kalapothakis et al., 1998b). In contrast to PhTx3, application of a purified peptide component of this fraction, *Phoneutria* toxin

Tx3-1, increased oscillation frequency, suggesting by this pharmacological profile that it could block K^+ channels.

Using whole-cell patch clamp, we show that a concentration of Tx3-1 effective to increase Ca^{2+} oscillation frequency significantly inhibits I_A , but does not alter BK currents, delayed-rectifying K^+ currents, $IK_{L,R}$, or Ba^{2+} currents through L- or T-type Ca^{2+} channels. These experiments show that Tx3-1 inhibited I_A rapidly, reversibly, and dose dependently.

GH₃ cells express Kv1.4 (which might generate an A current) and Kv1.5 and Kv2.1 (both delayed rectifiers) K^+ channel α subunits (Takimoto et al., 1995). The observation that in GH₃ cells, almost all Kv1.4 protein co-immunoprecipitates with Kv1.5 protein (Takimoto and Levitan, 1996) and that cardiac Kv1.4/Kv1.5 heteromers form A currents when expressed in *Xenopus* oocytes (Po et al., 1993) make this combination of subunits a possible molecular target for *Phoneutria* Tx3-1. However, further experiments using heterologously expressed Kv subunits will be necessary to test this hypothesis.

The A current is blocked by 4-AP, and 4-AP increases the frequency of APs in GH₃ cells (Sand et al., 1980; this report). This K^+ channel blocker, however, also inhibits the $IK_{L,R}$ in these cells, and $IK_{L,R}$ may play a role in determining AP frequency (Bauer et al., 1990; Barros et al., 1997; Weinsberg et al., 1997). Tx3-1 inhibits I_A without any effect on the $IK_{L,R}$ (Figs. 4 and 5). The observations that the only channel blocked by Tx3-1 is the A type and that its effects on Ca^{2+} oscillations can be reproduced by 4-AP strongly suggest that there is a causal relationship between inhibition of I_A and control of excitability of these cells. Thus, the results indicate that I_A is one of the determinants of the frequency of Ca^{2+} oscillations in unstimulated GH₃ cells. This observation agrees with the classic role of A currents in the spacing of repetitive firing in some types of nerves (Connor and Stevens, 1971; Hille, 1992). Therefore, variations in the level of I_A from cell to cell could explain some of the variation in AP and Ca^{2+} oscillation frequency universally observed in unstimulated GH₃ cells. Moreover, TRH changes the level of expression of voltage-sensitive K^+ channels in GH₃ cells (Takimoto et al., 1995), which could result in long-term changes in excitability. Consistent with our results, it has been reported that short-term exposure to TRH inhibits I_A and increases oscillation frequency (Dubinsky and Oxford, 1985). This last result, however, has been challenged (Simasko, 1991).

The effects of ChyTx, 4-AP, and *Phoneutria* Tx3-1 on whole-cell currents reverse rapidly on washout, whereas their effects on oscillation frequency persist after their removal. One possible explanation is that during the period of increased oscillation frequency, average intracellular Ca^{2+} is elevated, and Ca^{2+} -dependent signaling pathways thus activated could lead to changes that persist after removal of the drugs. For example, activation of protein kinases has been shown to increase electrical

excitability in GH₃/B6 cells (for review, see Hinkle et al., 1996).

Tx3-1 and 4-AP both increase Ca^{2+} oscillation frequency at concentrations that inhibit I_A by only 15–20%, indicating that the frequency of Ca^{2+} oscillations is strongly dependent on these channels. This trend was not observed by inhibition of BK by ChyTx, as at a concentration of 10 nM, ChyTx inhibited the Ca^{2+} -sensitive K^+ current by $37 \pm 5\%$ (mean \pm SD, $n = 2$), but at this concentration, ChyTx did not increase oscillation frequency (not shown). It is possible that the increase in oscillation frequency seen with 100 nM ChyTx could be mediated by nonspecific effects on other K^+ channels (Grissmer et al., 1994). In addition, we did not detect any effect of apamin (1 or 5 μ M) on Ca^{2+} oscillations, despite a report in the literature that 500 nM apamin increases AP frequency in GH₃ cells by inhibiting a slow after-hyperpolarization mediated by SK (Lang and Ritchie, 1990). This previous report, however, shows that the majority of cells tested did not respond to apamin. Therefore, it is unlikely that Tx3-1 would affect Ca^{2+} oscillations by blocking SK because Tx3-1 affected >90% of the cells studied.

An alternative interpretation, which could not be ruled out by our data, is that *Phoneutria* Tx3-1 has another target that is responsible for its effects on oscillation frequency. If the affinity for this other target were high, it might explain the delayed washout of the effect on oscillation frequency. However, delayed washout of the effect on oscillation frequency seems to be a generic result of elevated intracellular calcium, as all three treatments that increased oscillation frequency reversed only slowly after removal of the drug or toxin. Therefore, we favor the notion of a causal relationship between inhibition of A current and increase of oscillatory behavior for GH₃ cells.

One argument against the role of A currents to control excitability in these cells is that there might be little A current available at their normal resting potential. The following calculation shows that indeed very little current is needed to have a large impact on AP frequency. Between APs, oscillating GH₃ cells undergo a slow depolarization of ~ 10 mV/s (Kidokoro, 1975; Lang and Ritchie, 1990). These cells have a membrane capacitance of ~ 10 pF. Thus, the membrane current during the interspike period ($I = C dV/dt$) is on the order of 0.1 pA. We routinely measure A currents of 500–1,500 pA using the protocols described in Materials and Methods. Therefore, if a small fraction of A current were available at the resting potential, it should contribute significantly to the membrane current, thus directly affecting the rate at which the cell arrives at threshold.

Our experiments validate the use of Ca^{2+} oscillations in GH₃ cells as an assay for the screening of toxins. The techniques presented above use only the frequency of oscillations to detect effects of toxins, a method that allows rapid acquisition of data from many cells. As shown in Fig. 1, by using a line scan, high temporal resolution of an oscillation is possible, showing a rising

phase for 200 ms, followed by a slow mechanism of Ca^{2+} extrusion or buffering. This opens the possibility that changes in the form of oscillations, and not just the frequency, could be used to detect effects of toxins.

Molecular biology of Tx3-1

Analysis of a cDNA clone encoding the precursor to Tx3-1 showed the same overall organization found in several toxins cloned from the *P. nigriventer* venom gland (Kalapothakis et al., 1998a,b). Conserved features include a signal peptide, an intervening propeptide, and the mature toxin. In the case of Tx3-1, there are also six amino acids at the carboxy terminus that are not present in the mature toxin. Thus, the conversion of the precursor into mature polypeptide requires the excision of the signal peptide (Ala²¹–Glu²²), proteolysis at Arg³⁷, and removal of the last six residues at the carboxy terminus (Fig. 6).

The deduced amino acid sequence confirms that obtained by direct sequencing of the peptide (Cordeiro et al., 1993). Comparison of amino acid sequences shows that Tx3-1 is not related to other known K^+ channel blockers. The region of Tx3-1 bounded by Y-7 and C-34 [which contains the conserved Cys–Cys scaffold (Olivera et al., 1994)] has 42% identity with the Ca^{2+} blocking peptide ω -agatoxin-IVB. But despite this observation, Tx3-1 does not seem to affect Ca^{2+} channels (Prado et al., 1996; this study). Future experiments aimed at determining the site of interaction of this new pharmacological agent with heterologously expressed K^+ channels may provide new insights into the structure of the binding site in K^+ channels and mode of interaction of Tx3-1.

In conclusion, by using the screening assay described herein, we identified a new and selective agent to block A currents in GH₃ cells. The results obtained with this toxin provide direct evidence for a coupling between I_A and Ca^{2+} oscillation frequency and may be relevant to understanding the control of excitability in anterior pituitary cells, from which GH₃ cells are derived.

Acknowledgment: We are grateful to A. R. Massensini for help with the confocal microscope experiments, to R. M. Leão for his participation in preliminary patch clamp experiments, and to V. M. dos Santos, A. A. Guimarães, and A. A. Pereira for technical assistance. This work was supported by Finep, CNPq, PADCT, PRONEX, PRPq-UFMG, and a postdoctoral fellowship from FAPEMIG to C.K.

REFERENCES

- Altschul S. F., Gish W., Miller W., Myers E. W., and Lipman D. J. (1990) Basic local alignment search tool. *J. Mol. Biol.* **215**, 403–410.
- Araújo D. A., Cordeiro M. N., Diniz C. R., and Beirão P. S. (1993) Effects of a toxic fraction, PhTx2, from the spider *Phoneutria nigriventer* on the sodium current. *Naunyn-Schmiedeberg's Arch. Pharmacol.* **347**, 205–208.
- Armstrong C. M. and Bezanilla F. J. (1974) Charge movement associated with the opening and closing of the activation gates of the Na channels. *J. Gen. Physiol.* **63**, 533–552.
- Barros F., del Camino D., Pardo L. A., and de la Pena P. (1996) Caffeine enhancement of electrical activity through direct blockade of inward rectifying K^+ currents in GH₃ rat anterior pituitary cells. *Pflugers Arch.* **431**, 443–451.
- Barros F., del Camino D., Pardo L. A., Palomero T., Giraldez T., and de la Pena P. (1997) Demonstration of an inwardly rectifying K^+ current modulated by thyrotropin-releasing hormone and caffeine in GH₃ rat anterior pituitary cells. *Pflugers Arch.* **435**, 119–129.
- Bauer C. K., Meyerhof W., and Schwarz J. R. (1990) An inward-rectifying K^+ current in clonal rat pituitary cells and its modulation by thyrotrophin-releasing hormone. *J. Physiol. (Lond.)* **429**, 169–189.
- Cassola A. C., Jaffe H., Fales H. M., Castro Afeche S., Magnoli F., and Cipolla-Neto J. (1998) Omega-phonetoxin-IIA: a calcium channel blocker from the spider *Phoneutria nigriventer*. *Pflugers Arch.* **436**, 545–552.
- Chomczynski P. and Sacchi N. (1987) Single-step method of RNA isolation by acid guanidinium thiocyanate-phenol-chloroform extraction. *Anal. Biochem.* **162**, 156–159.
- Connor J. A. and Stevens C. F. (1971) Prediction of repetitive firing behaviour from voltage clamp data on an isolated neurone soma. *J. Physiol. (Lond.)* **213**, 31–53.
- Cordeiro M. N., Diniz C. R., Valentim A. C., von Eickstedt V. R., Gilroy J., and Richardson M. (1992) The purification and amino acid sequences of four Tx2 neurotoxins from the venom of the Brazilian "armed" spider *Phoneutria nigriventer* (Keys). *FEBS Lett.* **310**, 153–156.
- Cordeiro M. N., de Figueiredo S. G., Valentim A. C., Diniz C. R., von Eickstedt V. R., Gilroy J., and Richardson M. (1993) Purification and amino acid sequences of six Tx3 type neurotoxins from the venom of the Brazilian "armed" spider *Phoneutria nigriventer* (Keys). *Toxicon* **31**, 35–42.
- Diniz C. R., Cordeiro M. N., Junior L. R., Kelly P., Fischer S., Reimann F., Oliveira E. B., and Richardson M. (1990) The purification and amino acid sequence of the lethal neurotoxin Tx1 from the venom of the Brazilian "armed" spider *Phoneutria nigriventer*. *FEBS Lett.* **263**, 251–253.
- Dubinsky J. M. and Oxford G. S. (1985) Dual modulation of K channels by thyrotropin-releasing hormone in clonal pituitary cells. *Proc. Natl. Acad. Sci. USA* **82**, 4282–4286.
- Grissmer S., Nguyen A. N., Aiyar J., Hanson D. C., Mather R. J., Gutman G. A., Karmilowicz M. J., Auperin D. D., and Chandy K. G. (1994) Pharmacological characterization of five cloned voltage-gated K^+ channels, types Kv1.1, 1.2, 1.3, 1.5, and 3.1, stably expressed in mammalian cell lines. *Mol. Pharmacol.* **45**, 1227–1234.
- Grynkiewicz G., Poenie M., and Tsien R. Y. (1985) A new generation of Ca^{2+} indicators with greatly improved fluorescence properties. *J. Biol. Chem.* **260**, 3440–3450.
- Guatimosim C., Romano-Silva M. A., Cruz J. S., Beirão P. S., Kalapothakis E., Moraes-Santos T., Cordeiro M. N., Diniz C. R., Gomez M. V., and Prado M. A. (1997) A toxin from the spider *Phoneutria nigriventer* that blocks Ca^{2+} channels coupled to exocytosis. *Br. J. Pharmacol.* **122**, 591–597.
- Hamill O. P., Marty A., Neher E., Sakmann B., and Sigworth F. J. (1981) Improved patch-clamp techniques for high-resolution current recording from cells and cell-free membrane patches. *Pflugers Arch.* **391**, 85–100.
- Hille B. (1992) *Ionic Channels of Excitable Membranes*. Sinauer, Sunderland, MA.
- Hinkle P. M., Nelson E. J., and Ashworth R. (1996) Characterization of the calcium response to thyrotropin-releasing hormone in lactotrophs and GH cells. *Trends Endocrinol. Metab.* **7**, 370–374.
- Kalapothakis E., Penaforte C. L., Beirão P. S. L., Romano-Silva M. A., Cruz J. S., Prado M. A. M., Guimaraes P. E. M., Gomez M. V., and Prado V. F. (1998a) Cloning of cDNAs encoding neurotoxic peptides from the spider *Phoneutria nigriventer*. *Toxicon* **36**, 1843–1850.
- Kalapothakis E., Penaforte C. L., Leao R. M., Cruz J. S., Prado V. F., Cordeiro M. N., Diniz C. R., Romano-Silva M. A., Prado M. A. M., Gomez M. V., and Beirão P. S. L. (1998b) Cloning,

- cDNA sequence analysis and patch clamp studies of a toxin from the venom of the armed spider (*Phoneutria nigriventer*). *Toxicon* **36**, 1971–1980.
- Kidokoro Y. (1975) Spontaneous Ca^{++} action potentials in a clonal pituitary cell line and their relationship to prolactin secretion. *Nature* **258**, 741–742.
- Lang D. G. and Ritchie A. K. (1990) Tetraethylammonium blockade of apamin-sensitive and insensitive Ca^{2+} -activated K^+ channels in a pituitary cell line. *J. Physiol. (Lond.)* **425**, 117–132.
- Miranda D. M., Romano-Silva M. A., Kalapothakis E., Diniz C. R., Cordeiro M. N., Santos T. M., Prado M. A., and Gomez M. V. (1998) *Phoneutria nigriventer* toxins block tityustoxin-induced Ca^{++} influx in synaptosomes. *Neuroreport* **9**, 1371–1373.
- Olivera B. M., Rivier J., Clark C., Ramilo C. A., Corpuz G. P., Abogadie F. C., Mena E. E., Woodward S. R., Hillyard D. R., and Cruz L. J. (1990) Diversity of *Conus* neuropeptides. *Science* **249**, 257–263.
- Olivera B. M., Miljanich G. P., Ramachandran J., and Adams M. E. (1994) Ca^{++} channel diversity and neurotransmitter release: the omega-conotoxins and omega-agatoxins. *Annu. Rev. Biochem.* **63**, 823–867.
- Ozawa S. and Sand O. (1986) Electrophysiology of excitable endocrine cells. *Physiol. Rev.* **66**, 887–952.
- Po S., Roberds S., Snyders D. J., Tamkun M. M., and Bennett P. B. (1993) Heteromultimeric assembly of human potassium channels. Molecular basis of a transient outward current? *Circ. Res.* **72**, 1326–1336.
- Prado M. A., Guatimosim C., Gomez M. V., Diniz C. R., Cordeiro M. N., and Romano-Silva M. A. (1996) A novel tool for the investigation of glutamate release from rat cerebrocortical synaptosomes: the toxin Tx3-3 from the venom of the spider *Phoneutria nigriventer*. *Biochem. J.* **314**, 145–150.
- Press W. H., Flannery B. P., Teukolsky S. A., and Vetterling W. T. (1986) *Numerical Recipes*, p. 818. Cambridge University Press, Cambridge.
- Rezende L. Jr., Cordeiro M. N., Oliveira E. B., and Diniz C. R. (1991) Isolation of neurotoxic peptides from the venom of the "armed" spider *Phoneutria nigriventer*. *Toxicon* **29**, 1225–1233.
- Ritchie A. K. (1987) Two distinct Ca^{++} -activated potassium currents in a rat anterior pituitary cell line. *J. Physiol. (Lond.)* **385**, 591–609.
- Rogawski M. A. (1988) Transient outward current (I_A) in clonal anterior pituitary cells: blockade by aminopyridine analogs. *Nauyn Schmiedeberg's Arch. Pharmacol.* **338**, 125–132.
- Romano-Silva M. A., Ribeiro-Santos R., Ribeiro A. M., Gomez M. V., Diniz C. R., Cordeiro M. N., and Brammer M. J. (1993) Rat cortical synaptosomes have more than one mechanism for Ca^{2+} entry linked to rapid glutamate release: studies using the *Phoneutria nigriventer* toxin PhTX2 and potassium depolarization. *Biochem. J.* **296**, 313–319.
- Sambrook J., Fritsch E. F., and Maniatis T. (1989) *Molecular Cloning. A Laboratory Manual*. Cold Spring Harbor Laboratory Press, Cold Spring Harbor, NY.
- Sand O., Haug E., and Gautvik K. M. (1980) Effects of thyroliberin and 4-aminopyridine on action potentials and prolactin release and synthesis in rat pituitary cells in culture. *Acta Physiol. Scand.* **108**, 247–252.
- Schlegel W., Winiger B. P., Mollard P., Vacher P., Wuarin F., Zahnd G. R., Wollheim C. B., and Dufy B. (1987) Oscillations of cytosolic Ca^{2+} in pituitary cells due to action potentials. *Nature* **329**, 719–721.
- Simasko S. M. (1991) Reevaluation of the electrophysiological actions of thyrotropin-releasing hormone in a rat pituitary cell line (GH₃). *Endocrinology* **128**, 2015–2026.
- Simasko S. M., Weiland G. A., and Oswald R. E. (1988) Pharmacological characterization of two calcium currents in GH₃ cells. *Am. J. Physiol.* **254**, E328–E336.
- Takimoto K. and Levitan E. S. (1996) Altered K^+ channel subunit composition following hormone induction of Kv1.5 gene expression. *Biochemistry* **35**, 14149–14156.
- Takimoto K., Gealy R., Fomina A. F., Trimmer J. S., and Levitan E. S. (1995) Inhibition of voltage-gated K^+ channel gene expression by the neuropeptide thyrotropin-releasing hormone. *J. Neurosci.* **15**, 449–457.
- Weinsberg F., Bauer C. K., and Schwarz J. R. (1997) The class III antiarrhythmic agent E-4031 selectively blocks the inactivating inward-rectifying potassium current in rat anterior pituitary tumor cells (GH₃/B6 cells). *Pflugers Arch.* **434**, 1–10.



Halothane enhances exocytosis of [³H]-acetylcholine without increasing calcium influx in rat brain cortical slices

*¹R. S. Gomez, ²M. A. M. Prado, ³F. Carazza & ²M. V. Gomez

¹Departamento de Cirurgia, Sala 4000 Faculdade de Medicina da UFMG, Avenida Alfredo Balena, 190 CEP: 30130-100, Belo Horizonte-Minas Gerais-Brasil; ²Departamento de Farmacologia, ICB-UFMG, Avenida Alfredo Balena, 190 CEP: 30130-100, Belo Horizonte-Minas Gerais-Brasil and ³Departamento de Química, ICEX-UFMG, Avenida Alfredo Balena, 190 CEP: 30130-100, Belo Horizonte-Minas Gerais-Brasil

1 The effect of halothane on the release of [³H]-acetylcholine ([³H]-ACh) in rat brain cortical slices was investigated.

2 Halothane (0.018 mM) did not significantly affect the basal and the electrical field stimulation induced release of [³H]-ACh. However, halothane (0.063 mM) significantly increased the basal release of [³H]-ACh and this effect was additive with the electrical field stimulation induced release of [³H]-ACh.

3 The release of [³H]-ACh induced by 0.063 mM halothane was independent of the extracellular sodium and calcium ion concentration and was decreased by tetracaine, an inhibitor of Ca²⁺-release from intracellular stores or dantrolene, an inhibitor of Ca²⁺-release from ryanodine-sensitive stores.

4 Using 2-(4-phenylpiperidino)-cyclohexanol (vesamicol), a drug that blocks the storage of ACh in synaptic vesicles, we investigated whether exocytosis of this neurotransmitter is involved in the effect of halothane. Vesamicol significantly decreased the release of [³H]-ACh evoked by halothane.

5 It is suggested that halothane may cause a Ca²⁺ release from intracellular stores that increases [³H]-ACh exocytosis in rat brain cortical slices.

Keywords: Acetylcholine; transmitter release; anaesthetics, volatile; halothane; rat brain cortical slices; ions; intracellular Ca²⁺ release; exocytosis

Abbreviations: ACh, acetylcholine; EGTA, ethyleneglycol-bis-(β -aminoethyl ether) N,N,N',N'-tetraacetic acid; paraoxon, diethyl *p*-nitrophenyl phosphate; vesamicol, 2-(4-phenylpiperidino)-cyclohexanol

Introduction

There have been extensive efforts to characterize the mechanism of action of volatile anaesthetics, but their molecular and cellular actions are still a matter of debate. A possible site of action for general anaesthetics could be the presynaptic terminal as indicated by results showing that synaptic transmission is more sensitive to the effects of general anaesthetics than axonal conduction (Larrabee *et al.*, 1952; Richards, 1983; Griffiths & Norman, 1993). Thus, the investigation of the effects of anaesthetics on the release of neurotransmitters may provide information on the mechanisms that contribute to the general effect of these substances during anaesthesia.

Acetylcholine (ACh) is a transmitter implicated in memory, learning, cognitive behaviour and it is also of importance during sleep (Mitchell, 1963; Kanai & Szerb, 1965; Collier & Mitchell, 1967; Griffiths & Norman, 1993; Keifer *et al.*, 1994; Winkler *et al.*, 1995). Although there has been some reports of the action of volatile anaesthetics on ACh release, it is not clear how these drugs alter the release of this transmitter. Some authors reported significant inhibition of potassium-stimulated release of ACh in the presence of halothane (Johnson & Hartzell, 1985; Griffiths *et al.*, 1995) while others observed no effect (Bazil & Minneman, 1989a,b). However, to our knowledge all studies examined the release of ACh from the central nervous system (CNS) using high potassium stimula-

tion, and little effort has been made to follow the effects of anaesthetics on ACh release induced by electrical stimulation.

In the course of an investigation in brain cortical slices, we observed that halothane increased the basal release of ACh ([³H]-ACh). When associated with electrical stimulation, the release of this transmitter was additive. Therefore, the aim of the present work was to further investigate the mechanisms involved on halothane-induced release of [³H]-ACh in rat brain cortical slices.

Methods

Release of [³H]-ACh from rat brain cortical slices

All procedures were approved by the local ethics committee. Adult Wistar rats (200–250 g) of either sex were decapitated and had their brains removed. Slices of cerebral cortex (0.5 mm) were obtained using a McIlwain Tissue Slicer (Brinkman Instruments Inc., U.K.). The brain cortical slices were weighed (40 mg) and then placed into the incubating medium.

The release of [³H]-ACh into the incubating fluid was studied after labelling the tissue ACh with [methyl-³H]-choline chloride (78 Ci mmol⁻¹; Amersham Searle), as previously described by Gomez *et al.* (1996) and Casali *et al.* (1997). Briefly, endogenous ACh stores were first depleted by incubation at 37°C for 15 min in high-K⁺ (50 mM) salt medium (3.0 ml) and the slices were separated from the incubating medium by centrifugation (5000 × g for 10 min). To

*Author for correspondence; E-mail: gomez@mono.icb.ufmg.br

label the endogenous pools of ACh, the slices were incubated in salt medium for 30 min (37°C) with $0.11 \mu\text{Ci ml}^{-1}$ of [methyl- ^3H]-choline (free of choline carrier). The slices were then separated from the incubating fluid by centrifugation ($5000 \times g$ for 10 min) followed by two washes with a medium containing $1.0 \mu\text{M}$ choline.

Experimental protocol

Stock solutions of saturated halothane were prepared prior to each experimental session. 10 ml of incubating medium was equilibrated with liquid anaesthetic (100 or 400 μl) at 37°C in Teflon-capped glass vials for 30 min. Subsequently, 500 μl of stock, anaesthetic-saturated solution was added to 1.0 ml of the incubation medium with a glass syringe. The vial was immediately capped and mixed. In some experiments, slices were stimulated 5 min thereafter by electrical field stimulation with a platinum electrode (10 Hz, 0.5 ms, 10 V) for a further 5 min. In order to investigate the effect of halothane on the basal release of [^3H]-ACh, we also used halothane in the absence of electrical field stimulation.

To clarify the mechanism(s) by which halothane changes release of [^3H]-ACh, the slices were previously incubated for 15 min in the absence or presence of $0.5 \mu\text{M}$ tetrodotoxin, 2.0 mM EGTA, $100 \mu\text{M}$ Cd^{2+} , tetracaine (50 or 500 μM) or dantrolene ($0.1 - 100 \mu\text{M}$). Thereafter, the slices were incubated for 5 min in the absence or presence of halothane (0.063 mM). At this concentration and time the release of [^3H]-ACh was linear (data not shown). When the action of 2-(4-phenylpiperidino)-cyclohexanol (vesamicol) was examined, the drug was added to slices 10 min before incubation with [methyl- ^3H]-choline. In these conditions, a concentration of vesamicol ten times larger than that used in the present study does not alter the incorporation of ^3H label (Leão *et al.*, 1995). The incubation medium used contained (in mM): NaCl 136, KCl 2.7, CaCl_2 1.8, glucose 5.5, Tris base 10, and $20 \mu\text{M}$ diethyl *p*-nitrophenyl phosphate (paraoxon) to prevent hydrolysis of [^3H]-ACh. The final pH was adjusted to 7.4. The Ca^{2+} free solution was prepared by removing CaCl_2 and adding 2.0 mM ethyleneglycol-bis-(β -aminoethyl ether) N,N,N',N'-tetraacetic acid (EGTA).

The saturation of the stock solution and the aqueous concentration of halothane in the incubating medium after a 5 min incubation was confirmed by n-heptane extraction and measurement by gas chromatography using a Hewlett Packard Series II-5890 gas chromatograph (Rutledge *et al.*, 1963).

Measurement of [^3H]-ACh release

Aliquots (300 μl) of the samples were counted for radioactivity by liquid scintillation spectrophotometry using a Packard spectrophotometer. In each group of experiments, [^3H]-ACh and [^3H]-choline were separated from the supernatants by the choline kinase method (Goldberg & McCamman, 1973; Prado *et al.*, 1993) and [^3H]-ACh represented about 65% of the total radioactivity released. Confirming this data, the same magnitude of ^3H efflux induced by halothane was also obtained when paraoxon was replaced by $10 \mu\text{M}$ hemicholinium-3 (HC-3), suggesting that accumulation of ACh due to cholinesterase inhibition was not altering the release of transmitter (data not shown). In addition, there was little release of ^3H during halothane stimulation in the absence of paraoxon and HC-3 ($145 \pm 5\%$ of basal release, mean \pm s.e.mean for three experiments in the absence of paraoxon or HC-3 compared with $269 \pm 4\%$ in the presence of paraoxon), indicating that most [^3H]-ACh

released can be hydrolyzed and taken back by the slices in a HC-3 sensitive way.

Chemicals

Halothane was a generous gift from Halocarbon (River Edge, New Jersey, U.S.A.). Paraoxon, tetracaine, cadmium and dantrolene were obtained from Sigma Chemical Co. (St. Louis, MO, U.S.A.). The effective (–)-enantiomer of vesamicol was a gift of Professor S. M. Parsons (University of California at Santa Barbara CA, U.S.A.), and in this article the term vesamicol refers to the (–)-enantiomer. The n-heptane chromatography grade was obtained from Merck (Darmstadt, Germany). All other chemicals and reagents were of analytical grade and were obtained from the usual commercial sources.

Statistical analysis

Results are presented as mean \pm s.e.mean values. Difference between means were determined by analysis of variance (ANOVA) and multiple comparison tests.

Results

Effects of halothane on the resting and stimulated release of [^3H]-ACh

Table 1 shows that 0.018 mM halothane did not affect the basal or the electrical field induced release of [^3H]-ACh ($P > 0.05$). However, 0.063 mM halothane increased by 2.7 times the release of [^3H]-ACh ($P < 0.05$). This effect remained at higher concentrations of halothane (0.117 and 0.235 mM) and the release of [^3H]-ACh was linear up to 0.063 mM halothane and 5 min of incubation (data not shown). Moreover, the release of [^3H]-ACh in the presence of 0.063 mM halothane and electrical field stimulation was additive ($P < 0.05$).

Extracellular Na^+ and Ca^{2+} independence of halothane induced release of [^3H]-ACh

Halothane could affect the release of [^3H]-ACh through an alteration in Ca^{2+} or Na^+ influx, causing an increase in

Table 1 Effect of halothane on the release of acetylcholine induced by electrical field stimulation in rat brain cortical slices

Volatile anaesthetic	[^3H]-ACh (d.p.m. mg^{-1} of tissue)	
	Control	Electrical field stimulation (10 V, 0.5 ms, 10 Hz)
None	35.3 ± 2.9	$87.6 \pm 7.2^*$
Halothane (0.018 mM)	45.3 ± 5.9	$89.1 \pm 6.1^*$
Halothane (0.063 mM)	$94.9 \pm 5.2^{**}$	$189.2 \pm 15.6^{\dagger}$
Halothane (0.117 mM)	$105.8 \pm 4.8^{**}$	$193.2 \pm 13.2^{\dagger}$
Halothane (0.235 mM)	$104.7 \pm 6.2^{**}$	$196.3 \pm 16.5^{\dagger}$

*Statistically different from the control value, $P < 0.05$.

**Statistically different from the value without volatile anaesthetic, $P < 0.05$.

†Statistically different from the electrical field stimulation value, $P < 0.05$. Brain cortical slices (40 mg) loaded with [^3H]-choline were preincubated for 5 min in salt medium in the absence (control) or in the presence of halothane (0.018 or 0.063 mM) and then stimulated for 5 min with electrical field stimulation (10 V, 0.5 ms, 10 Hz). Data are mean \pm s.e.mean values from at least three different experiments performed in duplicate. For other details, see text.

transmitter output. Table 2 shows that tetrodotoxin, a known Na^+ channel blocker (Narahashi *et al.*, 1964), failed to affect the release of [3 H]-ACh induced by halothane. Moreover, these data also show that the release of [3 H]-ACh evoked by halothane was not affected by 2.0 mM EGTA (no calcium added to the medium) or 100 μM Cd^{2+} , a nonspecific blocker of calcium channels (Fox *et al.*, 1987). The lack of effect of external calcium on the action of halothane was also confirmed when $^{45}\text{Ca}^{2+}$ uptake in rat brain cortical synaptosomes was measured as previously described (Miranda *et al.*, 1998). In these experiments, the influx of $^{45}\text{Ca}^{2+}$ in synaptosomes after 30 s of exposure to 0.063 mM halothane (at 35°C) was not changed (mean \pm s.e.mean of three experiments performed in duplicate; control: 2760 ± 260 d.p.m. mg^{-1} protein; halothane: 2830 ± 218 d.p.m. mg^{-1} protein).

Table 2 Effect of tetrodotoxin, EGTA or Cd^{2+} on the release of acetylcholine induced by halothane in rat brain cortical slices

	[3 H]-ACh (d.p.m. $^{-1}$ of tissue)	
	Control	Halothane (0.063 mM)
Control	37.8 ± 2.4	$95.1 \pm 5.9^*$
Tetrodotoxin (0.5 μM)	32.5 ± 3.4	$91.5 \pm 4.8^*$
EGTA (2.0 mM)	38.8 ± 2.9	$90.1 \pm 6.8^*$
Cd^{2+} (100 μM)	39.1 ± 3.8	$101.7 \pm 8.1^*$

*Statistically different from the control value, $P < 0.05$. Brain cortical slices (40 mg) loaded with [3 H]-choline were preincubated for 15 min in salt medium in the absence (control) or in the presence of tetrodotoxin (0.5 μM), EGTA (2.0 mM) or Cd^{2+} (100 μM) and then incubated for 5 min in the absence (control) or presence of halothane (0.063 mM). The experiments with EGTA were performed in a calcium free medium. Data are mean \pm s.e.mean values from at least three different experiments performed in duplicate. For other details, see text.

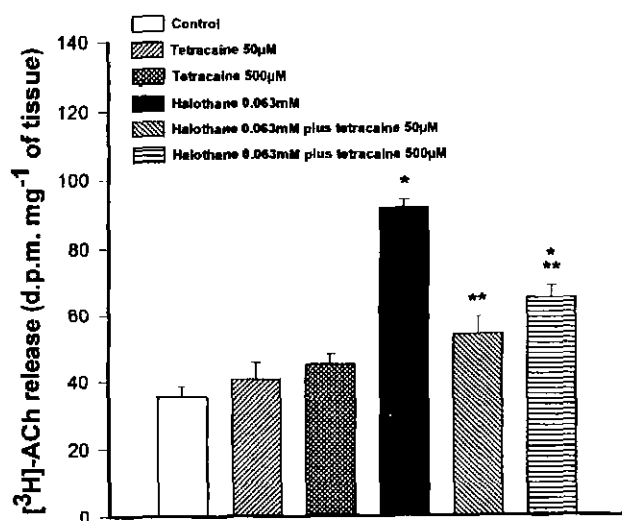


Figure 1 The effect of tetracaine on the release of [3 H]-ACh induced by halothane from rat brain cortical slices. Brain cortical slices (40 mg) loaded with [3 H]-choline were preincubated for 15 min in salt medium in the absence or in the presence of tetracaine (50 or 500 μM). They were then incubated for 5 min in the absence or presence of halothane (0.063 mM). Data are mean \pm s.e.mean (bars) values from at least three different experiments performed in duplicate. For other details, see text. *Statistically different from the control value, $P < 0.05$. **Statistically different from the halothane value, $P < 0.05$.

Effect of intracellular calcium stores blockers on the release of [3 H]-ACh evoked by halothane

It has been demonstrated that volatile anaesthetics, including halothane, stimulate Ca^{2+} release or leakage from the intracellular stores of cardiac (Wheeler *et al.*, 1988; Connolly & Coronado, 1994), skeletal (Palade, 1987; Nelson & Swco, 1988) and vascular smooth muscle cells (Tsuchida *et al.*, 1993) as well in synaptosomes (Daniell & Harris, 1988) and hippocampal slices (Mody *et al.*, 1991). Figure 1 illustrates the effect of 50 and 500 μM tetracaine on [3 H]-ACh release induced by halothane. At these concentrations, it has been demonstrated that tetracaine blocks calcium release from intracellular stores (Ohnishi *et al.*, 1979; Pike *et al.*, 1989; Györke *et al.*, 1997), and in our experiments decreased by 75.7 ± 4.0 and $64.4 \pm 3.5\%$, respectively, the release of [3 H]-ACh evoked by halothane ($P < 0.05$). There was also a trend for an increase in the rate of basal [3 H]-ACh release in the presence of tetracaine but it did not reach statistical significance.

We also investigated the effect of dantrolene (0.1–100 μM), a blocker of Ca^{2+} release from ryanodine-sensitive stores (Van Winkle, 1976; Morgan & Bryant, 1977; Ohta *et al.*, 1990), on the release of [3 H]-ACh stimulated by halothane. Dantrolene did not affect the basal release of [3 H]-ACh (data not shown) but caused a dose dependent reduction in volatile anaesthetic evoked ACh release (Figure 2, $P < 0.05$). The IC_{50} for dantrolene to inhibit [3 H]-ACh evoked release by halothane was close to 4.0 μM (Figure 2).

[3 H]-ACh exocytosis induced by halothane

To investigate the possibility that halothane increases the exocytotic release of [3 H]-ACh, vesamicol, a drug that blocks the storage of ACh in synaptic vesicles by inhibiting the vesicular ACh transporter (Parsons *et al.*, 1993), was used. As

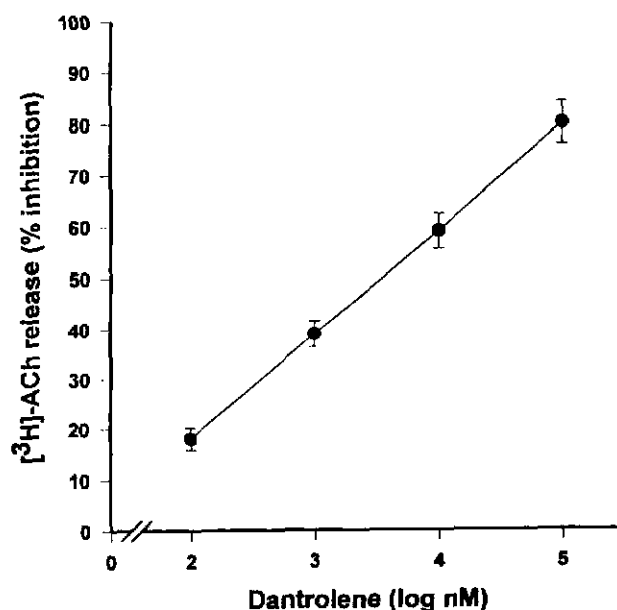


Figure 2 The effect of dantrolene concentration on the release of [3 H]-ACh induced by halothane from rat brain cortical slices. Brain cortical slices (40 mg) loaded with [3 H]-choline were preincubated for 15 min in salt medium in the presence of dantrolene at the indicated concentrations in abscissa. They were then incubated for 5 min in the presence of halothane (0.063 mM). Data are mean \pm s.e.mean (bars) values from at least three different experiments performed in duplicate. For other details, see text.

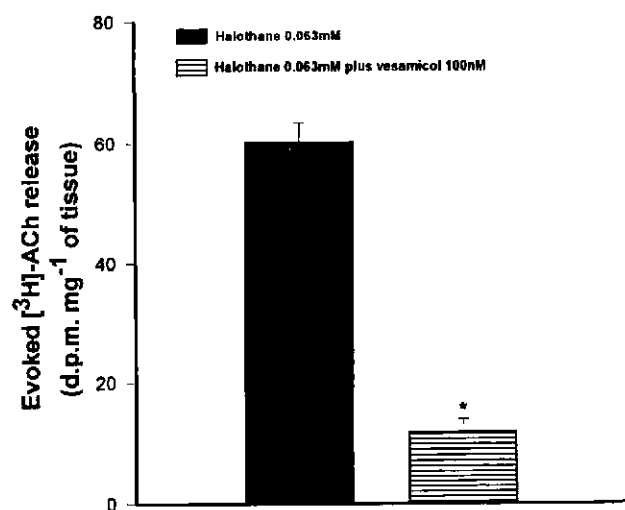


Figure 3 The effect of vesamicol on halothane-evoked [3 H]-ACh release from rat brain cortical slices. Brain cortical slices (40 mg) were first incubated for 10 min in the absence or presence of vesamicol (100 nM). They were then loaded with [3 H]-choline and after that incubated for 5 min in the absence or presence of halothane (0.063 mM). Data are shown as release of [3 H]-ACh evoked by halothane (total release minus basal in the absence or in the presence of vesamicol). Data are mean \pm s.e. mean (bars) values from at least three different experiments performed in duplicate. For other details, see text. *Statistically different from the halothane value, $P < 0.05$.

a consequence of vesamicol action, the vesicular release of ACh is suppressed. Vesamicol decreases basal release of ACh (Rigny & Collier, 1986), and in our experiments we observed a similar effect of 50% inhibition of basal [3 H]-ACh release. Thus the data in Figure 3 is shown as total release of [3 H]-ACh induced by halothane in the absence (filled bar) or in the presence of vesamicol (hatched bar) minus the value of basal release obtained in the absence or in the presence of the vesicular blocker, respectively. Figure 3 shows that vesamicol (100 nM) decreased ($80.4 \pm 4.9\%$) the evoked [3 H]-ACh release induced by halothane. Greater concentrations of vesamicol (up to $1.0 \mu\text{M}$) did not produce larger inhibition of the release of [3 H]-ACh evoked by the anaesthetic (data not shown).

Discussion

It is not completely clear how volatile anaesthetics cause anaesthesia, but one possible consequence of their action is to alter presynaptic activity and the release of neurotransmitters. Indeed, halothane has been shown to inhibit choline uptake into rat brain synaptosomes (Johnson & Hartzell, 1985; Griffiths & Norman, 1993; Griffiths *et al.*, 1994). We have studied here the effect of halothane on the release of [3 H]-ACh as an experimental model to determine how this volatile anaesthetic could affect neuronal secretion. To avoid any effect of halothane on choline uptake, the terminals were first loaded with radiolabelled choline in the absence of halothane and the release of [3 H]-ACh in the presence of this agent was determined.

There are few studies of the effect of volatile general anaesthetics on the release of ACh. In some of these studies, halothane was shown to decrease potassium-evoked ACh release from rat cortical synaptosomes (Johnson & Hartzell, 1985) and rat cortical slices (Griffiths *et al.*, 1995). In contrast, no effect on potassium-stimulated ACh release was observed in rat cerebral cortex in the presence of 1.25% halothane, 3%

enflurane or 0.2% methoxyflurane (Bazil & Minneman, 1989a, b). To our knowledge, all published studies investigated the effect of halothane in the CNS using only KCl depolarization, but did not investigate this effect following a more physiological and relevant stimulation, such as electrical field stimulation.

We observed that 0.018 mM halothane had no effect on the basal release of [3 H]-ACh (Table 1). At this concentration, the evoked release of [3 H]-ACh by electrical field stimulation was also not affected. In contrast, 0.063 mM halothane significantly increased the basal release of [3 H]-ACh. Interestingly, the association of field stimulation and 0.063 mM halothane caused additive release of [3 H]-ACh which result was not seen with 0.018 mM halothane. Both effects remained when higher concentrations of halothane (0.117 and 0.235 mM, Table 1) were used. In the cat sympathetic ganglion, Bosnjak *et al.* (1988) showed a decreased ACh release induced by electrical stimulation using higher concentration of halothane than those used in our experiments (0.28 and 0.59 mM). Although this apparent discrepancy could be explained by the halothane dose used, tissue and methodological differences should also be taken into account. Moreover, it is worth noting that, as in the present study, Griffiths *et al.* (1995) reported a trend to an increase in the release of ACh in brain cortical slices from unstimulated samples at all concentrations of halothane tested (0.037–1.19 mM).

The release of ACh evoked by electrical field stimulation is Na^+ and Ca^{2+} dependent and is inhibited by tetrodotoxin and the absence of calcium (Nakashima *et al.*, 1990; Yokoyama *et al.*, 1990). In our experiments, we demonstrated that EGTA, Cd^{2+} or tetrodotoxin did not significantly affect basal or halothane-induced ACh release. Moreover, halothane did not increase $^{45}\text{Ca}^{2+}$ influx in synaptosomes of rat brain cortical slices. Thus, the release of [3 H]-ACh in brain cortical slices induced by halothane is independent of the presence of extracellular Na^+ or Ca^{2+} and did not involve the entry of Ca^{2+} by calcium channels. Altogether, these results suggest the existence of different mechanisms for the release of [3 H]-ACh induced by halothane and electrical field stimulation from rat brain cortical slices.

Cellular activity is dependent on cytosolic free calcium concentration and intracellular Ca^{2+} stores have an important role in this process. The effect of tetracaine on the release of [3 H]-ACh evoked by halothane is consistent with the concept of calcium release from internal stores induced by halothane in cholinergic neurons, as previously described in synaptosomes (Daniell & Harris, 1988), hippocampal slices (Mody *et al.*, 1991) and in clonal pituitary cells (GH $_3$) (Hossain & Evers, 1994). The greater inhibition of tetracaine at 50 μM compared with 500 μM on halothane evoked [3 H]-ACh release could be explained by a dual effect of this drug on the calcium intracellular stores. Therefore, higher concentrations of tetracaine (above 1.0 mM) caused a gradual increase in intracellular store calcium load and subsequent activation of the Ca^{2+} -release channels by Ca^{2+} inside the internal stores (Pike *et al.*, 1989; Györke *et al.*, 1997). Indeed, we observed that tetracaine (1.0 and 2.0 mM) did not significantly affect the [3 H]-ACh release evoked by halothane (data not shown).

There is evidence indicating the presence of intracellular calcium stores in neurons that are sensitive to ryanodine receptor ligands such as caffeine and ryanodine (Miller, 1991; McPherson & Campbell, 1993). Indeed, our results showing a significant inhibition of halothane induced release of [3 H]-ACh by dantrolene suggests the involvement of ryanodine-sensitive stores in cholinergic neurons that are able to supply calcium for transmitter release.

It has long been known that the release of neurotransmitters requires the presence of extracellular Ca^{2+} . According to the calcium hypothesis, the synaptic release of neurotransmitters occurs through an exocytotic process triggered by Ca^{2+} inflow associated with presynaptic depolarization (Katz & Miledi, 1967). However, in recent years, evidence demonstrating transmitter release in the absence of external Ca^{2+} has been reported (reviewed by Adam-Vizi, 1992). Despite the large amount of contradictory data on this issue, one possibility is that neurotransmitter release under certain circumstances might be entirely independent of external Ca^{2+} , but triggered by the efflux of Ca^{2+} from internal stores (mitochondria, endoplasmic reticulum, etc.). Our results with EGTA, Cd^{2+} , tetracaine and dantrolene support this possibility. With respect to release in Ca^{2+} -free medium, most of the data in the literature suggests that transmitter release under these conditions occurs following efflux of transmitters from cytoplasmic sources. However, our experimental data with vesamicol, a compound known to inhibit the ACh transporter of cholinergic vesicles, suggests that most of the release of [³H]-

ACh induced by halothane from brain cortical slices occurs from an occluded tissue compartment, that uses the vesicular ACh transporter to accumulate ACh. The present results are thus distinct from the observation that extracellular Ca^{2+} -independent release does not require the vesicular ACh pool (Adam-Vizi et al., 1991; Adam-Vizi, 1992).

In conclusion, this study indicates that halothane may alter intracellular calcium homeostasis in cholinergic neurons, which effect could account for an extracellular Ca^{2+} -independent exocytotic release of ACh from rat brain cortical slices. Further investigations are necessary to identify the target by which halothane induces the release of ACh from cholinergic neurons.

We thank D.M. Miranda for her help with $^{45}\text{Ca}^{2+}$ influx experiments. We also thank Adriane A. Pereira, Andreia A. Guimarães and Antonio C.S. Gomes for technical assistance and Dr L.A. de Marco for reading and suggestions in this manuscript. Supported by FAPEMIG, CNPq, PADCT, FINEP, PRPq-UFGM and PRONEX.

References

- ADAM-VIZI, V. (1992). External Ca^{2+} -independent release of neurotransmitters. *J. Neurochem.*, **58**, 395–405.
- ADAM-VIZI, V., DERI, Z., VIZI, E.S., SERSHEN, H. & LAJTHA, A. (1991). Ca^{2+} -independent veratridine-evoked acetylcholine release from striatal slices is not inhibited by vesamicol (AH5183): mobilization of distinct transmitter pools. *J. Neurochem.*, **56**, 52–58.
- BAZIL, C.W. & MINNEMAN, K.P. (1989a). Effects of clinically effective concentrations of halothane on adrenergic and cholinergic synapses in rat brain in vitro. *J. Pharmacol. Exp. Ther.*, **248**, 143–148.
- BAZIL, C.W. & MINNEMAN, K.P. (1989b). Clinical concentrations of volatile anesthetics reduce depolarization-evoked release of [³H]norepinephrine, but not [³H]acetylcholine, from rat cerebral cortex. *J. Neurochem.*, **53**, 962–965.
- BOSNJAK, Z.J., DUJIC, Z., ROERIG, D.L. & KAMPINE, J.P. (1988). Effects of halothane on acetylcholine release and sympathetic ganglionic transmission. *Anesthesiology*, **69**, 500–506.
- CASALI, T.A.A., GOMEZ, R.S., MORAES-SANTOS, T., ROMANO-SILVA, M.A., PRADO, M.A.M. & GOMEZ, M.V. (1997). Different effects of reducing agents on ω -conotoxin GVIA inhibition of [³H]-acetylcholine release from cortical slices and guinea-pig myenteric plexus. *Br. J. Pharmacol.*, **120**, 88–92.
- COLLIER, B. & MITCHELL, J.F. (1967). Release of ACh during consciousness and after brain lesions. *J. Physiol. (Lond)*, **188**, 83–88.
- CONNELLY, T.J. & CORONADO, R. (1994). Activation of the Ca^{2+} release channel of cardiac sarcoplasmic reticulum by volatile anesthetics. *Anesthesiology*, **81**, 459–469.
- DANIELL, L.C. & HARRIS, R.A. (1988). Neuronal intracellular calcium concentrations are altered by anesthetics: Relationship to membrane fluidization. *J. Pharmacol. Exp. Ther.*, **245**, 1–7.
- FOX, A.P., NOWYCKY, M.C. & TSIEN, R.W. (1987). Kinetic and pharmacological properties distinguishing three types of calcium currents in chick sensory neurons. *J. Physiol. (Lond)*, **394**, 149–172.
- GOLDBERG, A.M. & MCCAMAN, R.E. (1973). The determination of picomole amounts of acetylcholine in mammalian brain. *J. Neurochem.*, **20**, 1–8.
- GOMEZ, R.S., GOMEZ, M.V. & PRADO, M.A.M. (1996). Inhibition of Na^+ , K^+ -ATPase by ouabain opens calcium channels coupled to acetylcholine release in guinea pig myenteric plexus. *J. Neurochem.*, **66**, 1440–1447.
- GRIFFITHS, R., GREIFF, J.M.C., BOYLE, E., ROWBOTHAM, D.J. & NORMAN, R.I. (1994). Volatile anesthetics inhibit choline uptake into rat synaptosomes. *Anesthesiology*, **81**, 953–958.
- GRIFFITHS, R., GREIFF, J.M.C., HAYCOCK, J., ELTON, C.D., ROWBOTHAM, D.J. & NORMAN, R.I. (1995). Inhibition by halothane of potassium-stimulated acetylcholine release from rat cortical slices. *Br. J. Pharmacol.*, **116**, 2310–2314.
- GRIFFITHS, R. & NORMAN, R.I. (1993). Effects of anaesthetics on uptake, synthesis and release of transmitters. *Br. J. Anaesth.*, **71**, 96–107.
- GYÖRKE, S., LUKYANENKO, V. & GYÖRKE, I. (1997). Dual effects of tetracaine on spontaneous calcium release in rat ventricular myocytes. *J. Physiol. (Lond)*, **500**, 297–309.
- HOSSAIN, M.D. & EVERS, A.S. (1994). Volatile anesthetic-induced efflux of calcium from IP_3 -gated stores in clonal (GH_3) pituitary cells. *Anesthesiology*, **80**, 1379–1389.
- JOHNSON, G.V.W. & HARTZELL, C.R. (1985). Choline uptake, acetylcholine synthesis and release, and halothane effects in synaptosomes. *Anesth. Analg.*, **64**, 395–399.
- KANAI, T. & SZERB, J.C. (1965). Mesencephalic reticular activating system and cortical acetylcholine output. *Nature*, **205**, 80–82.
- KATZ, B. & MILEDI, R. (1967). The timing of calcium action during neuromuscular transmission. *J. Physiol. (Lond)*, **189**, 533–544.
- KEIFER, J.C., BAGHDOYAN, H.A., BECKER, I. & LYDIC, R. (1994). Halothane anaesthesia causes decreased acetylcholine release in the pontine reticular formation and increased EEG spindles. *Neuroreport*, **5**, 577–580.
- LARRABEE, M.G. & POSTERNAK, J.M. (1952). Selective action of anesthetic on synapses and axons in mammalian sympathetic ganglia. *J. Neurophysiol.*, **15**, 92–114.
- LEÃO, R.M., GOMEZ, M.V., COLLIER, B. & PRADO, M.A.M. (1995). Inhibition of potassium-stimulated acetylcholine release from rat brain cortical slices by two high-affinity analogues of vesamicol. *Brain Res.*, **703**, 86–92.
- MCPHERSON, P.S. & CAMPBELL, K.P. (1993). The Ryanodine Receptor/ Ca^{2+} release channel. *J. Biol. Chem.*, **268**, 13765–13768.
- MILLER, R.J. (1991). The control of neuronal Ca^{2+} homeostasis. *Prog. Neurobiol.*, **37**, 255–285.
- MIRANDA, D.M., ROMANO-SILVA, M.A., KALAPOTHAKIS, E., DINIZ, C.R., CORDEIRO, M.N., MORAES-SANTOS, T., PRADO, M.A.M. & GOMEZ, M.V. (1998). *Phonotria nigriventer* toxins block tityustoxin-induced calcium influx in synaptosomes. *Neuroreport*, **9**, 1371–1373.
- MITCHELL, J.F. (1963). The spontaneous and evoked release of acetylcholine from the cerebral cortex. *J. Physiol. (Lond)*, **165**, 98–116.
- MODY, I., TANELIAN, D.L. & MACIVER, M.B. (1991). Halothane enhances tonic neuronal inhibition by elevating intracellular calcium. *Brain Res.*, **538**, 319–323.
- MORGAN, K.C. & BRYANT, S.H. (1977). The mechanism of action of dantrolene sodium. *J. Pharmacol. Exp. Ther.*, **201**, 138–147.
- NAKASHIMA, Y., SUGIYAMA, S., SHINDOH, J., TAKI, F., TAKAGI, K., SATAKE, T. & OZAWA, T. (1990). Effects of sodium channel blockers on electrical field stimulation-induced guinea-pig tracheal smooth muscle contraction. *Arch. Int. Pharmacodyn. Ther.*, **306**, 130–138.

- NARAHASHI, T., MOORE, J. & SCOTT, W.R. (1964). Tetrodotoxin blockage of sodium conductance increase in lobster giant axon. *J. Gen. Physiol.*, **147**, 965–974.
- NELSON, T.E. & SWEO, T. (1988). Ca^{2+} uptake and Ca^{2+} release by skeletal muscle sarcoplasmic reticulum. *Anesthesiology*, **69**, 571–577.
- OHNISHI, S.T. (1979). Calcium-induced calcium release from fragmented sarcoplasmic reticulum. *J. Biochem.*, **86**, 1147–1150.
- OHYA, T., ITO, S. & OHGA, A. (1990). Inhibitory action of dantrolene on Ca-induced Ca^{2+} release from sarcoplasmic reticulum in guinea pig skeletal muscle. *Eur. J. Pharmacol.*, **178**, 11–19.
- PALADE, P. (1987). Drug-induced Ca^{2+} release from isolated sarcoplasmic reticulum. II. Releases involving a Ca^{2+} -induced Ca^{2+} release channel. *J. Biol. Chem.*, **262**, 6141–6148.
- PARSONS, S.M., PRIOR, C. & MARSHALL, I.G. (1993). Acetylcholine transport, storage, and release. *Int. Rev. Neurobiol.*, **35**, 279–390.
- PIKE, G.K., ABRAMSON, J.J. & SALAMA, G. (1989). Effects of tetracaine and procaine on skinned muscle fibres depend on free calcium. *J. Musc. Res. Cell. Motil.*, **10**, 337–349.
- PRADO, M.A.M., GOMEZ, M.V. & COLLIER, B. (1993). Mobilization of a vesamicol-insensitive pool of acetylcholine from a sympathetic ganglion by ouabain. *J. Neurochem.*, **61**, 45–56.
- RICHARDS, C.D. (1983). Actions of general anaesthetics on synaptic transmission in the CNS. *Br. J. Anaesth.*, **55**, 201–207.
- RICNY, J. & COLLIER, B. (1986). Effect of 2-(4-phenylpiperidino)cyclohexanol on acetylcholine release and subcellular distribution in rat striatal slices. *J. Neurochem.*, **47**, 1627–1633.
- RUTLEDGE, C.O., SEIFEN, E., ALPER, M.H. & FLACKE, W. (1963). Analysis of halothane in gas and blood by gas chromatography. *Anesthesiology*, **24**, 862–867.
- TSUCHIDA, H., NAMBA, H., YAMAKAGE, M., FUJITA, S., NOTSUKI, E. & NAMIKI, A. (1993). Effects of halothane and isoflurane on cytosolic calcium ion concentrations and contraction in the vascular smooth muscle of the rat aorta. *Anesthesiology*, **78**, 531–540.
- VAN WINKLE, W.B. (1976). Calcium release from skeletal muscle sarcoplasmic reticulum; Site of action of dantrolene sodium? *Science*, **193**, 1130–1131.
- WHEELER, D.M., RICE, R.T., HANSFORD, R.G. & LAKATTA, E.G. (1988). The effect of halothane on the free intracellular calcium concentration of isolated rat heart cells. *Anesthesiology*, **69**, 578–583.
- WINKLER, J., SUHR, S.T., GAGE, F.H., THAL, L.J. & FISHER, L.J. (1995). Essential role of neocortical acetylcholine in spatial memory. *Nature*, **375**, 484–487.
- YOKOYAMA, K. & YAGASAKI, O. (1990). Effects of Ca^{2+} blockers on the various types of stimuli-induced acetylcholine release from guinea-pig ileum myenteric plexus. *Jpn. J. Pharmacol.*, **52**, 109–114.

(Received October 10, 1998

Revised March 8, 1999

Accepted March 17, 1999)

Expression of the Vesicular Acetylcholine Transporter, Proteins Involved in Exocytosis, and Functional Calcium Signaling in Varicosities and Soma of a Murine Septal Cell Line

J. Barbosa Jr., A. R. Massensini, *M. S. Santos, S. I. Meireles, †R. S. Gomez, M. V. Gomez, M. A. Romano-Silva, *V. F. Prado, and M. A. M. Prado

Laboratório de Neurofarmacologia, Departamento de Farmacologia; *Departamento de Bioquímica-Imunologia, Instituto de Ciências Biológicas; and †Departamento de Patologia, Faculdade de Odontologia, Universidade Federal de Minas Gerais, Belo Horizonte, Minas Gerais, Brasil

Abstract: The expression and localization of the vesicular acetylcholine transporter in a septal cell line, SN56, were investigated. Immunoprecipitation and immunoblot analysis of postnuclear supernatants indicated that this cell line expresses reasonable amounts of the transporter. Immunofluorescence and confocal microscopy experiments showed that the vesicular transporter is present in varicosities and also in the cell body of differentiated cells. Varicosities have the potential to be functional sites of transmitter release because they responded to depolarization with calcium influx through voltage-gated calcium channels and expressed the synaptic proteins synaptotagmin, SV2, synaptophysin, and a subunit of P/Q calcium channels. In the soma of SN56 cells, the transporter immunoreactivity was similar to that for synaptotagmin, and it colocalized with synaptophysin, but it did not colocalize with SV2. Labeling for SV2 appeared prominently in a defined perinuclear structure, whereas the two former proteins were widely distributed in the soma, where several endocytic compartments could be identified with the vital dye FM4-64. These data suggest that distinct synaptic vesicle proteins exist in different subcellular compartments, and consequently they may follow distinct pathways in neurites before reaching sites of transmitter storage and release in SN56 cells. **Key Words:** Confocal microscopy—Vesicular acetylcholine transporter—SN56 cells—Synaptic vesicles—Calcium imaging—Calcium channels.

J. Neurochem. 73, 1881–1893 (1999).

Studies of protein function and localization in neurons can be greatly facilitated by the use of cultured cells. Primary neuronal cultures can be used successfully to study diverse aspects of neuronal function, but they usually present neurochemical heterogeneity, which can be a problem for the study of a given neurotransmitter system. Cell lines expressing defined neurochemical phenotypes can help in circumventing this problem. SN56 cells have been generated by somatic fusion of mouse septal neurons (day 21) with a neuroblastoma cell line

(N18TG2) (see Hammond et al., 1990; Lee et al., 1990), resulting in a hybrid cell that possesses cholinergic features (Blusztajn et al., 1992). Recent studies have used SN56 cells to understand factors controlling the synthesis and release of acetylcholine (ACh) and vulnerability of cholinergic cells to amyloid peptides (Blusztajn et al., 1992; Pedersen et al., 1995, 1996; Le et al., 1997; Colom et al., 1998). Expression of two markers of cholinergic neurons, the enzyme choline acetyltransferase (ChAT) and the vesicular ACh transporter (VACHT), has also been studied at the mRNA level in these cells (Berse and Blusztajn, 1995). SN56 cells express ChAT protein (Blusztajn et al., 1992; Pedersen et al., 1995, 1996); however, it is not known whether VACHT is expressed at the protein level and directed to sites where synaptic vesicles presumably are present. This is of interest because another cell line that presents several cholinergic characteristics, NG108-15 (Hamprecht, 1977; McGee et al., 1978; McGee, 1980), has recently been shown to process VACHT incorrectly at the posttranslational level, and most likely VACHT is then mistargeted in this cell line (Diebler et al., 1998).

The deduced VACHT sequence predicts an integral membrane protein, with 12 transmembrane domains, cy-

Received May 26, 1999; revised manuscript received June 21, 1999; accepted June 22, 1999.

Address correspondence and reprint requests to Dr. M. A. M. Prado at Laboratório de Neurofarmacologia, Departamento de Farmacologia, Instituto de Ciências Biológicas, Universidade Federal de Minas Gerais, Avenida Antonio Carlos, 6627, Belo Horizonte, Minas Gerais, Brasil 31270-901.

The present address of Dr. S. I. Meireles is Ludwig Institute for Cancer Research, Rua Prof. Antonio Prudente 109, São Paulo, SP, Brasil 01509-010.

Abbreviations used: ACh, acetylcholine; ω -Aga IVA, ω -agatoxin IVA; AM, acetoxymethyl ester; ChAT, choline acetyltransferase; FITC, fluorescein isothiocyanate; MBP, maltose-binding protein; PAGE, polyacrylamide gel electrophoresis; SDS, sodium dodecyl sulfate; Syp, synaptophysin; Syt, synaptotagmin; TGN, trans-Golgi network; VACHT, vesicular acetylcholine transporter.

toplasmic N- and C-terminal regions, a large intravesicular loop with potential glycosylation sites, and a C-terminal consensus phosphorylation site for protein kinase C (Bejanin et al., 1994; Erickson et al., 1994; Roghani et al., 1994; Varoqui et al., 1994). Overexpression of VACHT has shown that the protein is targeted to endosomes in nonneuronal and to synaptic-like vesicles in neuronal models (Erickson et al., 1994; Liu and Edwards, 1997; Song et al., 1997; Tan et al., 1998). Recently, Varoqui and Erickson (1998) have demonstrated that in PC12 cells overexpressing VACHT, the cytoplasmic tail of the protein appears necessary for proper targeting to synaptic-like vesicles.

The present work investigated whether SN56 cells can express and target VACHT to sites where other synaptic vesicle proteins that participate in neurotransmitter release are present. Our results suggest that VACHT in SN56 cells is located in varicosities of neuritic processes, although immunoreactivity is also detected in large amounts in the soma, where endocytic organelles were readily identified with the styryl dye FM4-64. It is interesting that SV2, a putative transporter present in synaptic vesicles, was not present in the same somatic compartment as VACHT and other synaptic vesicle proteins. We also show that varicosities of SN56 cells respond to stimuli and present several components involved in synaptic vesicle exocytosis, such as neuronal calcium channels and synaptic vesicle proteins. Together these results indicate that several distinct aspects of cholinergic cell biology can be investigated in SN56 cells.

MATERIALS AND METHODS

Materials

Antiserum against VACHT has been previously characterized (Weihe et al., 1996) and was purchased from Phoenix Pharmaceuticals (Mountain View, CA, U.S.A.). SV2 monoclonal antibodies (Buckley and Kelly, 1985) were a kind gift of Dr. Sandra Bajjalieh (Department of Pharmacology, University of Washington, Seattle, WA, U.S.A.). The monoclonal antibody against synaptophysin (Syn) and the secondary antibodies coupled to fluorescein isothiocyanate (FITC) were from Sigma Chemical Co. (St. Louis, MO, U.S.A.). Antisera against synaptotagmin (Syn) and the calcium channel $\alpha 1A$ subunit were from Alomone Labs (Jerusalem, Israel). Secondary antibodies coupled to Alexa568 and fluo-3 acetoxymethyl ester (AM) were from Molecular Probes (Eugene, OR, U.S.A.). Fetal bovine serum was from GIBCO Life Technologies. All other reagents, unless otherwise stated, were from Sigma.

Mouse VACHT amplification by PCR

We used the relationship between rat and human VACHT to design primers to amplify the mouse VACHT gene. Primers used were as follows: 699F, 5'-TTCTGAGCTCGGG-GATATGA-3'; 859F, 5'-ATGGAACCCACCGCGCAAC-3'; 1282F, 5'-AGCGGGCCTTTCATTGATCG-3'; 2094R, 5'-GCGCACGTCCACCCAGAAAGG-3'; 2427R, 5'-GTCGT-CCTCGCACCCGTCAC-3'; 2104F, 5'-GTTCGAATTC-CAGTCTATGGCAGTGTCTA-3'; 2266F, 5'-TCTTGAATTC-CGTAATGTGGGCCTCCTTAC-3'; and 2544R, 5'-AAG-GCTGCAGGGTATTCATTAGAGGAGGT-3'. Numbering of primers indicates the 5' end of forward (F) and reverse (R)

primers according to the cloned rat VACHT sequence [GenBank accession no. U09211 (Erickson et al., 1994)]. Restriction sites (*EcoRI* or *PstI*, marked in italics in the above sequences) were introduced into some of the primers to facilitate successful cloning and correct orientation. DNA extracted from mouse BALB/c testis was used as template for PCR procedures. Amplified DNA segments were purified and cloned into pUC18. Recombinants were sequenced by the dideoxynucleotide chain-termination method using the Thermo Sequenase kit (Amersham).

C-terminal pMAL plasmid construction and expression

A fusion protein containing the C terminus (amino acids 470–530) of the mouse VACHT was produced with the pMAL bacterial expression system (New England BioLabs). The DNA encoding the carboxyl terminus was amplified by PCR using primers 2266F and 2544R, purified, and subcloned between the *EcoRI* and *PstI* sites of pMAL-c2 vector. Clones were sequenced by the dideoxynucleotide chain-termination method to confirm the reading frame.

The encoded fusion protein contains a 42.7-kDa maltose-binding protein (MBP) fused at the carboxyl end with the mouse VACHT C terminus (~6 kDa). The fusion protein was expressed in *Escherichia coli* (BL21 strain) cells transformed with pMAL plasmids according to the manufacturer's instructions. The induced bacteria were lysed by incubation with lysozyme and repeated freezing and thawing. The soluble fusion protein was affinity-purified from the bacterial lysates using amylose resin and eluted with 10 mM maltose. Purified fusion protein preparations were verified by sodium dodecyl sulfate (SDS)-polyacrylamide gel electrophoresis (PAGE) analysis, silver staining, and immunoblots using antiserum against the C-terminal region of VACHT.

Cell culture

SN56 cells were a generous gift of Prof. Bruce Wainer (Department of Pathology, Emory University School of Medicine, Atlanta, GA, U.S.A.). The cells were maintained in Dulbecco's modified Eagle's medium (Sigma), 10% fetal bovine serum (GIBCO Life Technologies), 2 mM L-glutamine, and 1% penicillin/streptomycin in 50-ml culture bottles in a 5% CO₂ atmosphere at 37°C. Cells were differentiated in the same medium above but lacking fetal bovine serum and supplemented with 1 mM dibutyryl-cyclic AMP for at least 3 days. Medium was changed every 2 days, except during differentiation, when it was changed every 24 h. For confocal analysis, cells were grown directly on coverslips and were exposed to the same differentiation protocol as described above. Passages up to 15 were used in the experiments.

Calcium measurements

Experiments were performed at room temperature (20–25°C). Cells on coverslips were incubated in HEPES-buffered salt solution [124 mM NaCl, 4 mM KCl, 2 mM CaCl₂, 1.2 mM MgCl₂, 10 mM glucose, and 25 mM HEPES (pH 7.4, adjusted with NaOH)] containing 10 μ M fluo-3 AM for 1 h. The coverslips were washed in dye-free HEPES-buffered salt solution and then transferred to a custom holder in which the coverslip formed the bottom of a 400- μ l bath that was perfused continuously. Imaging was performed with a Bio-Rad MRC 1024 laser scanning confocal system running the software Timecourse 1.0 coupled to a Zeiss microscope (Axiovert 100) with a water immersion objective (40 \times , 1.2 NA) as described (Kushmerick et al., 1999). In all the experiments, each cell or

varicosity was analyzed individually and used as its own control; thus, there was no need to calibrate the amount of fluo-3 present into the cells (see Kushmerick et al., 1999). However, preliminary experiments using indo-1 and UV illumination indicated that basal calcium in the cells we studied was around 50 nM and was raised to 200–300 nM on depolarization (A.R.M. et al., unpublished data).

Western analysis and immunoprecipitation

For preparation of a postnuclear supernatant, cells were collected in phosphate-buffered saline (pH 7.4) containing 5 mM EGTA and 200 μ l of a protease inhibitor mixture (complete protease inhibitor tablets; Boehringer Mannheim; twice the concentration suggested by the manufacturer) and centrifuged (800 g for 10 min). Cell pellets were resuspended in phosphate-buffered saline supplemented as above and homogenized, and cell debris were pelleted by centrifugation (800 g for 10 min at 4°C). In some experiments, mouse spinal cord was used as a positive control. The tissue was then dissected, homogenized in 0.32 M sucrose (pH 7.4), and centrifuged at 1,000 g for 10 min at 4°C. The supernatant was collected and centrifuged at 39,000 g for 15 min (4°C), and then the pellet was resuspended in phosphate-buffered saline containing the above concentration of protease inhibitor mixture. Aliquots of the cell extracts were frozen at –80°C until use. Proteins were resolved on 8% SDS-PAGE. After electrophoresis, proteins were transferred overnight to a nitrocellulose membrane as described (Towbin et al., 1979; Barbosa et al., 1997). For immunoblots, nitrocellulose membranes were blocked with phosphate-buffered saline containing 0.3% Tween and 5% non-fat milk, incubated with commercial antiserum against VACHT (1:1,000–1:5,000), washed, and then incubated with a secondary goat anti-rat antibody conjugated with peroxidase (1:10,000). Staining was revealed by enhanced chemiluminescence (ECL from Amersham Life Science).

For immunoprecipitation, cells were treated with RIPA buffer [final concentrations: 150 mM NaCl, 50 mM Tris, 5 mM EDTA, 10 mM NaF, 10 mM Na₄P₂O₇, 1% Nonidet P-40, 0.5% deoxycholate, 0.1% SDS, 0.1 mM phenylmethylsulfonyl fluoride, 10 μ g/ml leupeptin, and 5 μ g/ml aprotinin (pH 7.4 with HCl)], and all the manipulations were carried out at 4°C. Immunoprecipitation was performed using slight modifications of the method described by Ferguson et al. (1995) as detailed by Barbosa et al. (1997). After immunoprecipitation, the proteins were transferred to nitrocellulose, and immunostaining was performed as above. In some of the experiments, the VACHT antiserum was previously adsorbed with the MBP-VACHT fusion protein (50 μ M; mock immunoprecipitation). Control experiments in which the antiserum was adsorbed only with MBP indicated that the treated antiserum was able to immunoprecipitate VACHT and that adsorption occurred only in the presence of the C-terminal region of VACHT present in the fusion protein (data not shown).

Immunofluorescence and confocal microscopy

Cells were washed twice in 0.1 M phosphate buffer (pH 7.4) and then fixed with 4% paraformaldehyde in 0.1 M phosphate buffer for 20 min. Fixed cells were washed with phosphate buffer and 0.1 M Tris-buffered saline (pH 7.4) and incubated with primary antibodies (1:200–1:2,000 for VACHT, 1:300–1:1,500 for SV2, 1:200 for α 1A, 1:100 for Syt, and 1:100 for Syp) for 16 h at 4°C in Tris-buffered saline containing 1% normal goat serum and 0.1% Triton X-100. Cells were then washed, rinsed three times (10 min) with Tris-buffered saline, and incubated for 40 min with goat anti-rabbit or anti-mouse

antibodies conjugated to FITC or Alexa568 (in some experiments tetramethylrhodamine isothiocyanate was also used with similar results), depending on the primary antibody used. Cells were then washed three times with Tris-buffered saline and mounted on microscope slides with Hydromount. Controls to test for specific labeling consisted of omission of the primary antibody or, in the case of anti-VACHT, anti-Syt, and anti-calcium channels α 1A subunit, incubating the antisera with excess amount of the peptide (10 μ g) or recombinant protein (50 μ M). All the above manipulations impaired specific labeling (data not shown). In addition, control experiments, performed in parallel where one of the secondary antibodies was omitted to assess bleedthrough between the two channels used to image the fluorophores, indicated that very little contamination occurred between channels with the confocal settings used.

Imaging was performed with a Bio-Rad confocal system described above running the software Lasershar (version 3.1; Bio-Rad) with a water immersion 40 \times , 1.2 NA or an oil immersion 63 \times , 1.4 NA objective. A water-cooled argon UV laser (488 nm) or a krypton/argon laser was used to excite the preparation (through its 488 nm line or 568 nm line), and light emitted was selected with band pass filters (522/35 for FITC, 598/40 for Alexa568).

Z series or single optical sections were obtained with variable pinhole settings (between 1.8 and 5 mm). Image analysis and processing were performed with the Lasershar software, Adobe Photoshop, and Metamorph (Universal Imaging).

FM4-64 labeling

Cells were incubated with 1.5 μ M FM4-64 for 16 h as described previously (Maletic-Savatic and Malinow, 1998), and then cells were washed in HEPES-buffered salt solution three times before imaging with the confocal microscope. Excitation was with the 568 laser line, and emitted light was selected with a filter (680/32).

RESULTS

Varicosities of SN56 cells respond to depolarization

Previous characterization of SN56 cells indicates that they can synthesize and release ACh, and these features appear to improve on differentiation (Blusztajn et al., 1992). Before differentiation the hybrid cells are mainly round and extend few neuritic processes (see Hammond et al., 1990). However, after differentiation in medium containing dibutyryl-cyclic AMP, most of the SN cells develop a neuronal shape and extend processes that appear to make cell–cell contacts several microns away (Fig. 1A).

One property of neuronal cells is that they respond to depolarization with increases in intracellular calcium through specific neuronal voltage-gated calcium channels. To test whether this would occur to SN56 cells after differentiation, they were labeled with the calcium indicator fluo-3 AM, and changes in intracellular calcium were followed. Figure 1B shows two images of cells before and after depolarization with 60 mM KCl. The cells respond to depolarization by increasing intracellular calcium both in the soma and in the varicosities (Fig. 1B, arrows, and C). The increase in intracellular calcium was reversible and of similar magnitude when evoked in two sequential periods of depolarization (Fig. 1C1–3). This

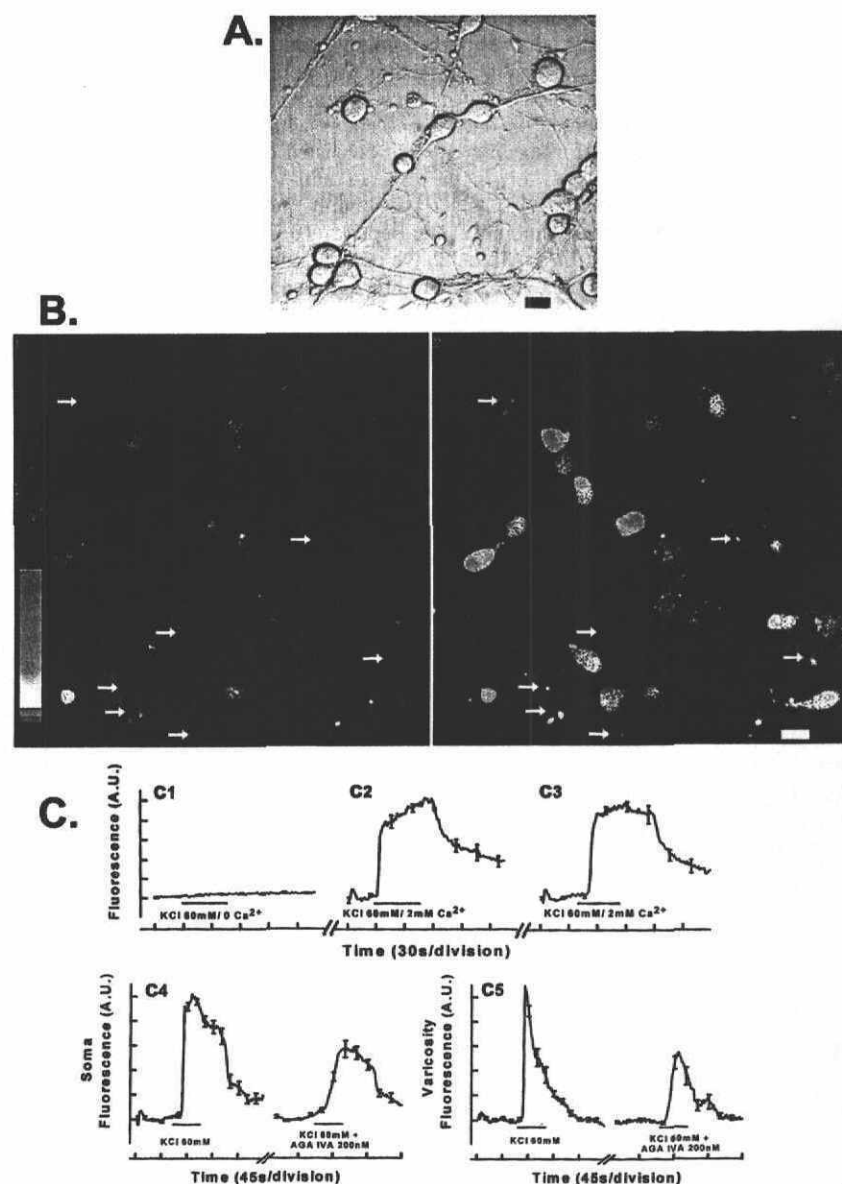


FIG. 1. SN56 cells respond to depolarization. **A:** Differential interference contrast image of typical SN56 cells differentiated with dibutyryl-cyclic AMP for 3 days. Note the abundance of varicosities in neuritic processes and the overall shape of the cells. Bar = 20 μ m. **B:** Confocal fluorescence pseudocolored images of differentiated SN56 cells from another culture labeled with fluo-3 before (1) and after (2) 60 mM KCl depolarization. Arrows indicate some of the varicosities that responded to depolarization. Images are representative of three experiments. Bar = 20 μ m. **C:** Quantification of fluo-3 fluorescence (A.U. = arbitrary units) for nine cells in which the culture was depolarized in the absence of calcium (C1) and after a period of rest the cells were challenged twice with 60 mM KCl (C2 and C3) in the presence of calcium. C4 and C5: Results of another experiment where the cells were first depolarized with KCl and then challenged again (60 mM KCl) in the presence of ω -Aga IVA (200 nM). Regions of interest were drawn around cells or varicosities, and the fluorescence intensity (256 gray levels) was obtained with Timecourse software during acquisition of fluorescence images. Data are mean \pm SEM (bars) values for nine individual cells (C4) and eight varicosities (C5). Similar results were obtained in two other experiments.

appeared to depend on entry of calcium via calcium channels, as in the absence of extracellular calcium the SN56 cells did not respond to depolarization (Fig. 1C1). The increase in calcium influx was diminished by ω -agatoxin IVA (ω -Aga IVA), a toxin that blocks neuronal P/Q calcium channels, in the soma and varicosities (Fig. 1C4 and 5), suggesting that these channels may be present in differentiated SN56 cells. Indeed, an anti-peptide antibody selective against the α 1A subunit, which codes for P/Q channels, stained SN56 cells (Fig. 2). Immunoreactivity in fixed cells was found in the cell body and also in growth cones or varicosities (see Fig. 2 for an example).

VACHT expression in SN56 cells

Because SN cells are derived from the mouse, we determined how related the deduced mouse protein is to

rat and human VACHT. The mouse VACHT DNA was amplified by PCR, cloned, and sequenced. The deduced amino acid sequence showed an overall homology to the rat and human sequences of 99.5 and 94.5%, respectively (data not shown). Moreover, sequence analysis suggested that the antiserum developed by Eiden and colleagues (Weihe et al., 1996) against the last 11 amino acids of the rat VACHT should recognize mouse VACHT (data not shown). This was confirmed by expressing the C-terminal region of mouse VACHT as an MBP fusion protein and performing immunoblot analysis of recombinant VACHT (Fig. 3A). The fusion protein was incubated with factor Xa protease as described by the manufacturer, and the resulting digestion product was resolved by SDS-PAGE, transferred to nitrocellulose, and probed with different antibodies. The VACHT antiserum

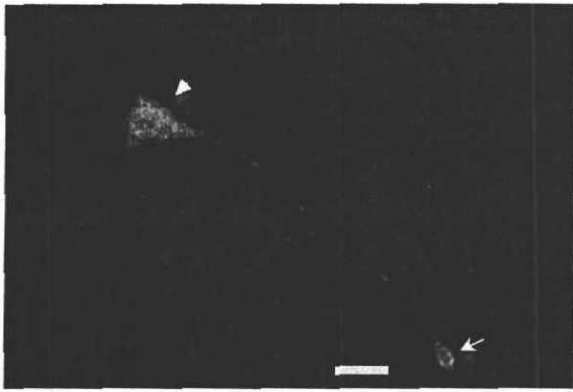


FIG. 2. SN56 cells express $\alpha 1A$ subunits of P/Q calcium channels. Confocal image of an SN56 cell stained with an antibody specific for the $\alpha 1A$ subunit and an FITC-labeled secondary antibody. The image shows a typical cell that presents heavy labeling in the cell body (arrowhead). In addition, the tip of the neurite presents localized immunoreactivity for $\alpha 1A$ (arrow). Bar = 20 μm .

recognizes MBP-VACHT fusion protein and the C-terminal region of VACHT after digestion of the fusion protein by factor Xa protease, which cleaves a region between MBP and the VACHT peptide (Fig. 3A, lane 3; the 49-kDa band represents the remaining MBP-VACHT, suggesting that digestion was not complete, and the 6-kDa band is the C-terminal fragment cleaved from the fusion protein). This immune reaction could be prevented by previously adsorbing the VACHT antiserum with an excess of the recombinant protein (Fig. 3A, lane 2). In addition, a control antibody against MBP does not recognize the C-terminal region (6 kDa), although it recognizes MBP (Fig. 3A, lane 1; note the difference in molecular weight compared with MBP-VACHT in lane 3). Finally, omission of the primary antibody indicates that there is no reaction against the expressed proteins, showing that staining was specific (Fig. 3A, lane 4).

To test whether SN56 cells expressed VACHT, we used the above antiserum to immunoprecipitate the protein from cell extracts. Figure 3B illustrates the results of the immunoprecipitation and subsequent immunoblot analysis of VACHT from differentiated SN56 cells. The antiserum precipitates one major band of somewhat variable molecular size (80–110 kDa, lower and upper limits for five experiments) that was subsequently recognized in immunoblots (Fig. 3B, lane 1). Mock immunoprecipitation, performed with the antiserum adsorbed with an excess of recombinant VACHT, indicates that this band represents the transporter from SN56 cells (Fig. 3B, lanes 1 and 2).

Immunoblot analysis of postnuclear supernatants of differentiated SN56 cells shows that VACHT can be detected as a major band of ~80 kDa that is abundantly expressed by the cells (Fig. 3C and D), but other molecular size forms may also be present in smaller amounts (Fig. 3D). The major immunolabeled protein electrophoresed in SDS gels with the same apparent molecular size

as the major immunolabeled protein in mouse spinal cord extracts (Fig. 3D).

Localization of VACHT and proteins involved in synaptic transmission

To investigate the localization of VACHT immunoreactivity in SN56 cells, we used indirect immunofluorescence and confocal microscopy. Figure 4A shows cells presenting neurites stained by the VACHT antiserum. Neuritic processes present localized immunoreactivity for VACHT, and this seemed to be contained mostly in dilations of neurite branches (Fig. 4A and B, arrows). VACHT immunoreactivity was also present at the cell

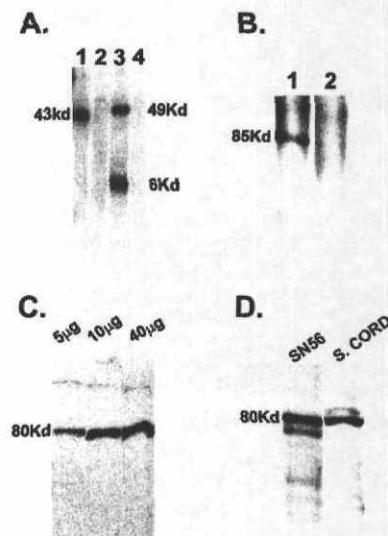


FIG. 3. Expression of VACHT by SN56 cells. **A:** Immunoblot analysis of bacterial-expressed C-terminal region of mouse VACHT. MBP-VACHT fusion protein was cleaved with factor Xa protease as described by the manufacturer, and proteins were separated by SDS-PAGE. Proteins were transferred to nitrocellulose and incubated with an MBP antiserum (lane 1), a rat VACHT antibody previously adsorbed with MBP-VACHT (lane 2), the VACHT antibody (lane 3), and omission of the primary antibody (lane 4). Staining was revealed by ECL (Amersham), and the 6-kDa fragment corresponds to the C-terminal VACHT peptide, the 49-kDa band represents the nondigested form of MBP-VACHT and the 43-kDa band of lane 1 represents MBP (calculated molecular size by the deduced sequence is 42.5 kDa) after digestion. **B:** Differentiated SN56 cell extracts were used to immunoprecipitate VACHT using the VACHT antibody. After immunoprecipitation, the proteins were resolved by SDS-PAGE, transferred to nitrocellulose membrane, and immunostained as described in the text. One major band was detected (lane 1). Lane 2 shows a similar experiment but one in which the VACHT antibody was first adsorbed with the recombinant VACHT peptide (mock immunoprecipitation). **C:** Postnuclear supernatants of SN56 cells were separated by SDS-PAGE, and immunoblot analysis was performed. The bands represent immunoreactivity against VACHT detected in 5, 10, or 40 μg of protein extract loaded in the gel. **D:** Postnuclear supernatant proteins of SN56 cells and mouse spinal cord were separated by SDS-PAGE and immunostained with the VACHT antibody. Two major bands of ~80 kDa were detected in both extracts, although other molecular size forms of VACHT were also detected in both samples after overexposure of the membranes. The blots were representative of at least six (SN56) and two (spinal cord) different experiments.

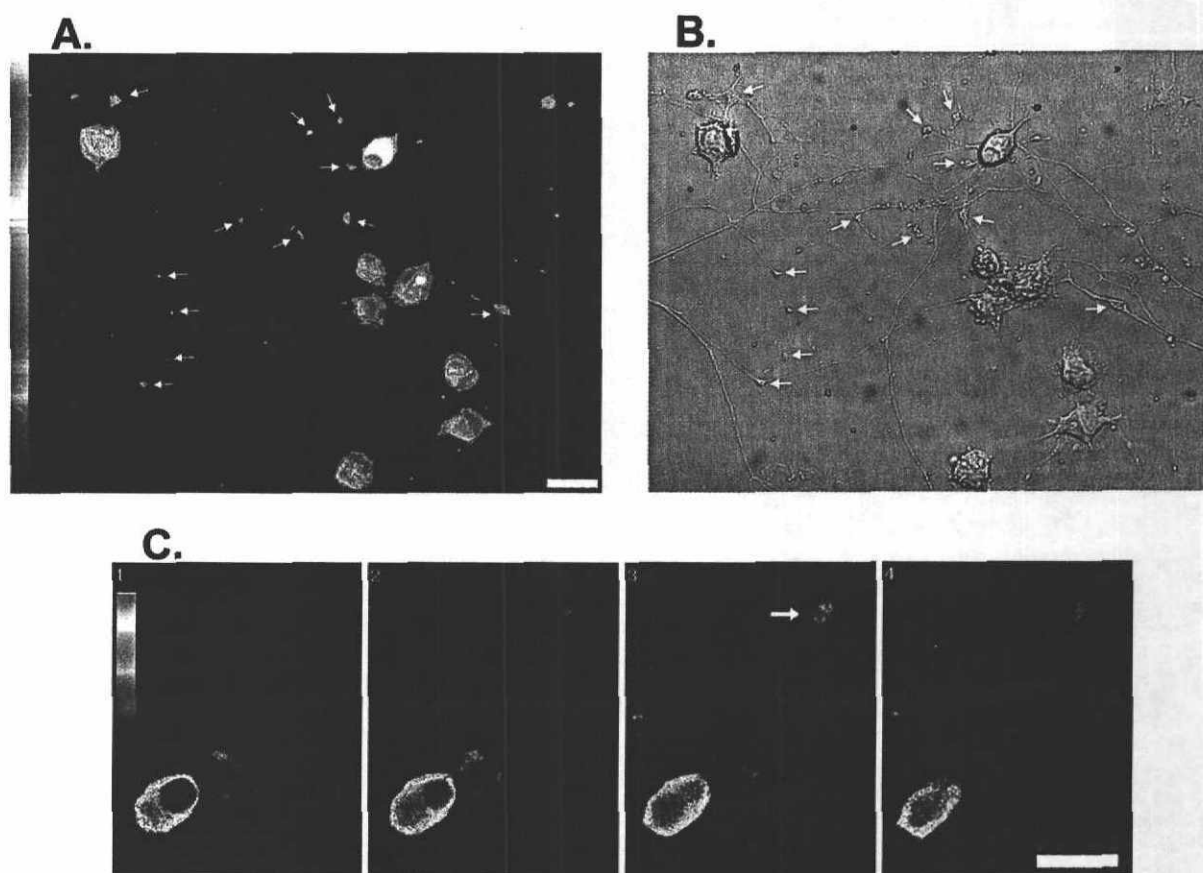


FIG. 4. Localization of VACHT immunoreactivity in SN56 cells. **A:** Confocal image of a field of SN56 cells containing neuritic process that were labeled with VACHT antiserum and FITC-labeled secondary goat anti-rat antibody. Arrows indicate varicosities. Bar = 20 μ m. **B:** Corresponding bright-field image of cells in A. **C1–4:** Confocal Z series of a cell stained for VACHT. Regions of variable fluorescence can be distinguished in the pseudocolored image of the soma. Arrow in slice 3 shows a varicosity from a neuritic process of the same cell. Each optical section is 1.8 μ m apart. Bar = 20 μ m.

body (Fig. 4A and C), but it was not homogeneous, and regions of stronger fluorescence could be readily identified in the pseudocolor image. Note in Fig. 4C, section 1, that fluorescence was absent from the nucleus and that moving the plane of focus further (sections 2–4; every section is 1.8 μ m apart) reveals also immunolabeling of a varicosity (arrow). Overall, most cells were labeled with VACHT antibody, and that was totally prevented by adsorption of the antiserum or omission of the primary antiserum (data not shown). These results suggest that VACHT expressed by SN56 cells reaches varicosities; however, most of the protein in the conditions we studied is present in the cell body, possibly in endosomes, as described before for PC12 cells overexpressing VACHT (Liu and Edwards, 1997).

To test whether this location pattern is common to other synaptic vesicle proteins in SN56 cells, a monoclonal antibody against the synaptic vesicle protein SV2 (Buckley and Kelly, 1985), an anti-peptide antibody against Syt [residues 1–19 (Mundigl et al., 1993)], and a monoclonal antibody against Syp were used. Labeling with the monoclonal antibody against SV2 identified most of the varicosities in SN56 cultures, and the immu-

noreactivity was totally prevented by omission of the primary antibody (data not shown). Indeed, the neurite–cell contacts were much more readily identified with the SV2 antibody than with the other antibodies used in this study. The experiment of Fig. 5A shows a cell immunoreactive for SV2 that contains few growth cones and varicosities. Note that the varicosities in the processes show intense immunolabeling with the SV2 antibody. The pattern of labeling in the soma was distinct from that seen for VACHT (compare Fig. 5A and B). The SV2 antibody (red) usually labeled a localized region that was close to the nucleus, whereas VACHT (green) labeled the cell body less discretely as shown before (Figs. 4 and 5). Superimposition of VACHT and SV2 immunoreactivities shows on Fig. 5A that SV2 antibodies label varicosities strongly, whereas in this example VACHT labeling was not very strong in the varicosities (arrow) compared with the staining in the soma. The series of optical sections of Fig. 5B for another cell gives some insight in the sub-cellular distribution of immunoreactivities. The data indicate that SV2 (red) is surrounded by VACHT (green), as if the former was present mainly in one well-defined compartment toward the middle of the cell.

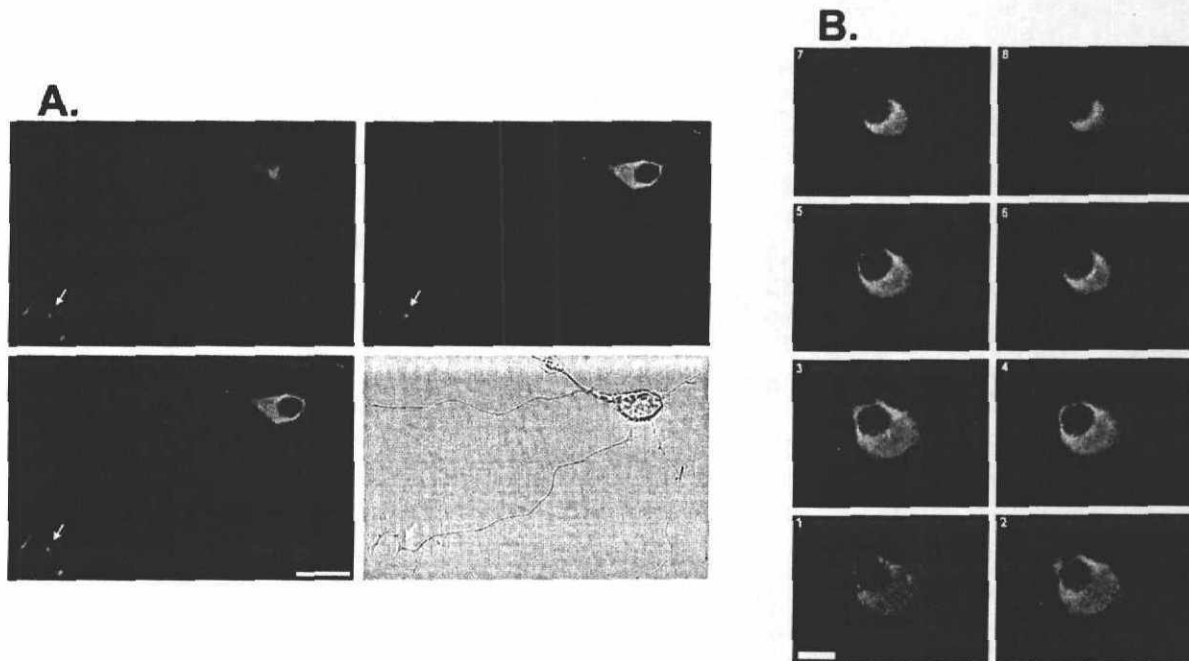


FIG. 5. Localization of VACHT and SV2 in SN56 cells. **A:** Red panel shows an optical section of SN56 cells stained with a monoclonal antibody against SV2 and visualized with secondary goat anti-mouse antibody labeled with Alexa568. Note the discrete immunolocalization of SV2 in the soma and the strong labeling of varicosities and growth cones in the bottom of the image. Green panel shows the same optical section stained with the rabbit anti-VACHT antibody and a secondary FITC-labeled goat anti-rabbit antibody. Note that with the setting used to obtain this image, VACHT immunolabeling of the varicosities is weak compared with that of SV2 (arrow). The two optical sections were obtained simultaneously with the 488 and 568 line of the argon/krypton laser and the proper set of filters. The bottom images show the overlay for SV2 and VACHT immunolabeling and the corresponding bright-field image. Bar = 20 μ m. **B1-8:** Series of optical sections show the combined immunolocalization of VACHT and SV2. A simultaneous Z series of a VACHT- and SV2-immunolabeled cell was acquired with an interval of 0.6 μ m. Note that VACHT immunoreactivity appears to be closer to the cell periphery than SV2 and that the latter is found in a region proximal to the nucleus. Bar = 10 μ m.

In contrast to SV2 labeling, immunostaining with an antibody against Syt appears similar to that observed for VACHT (Fig. 6A). The soma is immunopositive for Syt, with variable levels of fluorescence, and varicosities (arrows) are also positive. Syt immunostaining was blocked by previous adsorption of the antibody with excess of Syt peptide (10 μ g; data not shown). It is interesting that double labeling experiments using antibodies against Syt (Fig. 6C, green) and SV2 (Fig. 6C, red) showed that these proteins seem to be differentially distributed in the soma, similar to what was observed for VACHT and SV2 labeling (Fig. 6C).

We have also investigated where another synaptic vesicle protein, Syp, is localized in SN56 cells. Syp has been shown to be present in endosomes in cultured neurons (Cameron et al., 1991). Indeed, in SN56 cells Syp immunoreactivity, detected with a monoclonal antibody, is found in the soma and varicosities, and its pattern of localization was somewhat similar to those of VACHT and Syt. Figure 7 shows double labeling experiments performed with Syp (red) and VACHT (green) antibodies. There is good colocalization of immunoreactivities for these proteins, which is shown in yellow in the overlay.

The presence of large amounts of synaptic proteins widely distributed in the soma of SN56 cells suggests the

existence of an extensive network of endomembranes therein. To visualize endocytic membranes into the cells, we used the vital dye FM4-64 to label organelles that suffered exocytosis/endocytosis during a period of 16 h. Incubation with FM4-64 labeled the soma, compatible with the presence of large membranous structures in the cell body (Fig. 8). Arrows indicate that some varicosities were also able to incorporate the dye, possibly in endosomal compartments.

DISCUSSION

A putative cDNA coding for VACHT was first isolated from a *Caenorhabditis elegans* mutant, *unc-17* (Alfonso et al., 1993), which presents defective cholinergic transmission and, as a consequence of that, resistance to cholinesterase inhibitors. This earlier work provided the molecular tools to isolate homologous cDNAs from vertebrates (Erickson et al., 1994; Roghani et al., 1994; Varoqui et al., 1994) and to show that this gene coded for a vesamicol-sensitive VACHT (Erickson et al., 1994; Liu and Edwards, 1997; Varoqui and Erickson, 1997). The VACHT gene has a unique genomic organization, and it is present within the first intron of the ChAT gene, in what has been proposed to be a "cholinergic gene locus" (see reviews by Usdin et al., 1995; Eiden, 1998). Regu-

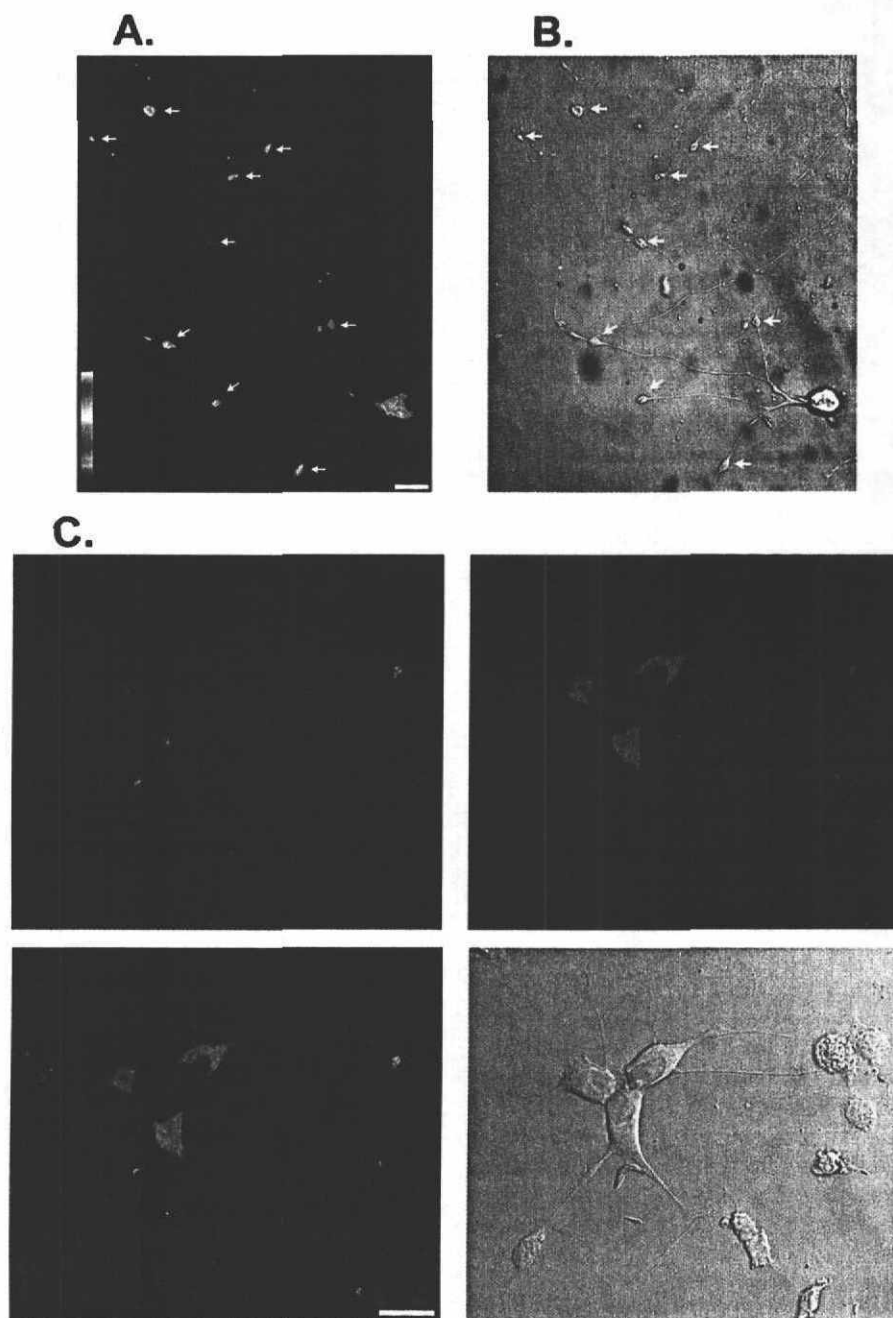


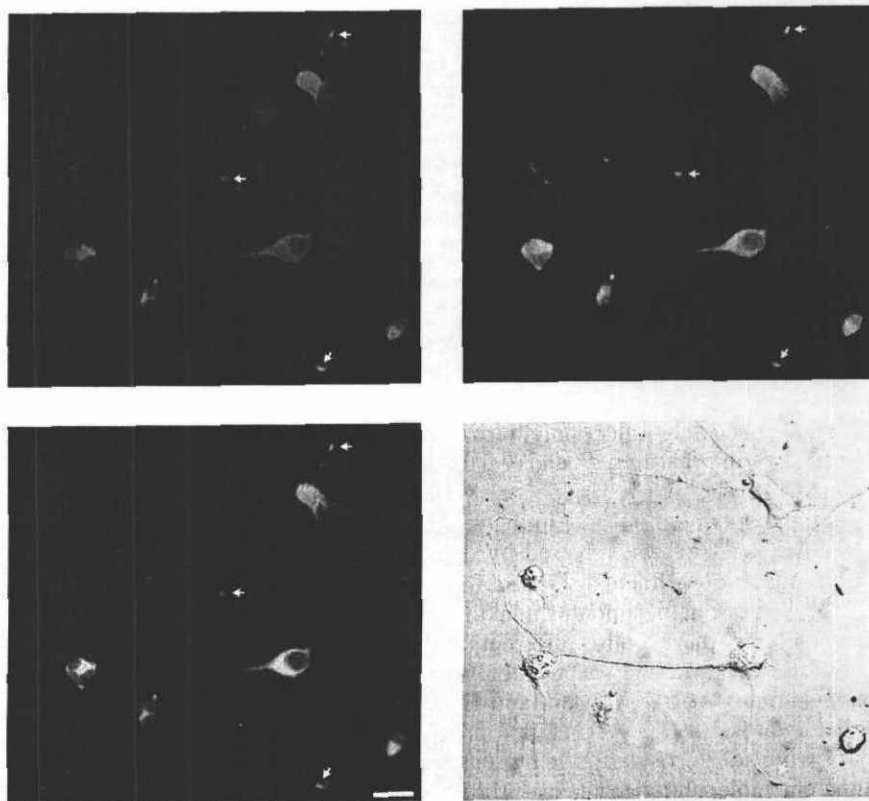
FIG. 6. Immunolocalization of Syt in SN56 cells. **A:** Confocal section of a cell labeled with a rabbit antibody against Syt and an FITC-labeled secondary goat anti-rabbit antibody. Note that immunoreactivity in the soma of the pseudocolored image is not homogeneous. Arrows indicate Syt-positive varicosities. Bar = 20 μ m. **B:** Bright-field image of the same cell in A. **C:** Optical section of cell labeled with SV2 (red, visualized with a secondary antibody coupled to Alexa568) and VACHT (green, visualized with an FITC-labeled secondary antibody) antibodies and the corresponding bright-field image. Note that, again, SV2 immunoreactivity is present in a region closer to nucleus, but in this example, it also appears as some punctated peripheral localization. Bar = 20 μ m.

lation of VACHT expression (Bejanin et al., 1994; Berard et al., 1995; Berse and Blusztajn, 1995; Cervini et al., 1995; Misawa et al., 1995), its sorting to synaptic-like vesicles (Gilmor et al., 1996; Weihe et al., 1996; Varoqui and Erickson, 1998), and regulation of its activity (Noremborg and Parsons, 1989; Van der Kloot, 1991; Barbosa et al., 1997) have all been the focus of extensive research.

SN56 cells may provide an alternative model to study VACHT because the cells should normally express the transporter as an inherited characteristic from their cholinergic parent cell. However, whether VACHT is ex-

pressed by this cell line has not been yet determined. The present experiments have confirmed and extended some of the findings relating SN56 cells to a neuronal phenotype. First, we show that differentiated SN56 cells respond to depolarization by increasing intracellular calcium, and this seems to relate, at least partially, to entry of calcium through P/Q type calcium channels. Two complementary pieces of evidence indicated that this neuronal-type channel is present in the cells in the correct location: (a) blockage of Ca^{2+} concentration increases in the soma and in varicosities of SN56 by ω -Aga IVA and (b) the detection of expression of the $\alpha 1A$

FIG. 7. Colocalization of VAcHT and Syp in SN56 cells, shown in an optical section of cells labeled with a monoclonal antibody against Syp (red) and also with the VAcHT antibody (green) and the corresponding bright-field image. The overlay image shows a similar pattern of labeling for both antibodies (yellow). Arrows indicate some of the varicosities that are immunopositive. Bar = 20 μ m.



subunit of voltage-gated Ca^{2+} channels [which are likely to form P/Q channels (Sather et al., 1993; Stea et al., 1994)] in the cell body and varicosities or growth cones of processes. P/Q calcium channels are generally present in neurons (Westenbroek et al., 1995) where they control neurotransmitter exocytosis (Turner et al., 1992; Mintz et al., 1995; Guatimosim et al., 1997). It is interesting that the parental cell line for SN56, N18TG2, does not seem to express neuronal-type calcium channels (Crawford et

al., 1992). Moreover, 30% of high-voltage-activated calcium currents in neurons of nucleus basalis from guinea pig are sensitive to ω -Aga IVA [P/Q type channels (Williams et al., 1997)], a result somewhat similar to that presently obtained for SN56 cells. Overall, calcium measurements suggest that the cells are viable after differentiation and are able to increase intracellular calcium levels in response to depolarization through a neuronal-type calcium channel. This response occurs also in sites

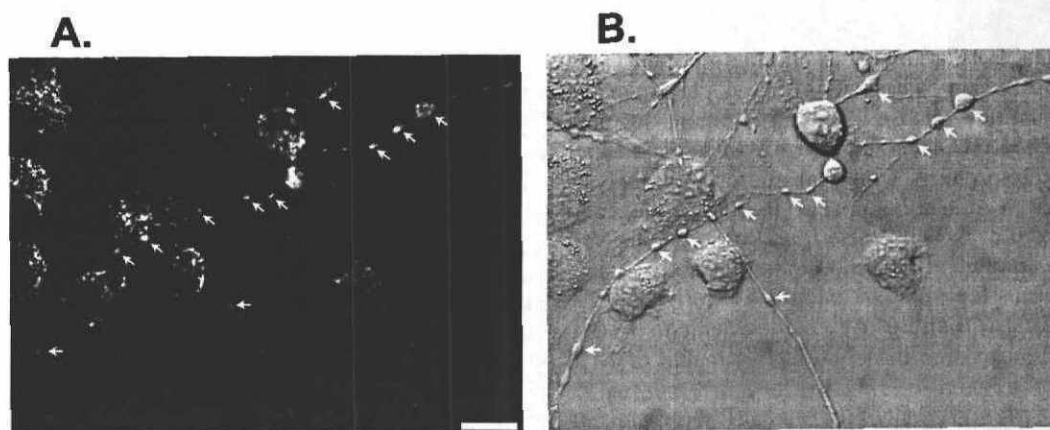


FIG. 8. Labeling of endocytic organelles in SN56 cells by the vital dye FM4-64. **A:** Field of view of SN56 cells labeled with the impermeant membrane dye FM4-64 for 16 h. The cells present staining compatible with the presence of the impermeant dye inside membranous structures. Arrows indicate varicosities that were also able to internalize the dye owing to endocytic activity. **B:** Corresponding bright-field image of the same cells on A. Bar = 20 μ m.

possessing morphological and functional features of relevance for neurotransmitter release, supporting the notion that calcium signaling in these cells is an inherited feature of their cholinergic parental cells.

To study VACHT expression, we first amplified, cloned, and sequenced mouse VACHT (data not shown). Sequence analysis suggested that mouse VACHT is, as expected, very homologous to human and rat VACHT. It is noteworthy that comparison of the mouse sequence obtained in the present study with the published sequence described by Naciff et al. (1997) indicates two amino acid differences: Leu at position 178 and Met at position 497 instead of Phe and Val, respectively. Because the sequences came from distinct mouse strains, the differences may reflect polymorphism of the protein. It is interesting that Leu¹⁷⁸ and Val⁴⁹⁷ are conserved in other mammals.

Immunoprecipitation and immunoblot analysis indicated that VACHT is expressed by differentiated SN56 cells. These experiments showed that VACHT is expressed in reasonable amounts, making the protein easily detectable in these cells, different from native PC12 cells, for example, that express only small amounts of endogenous VACHT (Varoqui and Erickson, 1996; Liu and Edwards, 1997). VACHT is a protein of ~56 kDa, but owing to glycosylation it presents, in SDS gels, an apparent molecular size of 70–80 kDa in brain tissues (Gilmor et al., 1996; Barbosa et al., 1997; Liu and Edwards, 1997). The immunodetected VACHT from SN56 cells also showed an apparent molecular size around 80 kDa. Moreover, the protein migrated similarly to immunodetected VACHT present in mouse spinal cord, suggesting that if there are differences in posttranslational modifications, these do not change the electrophoretic behavior of VACHT. It should be noted that very little, if any, VACHT protein was detected at 39 kDa, as shown before for another neuroblastoma cell line [NG108-15 (Diebler et al., 1998)], which, according to Varoqui and Erickson (1996), corresponds to a deglycosylated form of VACHT. Thus, it seems that although certain neuroblastoma cell lines are unable to process VACHT correctly, the hybrid SN56 is capable of expressing the protein more similarly to cholinergic neurons.

SN56 cells present varicosities that could represent sites of transmitter release. One requirement for that would be the correct localization of VACHT and other synaptic vesicle proteins. Confocal microscopy analysis indicated that VACHT is present in varicosities and growth cones; however, it is also found in soma of SN56 cells in large amounts. In addition, other synaptic vesicle proteins, such as the putative calcium sensor Syt, SV2, and Syp were also found in varicosities, which strongly supports the notion that these sites are capable of ACh release.

The labeling for VACHT in the soma of SN56 appears similar to that found in PC12 cells overexpressing the transporter, consistent with the notion that VACHT is present in endosomes (Liu and Edwards, 1997). VACHT immunolabeling appears to be similar to that of Syt and

Syp in the soma and varicosities. Synaptic vesicle proteins are believed to pass through an endosomal intermediate before reaching mature synaptic vesicles (Johnston et al., 1989; Cameron et al., 1991; Regnier-Vigouroux et al., 1991), which would support the idea that in SN56 cells at least part of the VACHT is present in endosomes in the cell body. Indeed, labeling with FM4-64 has shown that SN56 cells present a large number of endosomal-like structures. This dye has been used as a probe for endocytosis in various preparations and behaves essentially like FM1-43 in labeling endocytic structures (Cochilla et al., 1999). Consistent with that, transfection of a VACHT fluorescently tagged with green fluorescent protein in SN56 cells indicated that VACHT is present in the cell body in organelles that can be labeled with FM4-64 (M. S. Santos et al., manuscript in preparation).

Immunocytochemistry analysis of cholinergic neurons, including those of the basal forebrain in the rat, shows that some cholinergic cell bodies are heavily labeled by VACHT antibodies (Roghani et al., 1998; Schaffer et al., 1998). Thus, cholinergic neurons may also have VACHT in endosomes, and this may be part of the constitutive pathway used by the transporter to reach nerve terminals (see Regnier-Vigouroux et al., 1991; Nakata et al., 1998).

Another possibility is that some VACHT may be present in a storage organelle that could be involved in soma exocytosis. It is noteworthy that some treatments that yield neurochemical differentiation of SN56 cells, i.e., ability to synthesize and release ACh, do not produce morphological differentiation, i.e., formation of synaptic-like contacts (Blusztajn et al., 1992), which would support an active role for VACHT present in the soma. For example, dopamine can be released from the dendrites and cell bodies of midbrain neurons (Kalivas and Duffy, 1993; Heeringa and Abercrombie, 1995), and the vesicular monoamine transporter VMAT2 is found in tubulovesicular organelles in dendrites and soma of dopaminergic cells (Nirenberg et al., 1995; see review by Reimer et al., 1998). Moreover, primary cultured neurons also seem to have robust cell body exocytosis (Maretic-Savatic and Malinow, 1998), which has been suggested to participate in synaptic plasticity.

It is remarkable that SV2, a protein with structural similarities to VACHT and other transporters, shows a distinct pattern of labeling when compared with VACHT, Syt, and Syp. Immunoreactivity in the cell body showed important differences compared with other synaptic vesicle proteins. SV2 immunoreactivity was less distributed in the soma than immunolabeling against other synaptic vesicle proteins, where it appeared to label a defined structure. Although not tested directly, the pattern of labeling by SV2 could represent *trans*-Golgi network (TGN) staining. SV2 is a 12-transmembrane domain protein found in synaptic vesicles and large dense-core vesicles, which has structural features of a transporter (Bajjalieh et al., 1992; Feany et al., 1992; Gingrich et al., 1992), but as far as we are aware no substrate has been

found in nerve endings that is transported by SV2. Immunoelectron microscopy analysis indicates that when the subcellular distribution of SV2 is compared with that of Syp, it presents a ratio of 9:1 in granules (SV2 to Syp) and 1:1 in synaptic-like vesicles from nerve growth factor-treated PC12 cells (Tanner et al., 1996). These results suggest that SV2 may in fact show differences in targeting to secretory vesicles when compared with other synaptic vesicle proteins. Indeed, transfection of Chinese hamster ovary cells with SV2 cDNA shows that the protein sorts to a population of large vesicles distinct from endosomes (Feany et al., 1993). Inasmuch as the location of SV2 in the TGN is a speculative suggestion, sorting of proteins to large dense-core granules occurs at the TGN (see reviews by Tooze, 1991, 1998), which would then favor the notion that SV2 is present in dense vesicles in SN56 cells. Electron microscopy analysis has indicated the presence of such secretory organelles in SN cell lines, as well as small clear synaptic-like vesicles that are found in varicosities (Hammond et al., 1990).

Another interesting aspect of sorting of SV2 comes from investigations of synaptic vesicle precursors trafficking in axons by the kinesin superfamily of proteins. Hirokawa and collaborators (Okada et al., 1995) have shown that although most of the synaptic vesicle proteins use KIF1a (a member of this kinesin superfamily), SV2 and membrane proteins appear to be transported to axonal tips by another motor protein, which would support the idea of distinct intermediates in trafficking for SV2 and other synaptic vesicle proteins. Thus, the present results showing that SV2 antibody labels varicosities and growth cones, as do other synaptic vesicle proteins, but does not stain the same cytoplasmic structures agree with these previous reports.

SN56 cells synthesize and release endogenous ACh (Blusztajn et al., 1992) and several synaptic proteins, such as calcium channels and synaptic vesicle proteins, including VACHT, Syp, SV2, and Syp, are present in their varicosities, suggesting that varicosities may have a population of functional synaptic vesicles and endocytic organelles, as seen in ultrastructural studies of other SN lines (Hammond et al., 1990). The distribution of distinct synaptic vesicle proteins in different cellular compartments suggests that SN56 cells may provide an alternative paradigm to study the genesis of small synaptic vesicles, molecular determinants of neuronal polarity, and the trafficking of synaptic vesicle proteins to sites of ACh storage and release.

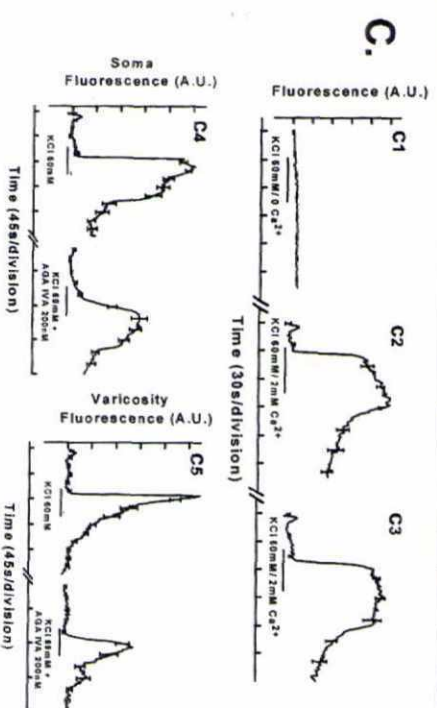
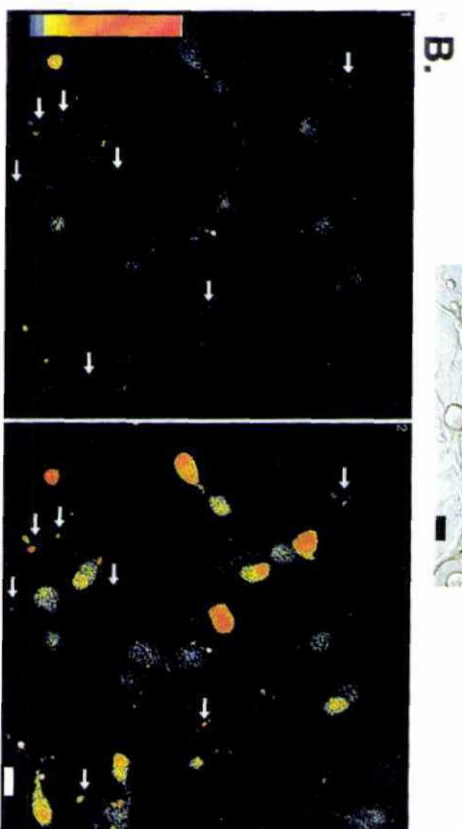
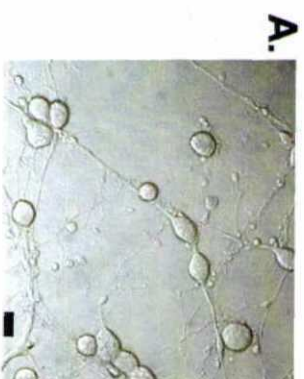
Acknowledgment: We wish to thank CAPES, CNPq, PADCT, PRONEX, FINEP, and PRPq-UFMG for financial support. We also thank Prof. Bruce Wainer for his generous gift of SN56 cells and Dr. S. Bajjalieh for the SV2 antibody. The technical help of Ms. A. Pereira and A. Guimaraes is appreciated. We also acknowledge Dr. Alain Beaudet (Montreal Neurological Institute) for help with immunofluorescence and several discussions.

REFERENCES

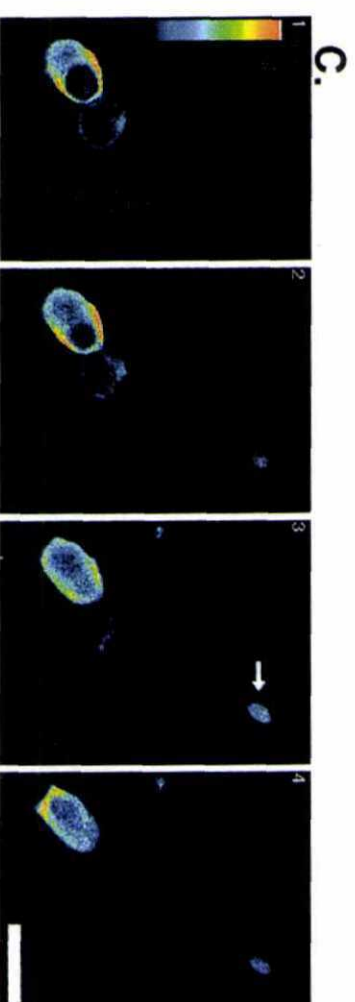
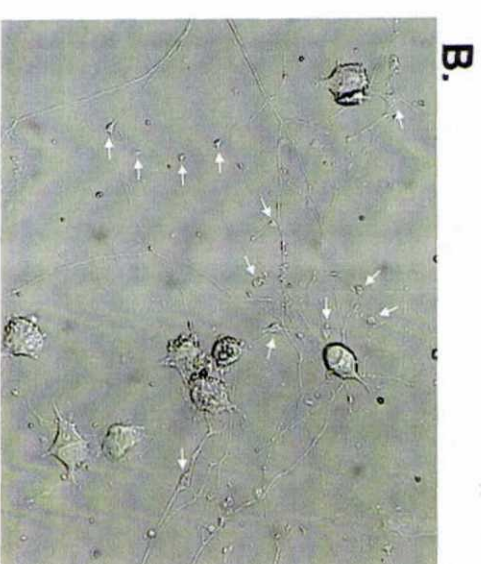
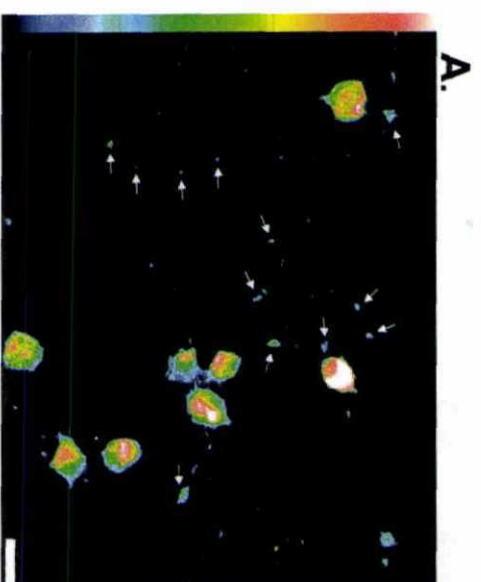
- Alfonso A., Grundahl K., Duerr J. S., Han H.-P., and Rand J. B. (1993) The *Caenorhabditis elegans unc-17* gene: a putative vesicular acetylcholine transporter. *Science* **261**, 617–619.
- Bajjalieh S. M., Peterson K., Shinghal R., and Scheller R. H. (1992) SV2, a brain synaptic vesicle protein homologous to bacterial transporters. *Science* **257**, 1271–1273.
- Barbosa J. Jr., Clarizia A. D., Gomez M. V., Romano-Silva M. A., Prado V. F., and Prado M. A. M. (1997) Effects of protein kinase C activation on the release of [³H]acetylcholine in the presence of vesamicol. *J. Neurochem.* **69**, 2608–2611.
- Bejanin S., Cervini R., Mallet J., and Berrard S. (1994) A unique gene organization for two cholinergic markers, choline acetyltransferase and a putative vesicular transporter of acetylcholine. *J. Biol. Chem.* **269**, 21944–21947.
- Berrard S., Varoqui H., Cervini R., Israël M., Mallet J., and Diebler M. F. (1995) Coregulation of two embedded gene products, choline acetyltransferase and the vesicular acetylcholine transporter. *J. Neurochem.* **65**, 939–942.
- Berse B. and Blusztajn J. K. (1995) Coordinated up-regulation of choline acetyltransferase and vesicular acetylcholine transporter gene expression by the retinoic acid receptor α , cAMP, and leukemia inhibitory factor/ciliary neurotrophic factor signaling pathways in a murine septal cell line. *J. Biol. Chem.* **270**, 22101–22104.
- Blusztajn J. K., Venturini A., Jackson D. A., Lee H. J., and Wainer B. H. (1992) Acetylcholine synthesis and release is enhanced by dibutyryl cyclic AMP in a neuronal cell line derived from mouse septum. *J. Neurosci.* **12**, 793–799.
- Buckley K. and Kelly R. B. (1985) Identification of a transmembrane glycoprotein specific for secretory vesicles of neural and endocrine cells. *J. Cell Biol.* **100**, 1284–1294.
- Cameron P. L., Sudhof T. C., Jahn R., and De Camilli P. (1991) Colocalization of synaptophysin with transferrin receptors: implications for synaptic vesicle biogenesis. *J. Cell Biol.* **115**, 151–164.
- Cervini R., Houhou L., Pradat P.-F., Bejanin S., Mallet J., and Berrard S. (1995) Specific vesicular acetylcholine transporter promoters lie within the first intron of the rat choline acetyltransferase gene. *J. Biol. Chem.* **270**, 24654–24657.
- Cochilla A. J., Angleson J. K., and Betz W. J. (1999) Monitoring secretory membrane with FM1–43 fluorescence. *Annu. Rev. Neurosci.* **22**, 1–10.
- Colom L. V., Diaz M. E., Beers D. R., Neely A., Xie W. J., and Appel S. H. (1998) Role of potassium channels in amyloid-induced cell death. *J. Neurochem.* **70**, 1925–1934.
- Crawford G. D. Jr., Le W. D., Smith R. G., Xie W. J., Stefani E., and Appel S. H. (1992) A novel N18TG2 \times mesencephalon cell hybrid expresses properties that suggest a dopaminergic cell line of substantia nigra origin. *J. Neurosci.* **12**, 3392–3398.
- Diebler M. F., Tomasi M., Meunier F. M., Israël M., and Dolezal V. (1998) Influence of retinoic acid and of cyclic AMP on the expression of choline acetyltransferase and of vesicular acetylcholine transporter in NG108–15 cells. *J. Physiol. (Paris)* **92**, 379–384.
- Eiden L. E. (1998) The cholinergic gene locus. *J. Neurochem.* **70**, 2227–2240.
- Erickson J. D., Varoqui H., Schäfer M. K.-H., Modi W., Diebler M.-F., Weihe E., Eiden L. E., Bonner T. I., and Usdin T. B. (1994) Functional identification of a vesicular acetylcholine transporter and its expression from a 'cholinergic' gene locus. *J. Biol. Chem.* **269**, 21929–21932.
- Feany M. B., Lee S., Edwards R. H., and Buckley K. M. (1992) The synaptic vesicle protein SV2 is a novel type of transmembrane transporter. *Cell* **70**, 861–867.
- Feany M. B., Yee A. G., Delvy M. L., and Buckley K. M. (1993) The synaptic vesicle proteins SV2, synaptotagmin and synaptophysin are sorted to separate cellular compartments in CHO fibroblasts. *J. Cell Biol.* **123**, 575–584.
- Ferguson S. S., Menard L., Barak L. S., Koch W. J., Colapietro A. M., and Caron M. G. (1995) Role of phosphorylation in agonist-promoted beta 2-adrenergic receptor sequestration. Rescue of a

- sequestration-defective mutant receptor by beta ARK1. *J. Biol. Chem.* **270**, 24782–24789.
- Gilmor M. L., Nash N. R., Roghani A., Edwards R. H., Yi H., Hersch S. M., and Levey A. I. (1996) Expression of the putative vesicular acetylcholine transporter in rat brain and localization in cholinergic synaptic vesicles. *J. Neurosci.* **16**, 2179–2190.
- Gingrich J. A., Andersen P. H., Tiberi M., El Mestikawy S., Jorgensen P. N., Freneau R. T. Jr., and Caron M. G. (1992) Identification, characterization, and molecular cloning of a novel transporter-like protein localized to the central nervous system. *FEBS Lett.* **312**, 115–122.
- Guatimosim C., Romano-Silva M. A., Cruz J. S., Beirão P. S., Kalapothakis E., Moraes-Santos T., Cordeiro M. N., Diniz C. R., Gomez M. V., and Prado M. A. (1997) A toxin from the spider *Phoneutria nigriventer* that blocks calcium channels coupled to exocytosis. *Br. J. Pharmacol.* **122**, 591–597.
- Hammond D. N., Lee H. J., Tongard J. H., and Wainer B. H. (1990) Development and characterization of clonal cell lines derived from septal cholinergic neurons. *Brain Res.* **512**, 190–200.
- Hamprecht B. (1977) Structural, electrophysiological, biochemical, and pharmacological properties of neuroblastoma–glioma cell hybrids in cell culture. *Int. Rev. Cytol.* **49**, 99–170.
- Heeringa M. J. and Abercrombie E. D. (1995) Biochemistry of somatodendritic dopamine release in substantia nigra: an in vivo comparison with striatal dopamine release. *J. Neurochem.* **65**, 192–200.
- Johnston P. A., Cameron P. L., Stukenbrok H., Jahn R., De Camilli P., and Südhof T. C. (1989) Synaptophysin is targeted to similar microvesicles in CHO and PC12 cells. *EMBO J.* **8**, 2863–2872.
- Kalivas P. W. and Duffy P. (1993) Time course of extracellular dopamine and behavioral sensitization to cocaine. II. Dopamine perikarya. *J. Neurosci.* **13**, 276–284.
- Kushmerick C., Kalapothakis E., Beirão P. S. L., Penaforte C. L., Prado V. F., Cruz J. S., Diniz C. R., Cordeiro M. N., Gomez M. V., Romano-Silva M. A., and Prado M. A. M. (1999) *Phoneutria nigriventer* toxin Tx3-1 blocks A-type K⁺ currents controlling Ca²⁺ oscillation frequency in GH₃ cells. *J. Neurochem.* **72**, 1472–1481.
- Le W. D., Xie W. J., Kong R., and Appel S. H. (1997) β -Amyloid-induced neurotoxicity of a hybrid septal cell line associated with increased tau phosphorylation and expression of β -amyloid precursor protein. *J. Neurochem.* **69**, 978–985.
- Lee H. J., Hammond D. N., Large T. H., and Wainer B. H. (1990) Immortalized young adult neurons from the septal region: generation and characterization. *Brain Res. Dev. Brain Res.* **52**, 219–228.
- Liu Y. and Edwards R. H. (1997) Differential localization of vesicular acetylcholine and monoamine transporters in PC12 cells but not CHO cells. *J. Cell Biol.* **139**, 907–916.
- Maletic-Savatic M. and Malinow R. (1998) Calcium-evoked dendritic exocytosis in cultured hippocampal neurons. Part I: *trans*-Golgi network-derived organelles undergo regulated exocytosis. *J. Neurosci.* **18**, 6803–6813.
- McGee R. Jr. (1980) Choline uptake by the neuroblastoma \times glioma hybrid, NG108–15. *J. Neurochem.* **35**, 829–837.
- McGee R., Simpson P., Christian C., Mata M., Nelson P., and Nirenberg M. (1978) Regulation of acetylcholine release from neuroblastoma \times glioma hybrid cells. *Proc. Natl. Acad. Sci. USA* **75**, 1314–1318.
- Mintz J. M., Sabatini B. L., and Regehr W. G. (1995) Calcium control of transmitter release at a cerebellar synapse. *Neuron* **15**, 675–688.
- Misawa H., Takahashi R., and Deguchi T. (1995) Coordinate expression of vesicular acetylcholine transporter and choline acetyltransferase in sympathetic superior cervical neurones. *Neuroreport* **7**, 965–968.
- Mundigl O., Matteoli M., Daniell L., Thomas-Reetz A., Metcalf A., Jahn R., and De Camilli P. (1993) Synaptic vesicle proteins and early endosomes in cultured hippocampal neurons: differential effects of brefeldin A in axon and dendrites. *J. Cell Biol.* **122**, 1207–1221.
- Naciff J. M., Misawa H., and Dedman J. R. (1997) Molecular characterization of the mouse vesicular acetylcholine transporter gene. *Neuroreport* **8**, 3467–3473.
- Nakata T., Terada S., and Hirokawa N. J. (1998) Visualization of the dynamics of synaptic vesicle and plasma membrane proteins in living axons. *J. Cell Biol.* **140**, 659–674.
- Nirenberg M. J., Liu Y., Peter D., Edwards R. H., and Pickel V. M. (1995) The vesicular monoamine transporter 2 is present in small synaptic vesicles and preferentially localizes to large dense core vesicles in rat solitary tract nuclei. *Proc. Natl. Acad. Sci. USA* **92**, 8773–8777.
- Norenberg K. and Parsons S. M. (1989) Regulation of the vesamicol receptor in cholinergic synaptic vesicles by acetylcholine and an endogenous factor. *J. Neurochem.* **52**, 913–920.
- Okada Y., Yamazaki H., Sekine-Aizawa Y., and Hirokawa N. (1995) The neuron-specific kinesin superfamily protein KIF1A is a unique monomeric motor for anterograde axonal transport of synaptic vesicle precursors. *Cell* **81**, 769–780.
- Pedersen W. A., Berse B., Schüler U., Wainer B. H., and Blusztajn J. K. (1995) All-*trans*- and 9-*cis*-retinoic acid enhance the cholinergic properties of a murine septal cell line: evidence that the effects are mediated by activation of retinoic acid receptor- α . *J. Neurochem.* **65**, 50–58.
- Pedersen W. A., Kloczewiak M. A., and Blusztajn J. K. (1996) Amyloid beta-protein reduces acetylcholine synthesis in a cell line derived from cholinergic neurons of the basal forebrain. *Proc. Natl. Acad. Sci. USA* **93**, 8068–8071.
- Regnier-Vigouroux A., Tooze S. A., and Hüttner W. B. (1991) Newly synthesized synaptophysin is transported to synaptic-like microvesicles via constitutive secretory vesicles and the plasma membrane. *EMBO J.* **10**, 3589–3601.
- Reimer R. J., Fon E. A., and Edwards R. H. (1998) Vesicular neurotransmitter transport and the presynaptic regulation of quantal size. *Curr. Opin. Neurobiol.* **8**, 405–412.
- Roghani A., Feldman J., Kohan S. A., Shirzadi A., Gundersen C. B., Brecha N., and Edwards R. H. (1994) Molecular cloning of a putative vesicular transporter for acetylcholine. *Proc. Natl. Acad. Sci. USA* **91**, 10620–10624.
- Roghani A., Shirzadi A., Butcher L. L., and Edwards R. H. (1998) Distribution of the vesicular transporter for acetylcholine in the rat central nervous system. *Neuroscience* **82**, 1195–1212.
- Sather W. A., Tanabe T., Zhang J. F., Mori Y., Adams M. E., and Tsien R. W. (1993) Distinctive biophysical and pharmacological properties of class A (B1) calcium channel α 1 subunits. *Neuron* **11**, 291–303.
- Schafer M. K., Eiden L. E., and Weihe E. (1998) Cholinergic neurons and terminal fields revealed by immunohistochemistry for the vesicular acetylcholine transporter. I. Central nervous system. *Neuroscience* **84**, 331–359.
- Song H., Ming G., Fon E., Bellocchio E., Edwards R. H., and Poo M. (1997) Expression of a putative vesicular acetylcholine transporter facilitates quantal transmitter packaging. *Neuron* **18**, 815–826.
- Stein A., Tomlinson W. J., Soong T. W., Bourinet E., Dubel S. J., Vincent S. R., and Snutch T. P. (1994) Localization and functional properties of a rat brain α 1A calcium channel reflect similarities to neuronal Q- and P-type channels. *Proc. Natl. Acad. Sci. USA* **91**, 10576–10580.
- Tan P. K., Waites C., Liu Y., Krantz D. E., and Edwards R. H. (1998) A leucine-based motif mediates the endocytosis of vesicular monoamine and acetylcholine transporters. *J. Biol. Chem.* **273**, 17351–17360.
- Tanner V. A., Ploug T., and Tao-Cheng J. H. (1996) Subcellular localization of SV2 and other secretory vesicle components in PC12 cells by an efficient method of preembedding EM immunocytochemistry for cell cultures. *J. Histochem. Cytochem.* **44**, 1481–1488.
- Tooze S. A. (1991) Biogenesis of secretory granules. Implications arising from the immature secretory granule in the regulated pathway of secretion. *FEBS Lett.* **285**, 220–224.
- Tooze S. A. (1998) Biogenesis of secretory granules in the *trans*-Golgi network of neuroendocrine and endocrine cells. *Biochim. Biophys. Acta* **1404**, 231–244.
- Towbin H., Staehelin T., and Gordon J. (1979) Electrophoretic transfer of proteins from polyacrylamide gels to nitrocellulose sheets:

- procedure and some applications. *Proc. Natl. Acad. Sci. USA* **76**, 4350–4354.
- Turner T. J., Adams M. E., and Dunlap K. (1992) Calcium channels coupled to glutamate release identified by omega-Aga-IVA. *Science* **258**, 310–313.
- Usdin T. B., Eiden L. E., Bonner T. I., and Erickson J. D. (1995) Molecular biology of the vesicular ACh transporter. *Trends Neurosci.* **18**, 218–224.
- Van der Kloot W. (1991) Down-regulation of quantal size at frog neuromuscular junctions: possible roles for elevated intracellular calcium and for protein kinase C. *J. Neurobiol.* **22**, 204–214.
- Varoqui H. and Erickson J. D. (1996) Active transport of acetylcholine by the human vesicular acetylcholine transporter. *J. Biol. Chem.* **271**, 27229–27232.
- Varoqui H. and Erickson J. D. (1997) Vesicular neurotransmitter transporters. Potential sites for the regulation of synaptic function. *Mol. Neurobiol.* **15**, 165–191.
- Varoqui H. and Erickson J. D. (1998) The cytoplasmic tail of the vesicular acetylcholine transporter contains a synaptic vesicle targeting signal. *J. Biol. Chem.* **273**, 9094–9098.
- Varoqui H., Diebler M.-F., Meunier F.-M., Rand J. B., Usdin T. B., Bonner T. I., Eiden L. E., and Erickson J. D. (1994) Cloning and expression of the vesamicol binding protein from the marine ray *Torpedo*. Homology with the putative vesicular acetylcholine transporter UNC-17 from *Caenorhabditis elegans*. *FEBS Lett.* **342**, 97–102.
- Weihe E., Tao-Cheng J.-H., Schäfer M. K.-H., Erickson J. D., and Eiden L. E. (1996) Visualization of the vesicular acetylcholine transporter in cholinergic nerve terminals and its targeting to a specific population of small synaptic vesicles. *Proc. Natl. Acad. Sci. USA* **93**, 3547–3552.
- Westenbroek R. E., Sakurai T., Elliott E. M., Hell J. W., Starr T. V., Snutch T. P., and Catterall W. A. (1995) Immunochemical identification and subcellular distribution of the alpha 1A subunits of brain calcium channels. *J. Neurosci.* **15**, 6403–6418.
- Williams S., Serafin M., Muhlethaler M., and Bernheim L. (1997) Facilitation of N-type calcium current is dependent on the frequency of action potential-like depolarizations in dissociated cholinergic basal forebrain neurons of the guinea pig. *J. Neurosci.* **17**, 1625–1632.

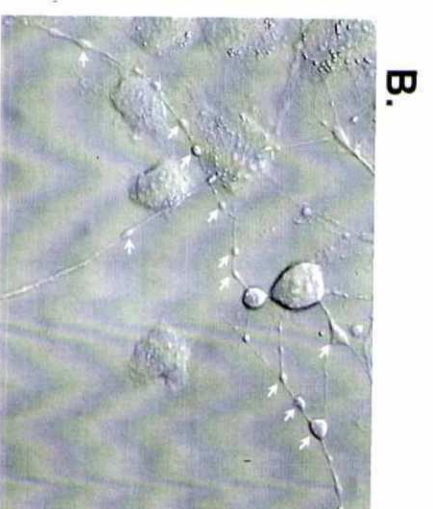
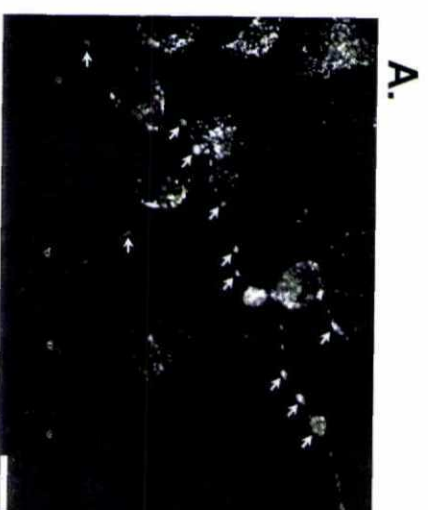


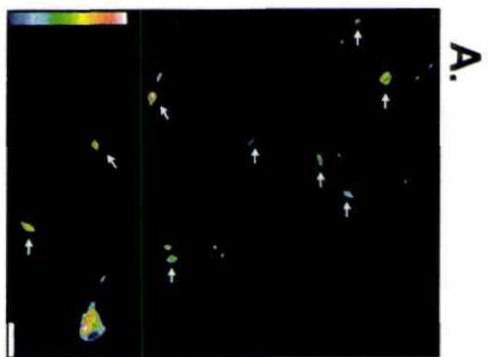
1h1190629001



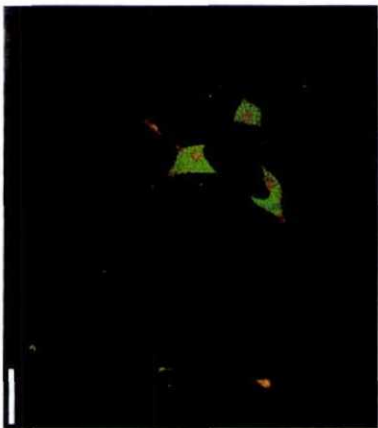
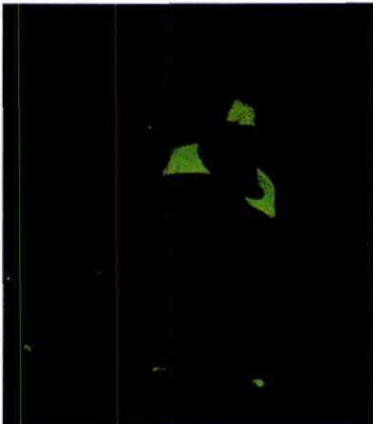
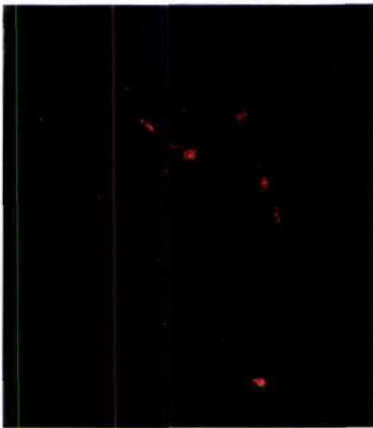
1h1190629004

1h1190629008

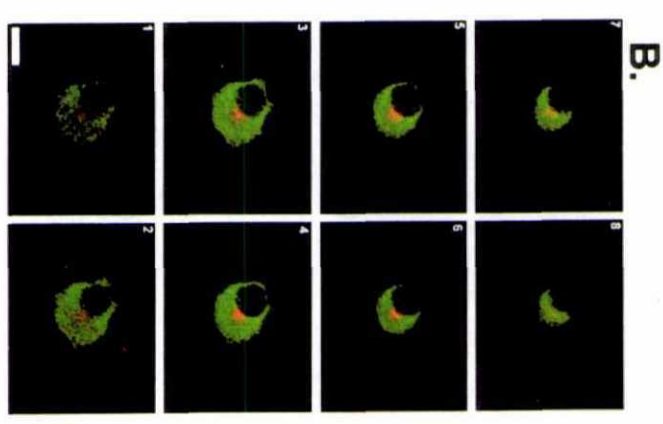
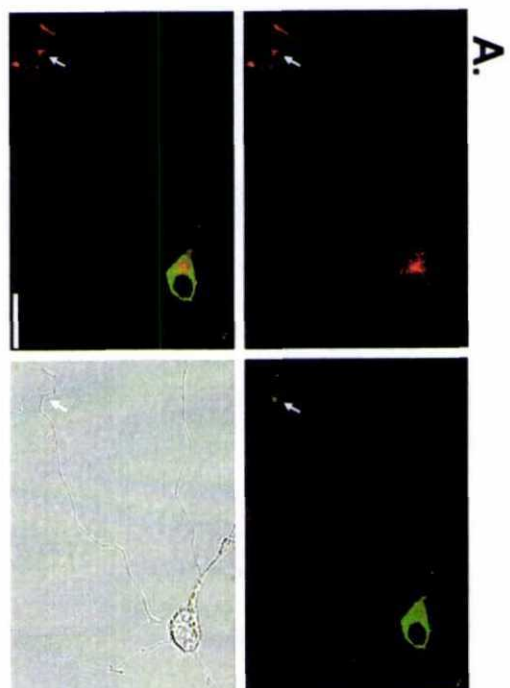
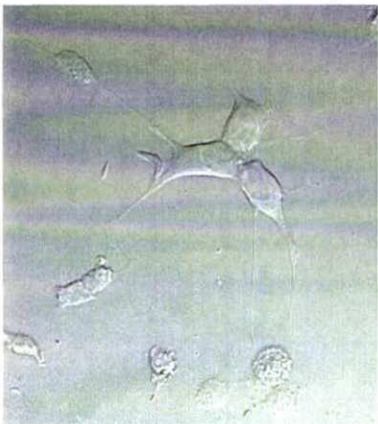




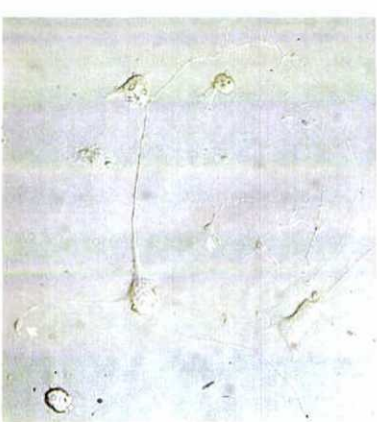
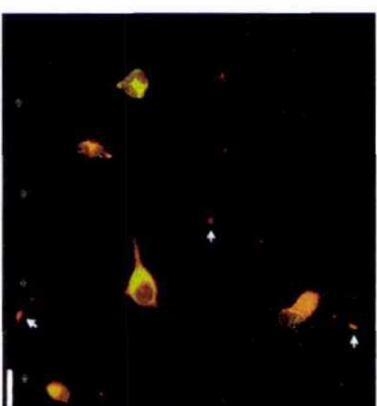
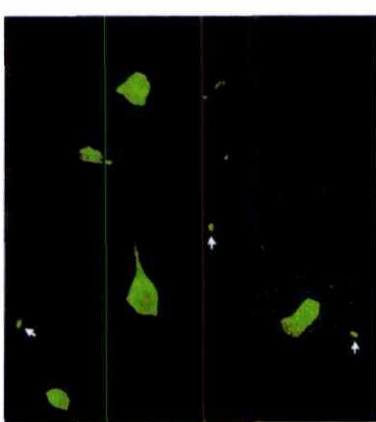
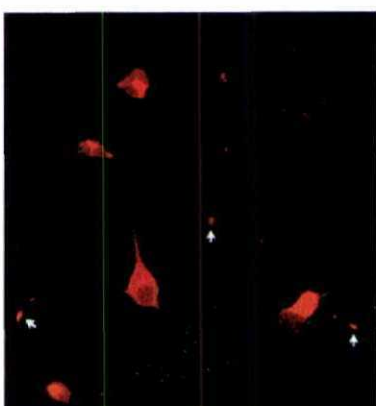
C.



1h1190629006



1h1190



1h1190629007

4-AMINOZENOVESAMICOL was used to test whether activation of protein kinase C protects the vesicular acetylcholine transporter from interaction with vesamicol-like drugs. The essentially irreversible vesamicol analog inhibits the release of newly synthesized [^3H]acetylcholine from stimulated hippocampal slices. Prior activation of protein kinase C with a phorbol ester prevented the inhibition of [^3H]acetylcholine release, but activation of protein kinase C after the exposure to the irreversible analog did not prevent the effect of the drug. Binding of 4-aminobenzenovesamicol in hippocampal synaptosomes, assayed using [^3H]vesamicol and back-titration, was decreased by activation of protein kinase C prior to analog exposure but not by activation subsequent to exposure. We propose that phosphorylation of the vesicular acetylcholine transporter prevents the binding of vesamicol-like drugs. *NeuroReport* 10:2783–2787 © 1999 Lippincott Williams & Wilkins.

Key words: Acetylcholine; Acetylcholine storage; Synaptic vesicles; Vesamicol; Vesicular acetylcholine transporter

Control of the binding of a vesamicol analog to the vesicular acetylcholine transporter

Alessandra D. Clarizia,
Marcus V. Gomez,
Marco A. Romano-Silva,
Stanley M. Parsons,¹ Vania F. Prado²
and Marco A. M. Prado^{CA}

Laboratório de Neurofarmacologia, Departamentos de Farmacologia ²e Bioquímica-Imunologia, ICB, Universidade Federal de Minas Gerais, Av. Antonio Carlos, 6627, Belo Horizonte, Minas Gerais, Brazil 31270-901; ¹Department of Chemistry, University of California, Santa Barbara, CA 93106, USA

^{CA}Corresponding Author

Introduction

Synaptic communication depends on the concerted action of many proteins to trigger exocytosis of neurotransmitter-loaded synaptic vesicles. The accumulation of transmitter into vesicles determines how much of the chemical mediator a given vesicle will release, and thus is of relevance for proper synaptic communication in the nervous system. Storage of acetylcholine (ACh) by synaptic vesicles depends on the activity of a vesicular acetylcholine transporter (VACHT), which uses a proton electrochemical gradient to move ACh to the inside of the organelle [1–3]. Inhibition of the transporter by drugs such as vesamicol has shown that ACh storage is critical for maintenance of ACh release during prolonged stimulation [1,4].

Experiments by Van der Kloot [5–7] demonstrate that the size of ACh quanta can be pharmacologically increased, apparently by manipulation of second-messenger levels and protein kinase activity. Pharmacological manipulation of protein phosphatase activity can also affect the amount of ACh present in synaptic vesicles [8]. Over-expression of VACHT by immature *Xenopus* motoneurons increases quantal size several-fold [9]. Thus, quantal

size is variable, and the plasticity in quantal size has been linked to VACHT in at least one circumstance. Regulation of VACHT might control synaptic strength.

We recently showed that VACHT is phosphorylated in hippocampal synaptosomes and that the phosphorylation level increases in response to activation of protein kinase C (PKC) [10]. Indeed, the deduced amino acid sequence of VACHT indicates a region of consensus for PKC phosphorylation (Ser-480) [11,12]. The vesicular monoamine transporter (VMAT) has also been shown to be phosphorylated [13].

The role of VACHT phosphorylation in the storage of ACh is not yet clear. Previous experiments demonstrated that vesamicol-treated cholinergic terminals, which normally fail to release ACh in response to stimulation, can become release-competent by activation of PKC, as if phosphorylation could interfere with the ability of vesamicol to block ACh transport [10,14]. The present study provides a more robust test of this possibility by use of the essentially irreversible vesamicol analog 4-aminobenzenovesamicol (ABV) [15,16]. We also measured [^3H]vesamicol binding sites in membranes prepared from manipulated synaptosomes to assess whether

PKC activation blocks the binding of vesamicol-like drugs to VACHT. Our results suggest that prior PKC activation prevents ABV blockade of ACh storage by preventing binding of ABV to VACHT.

Materials and Methods

[³H]vesamicol (35 Ci/mmol), and [³H-methyl]choline (60–90 Ci/mmol) were from New England Nuclear, a division of DuPont, Inc. (USA). Percoll and diethyl *p*-nitrophenylphosphate (paraoxon) were from Sigma Chemical Co. (USA). Phorbol myristate acetate (PMA), and α -PMA were from Research Biochemicals International (USA). Vesamicol and ABV were synthesized as described [17]. All other chemicals and reagents were of analytical grade obtained from usual commercial sources.

Rat brain hippocampal slices: Animal use was in accordance with the guidelines of the Brazilian Research Council (CNPq), and the procedures were approved by the local Animal Care Committee in Brazil. Wistar rats of both sexes (180–200 g) were decapitated. Their hippocampi were removed and put in ice-cold medium (see below) immediately. Slices (300 μ m) were obtained with a McIlwain tissue chopper.

Release of [³H]ACh from rat brain hippocampal slices: The release of [³H]ACh was followed after labeling hippocampal slices with [³H]choline chloride, essentially as described [10,16] at 37°C. When the action of ABV was examined the drug was added to slices 15 min prior to incubation with [³H]choline. In these conditions, ABV does not alter the uptake of [³H]choline [16]. After incubation with [³H]choline, the slices were washed twice before stimulation at 15 Hz through a platinum electrode (field stimulation, square wave pulses, 10 V/cm, 0.5 ms). Since ABV affects VACHT in an essentially irreversible way [15,16] the drug did not need to be maintained in the incubation medium during the stimulation period to block ACh release. Slices were separated from the incubation medium by centrifugation, and [³H]ACh in the supernatant was separated and measured as described [16] by extraction with tetraphenylboron in 3-heptanone and the choline kinase assay. The incubation medium contained (in mM) 124 NaCl, 4 KCl, 1.2 MgSO₄, 2 CaCl₂, 10 glucose, 25 Hepes, pH 7.4 with NaOH and 20 μ M paraoxon to prevent hydrolysis of [³H]ACh.

Purification of hippocampal synaptosomes and binding of [³H]vesamicol: Hippocampal synaptosomes were isolated from an S1 fraction of homogenized

hippocampi by discontinuous Percoll density gradient centrifugation [18] as described [19]. In order to determine whether PKC activation interfered with ABV (and consequently vesamicol) binding, we sought to design an experiment that would reproduce the conditions used for the experiments that investigated the release of newly synthesized transmitter. Moreover, it was of interest to use conditions that have been previously determined to increase the phosphorylation of VACHT [10]. Therefore, [³H]vesamicol binding was carried out in the following way to investigate the role of PKC on ABV binding. First, synaptosomes (~600 μ g determined in preliminary experiments to be optimal for specific binding of [³H]-vesamicol) were incubated with PMA (200 nM), α -PMA (200 nM) or no drugs for 15 min and then ABV (1 μ M) was added for a further 15 min when necessary. In one of the protocols ABV was added before the treatment with PMA. Since the binding of ABV is irreversible for the time period of this experiment [15] the results should reveal the sensitivity of VACHT to ABV in intact synaptosomes. The binding sites remaining after the treatments above could be determined with [³H]-vesamicol (100 nM). After the incubation with ABV, synaptosomes were then separated from the incubation medium by centrifugation and were resuspended in 10 mM Tris (pH 7.4 with HCl) containing 2 mM of CHAPS in a homogenizer, with the objective of disrupting the nerve terminals. The synaptosomal extract was then incubated for 40 min (room temperature) with 100 nM of [³H]vesamicol, and bound vesamicol was separated from the free drug by filtration through GF/F filters previously treated with polyethylenimine (1%). Non-specific binding was determined in the presence of 30 μ M (–)-vesamicol. The K_d for [³H]vesamicol in synaptosomal extracts was obtained similarly as above, but without the pretreatments with drugs. The extract was incubated with increasing concentrations of [³H]vesamicol and the experiment performed as above. The data were plotted using Sigmaplot and the K_d obtained by computer-assisted regression (hyperbolic fit).

Results

Hippocampal slices release newly synthesized [³H]ACh upon stimulation (15 Hz, 5 min), and the amount of evoked release is several-fold higher than the basal release (Fig. 1A). Previous work has shown that vesamicol blocks evoked release of newly synthesized [³H]ACh by blocking storage and the phorbol ester PMA prevents the vesamicol effect. The effect of PMA is due to activation of PKC and has been suggested to be related to phosphorylation

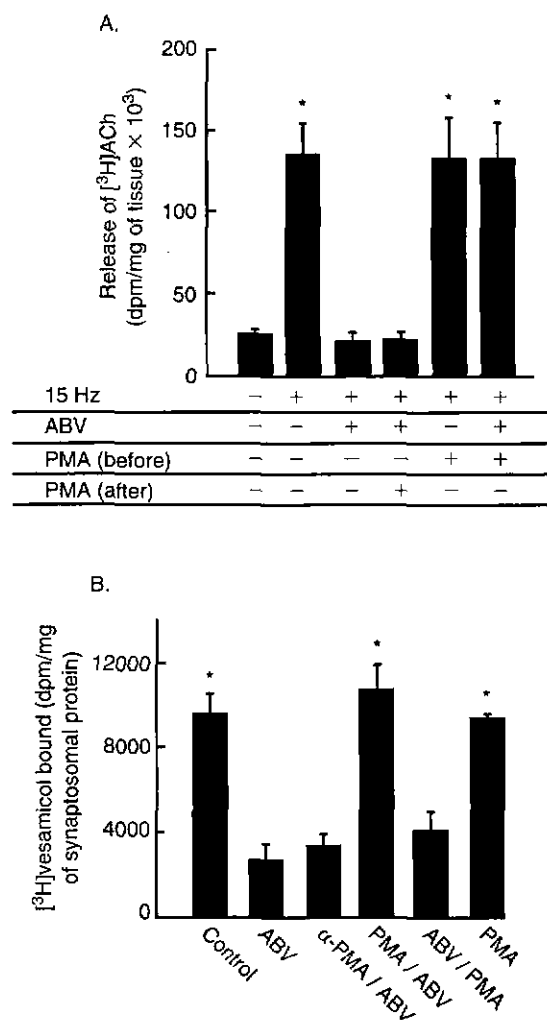


FIG. 1. Effect of PKC activation on ABV action. (A) Hippocampal slices were incubated in the presence or absence of ABV ($1 \mu\text{M}$) for 15 min and then with [^3H]choline for 45 min. Released [^3H]ACh was measured as described [10] with or without electrical stimulation (5 min, 15 Hz) in the conditions described in the panel. PMA (200 nM) was added 15 min before exposure to ABV and was maintained during the period of labelling with [^3H]choline (before) or was added only 15 min prior to electrical stimulation (after). The bars are means \pm s.e.m. for four experiments performed in duplicate. *Statistically different from slices stimulated in the presence of ABV ($p < 0.05$, ANOVA and adjusted t -test with p values corrected by the Bonferroni method for comparison between groups). (B) Binding of ABV in intact synaptosomes assessed by back-titration with [^3H]vesamicol. Synaptosomes were exposed to PMA (200 nM) or α -PMA (200 nM) for 15 min and then incubated with ABV ($1 \mu\text{M}$) for 15 min. In some experiments ABV was not added to synaptosomes (control) and in others PMA was added after exposure to ABV (ABV/PMA). After the incubation, membranes were prepared as described in Materials and Methods and the specific binding for [^3H]vesamicol was determined. Results are mean \pm s.e.m. for six (control, ABV, PMA/ABV) and three (α -PMA, ABV/PMA and PMA) experiments performed in triplicate. *Significantly different from those obtained in the presence of ABV ($1 \mu\text{M}$, $p < 0.05$ ANOVA and adjusted t -test with p values corrected by the Bonferroni method for comparison between groups).

of VACHT [10,14]. Here we tested whether blockade of evoked release (and thus storage) by the essentially irreversible vesamicol analog ABV can also be prevented by activation of PKC. Moreover,

because of the near irreversibility of ABV action on VACHT, we could ask whether the order of addition of PMA and ABV produces different outcomes.

Like vesamicol, ABV blocks the evoked release of newly-synthesized transmitter when it is present during uptake of [^3H]choline (Fig. 1A). To test prior PKC activation, slices were treated sequentially with PMA (200 nM), ABV ($1 \mu\text{M}$) and radiolabeled choline. In this condition, activation of PKC prevents blockade of evoked release by ABV (Fig. 1A). PMA does not affect the evoked release of [^3H]ACh in the absence of ABV, suggesting that the PMA effect is linked to VACHT (Fig. 1A). In contrast, when the slices were treated sequentially with ABV and radiolabeled choline, then activation of PKC with PMA did not prevent blockade of evoked release by ABV (Fig. 1A). The ABV behavior contrasts with that of vesamicol, for which PMA prevents blockade of evoked release no matter the order of addition [10].

The evidence presented so far suggests that activation of PKC prevents the association of vesamicol and its analogs with the transporter. To test this hypothesis, binding of ABV to VACHT was investigated in intact synaptosomes using a back-titration technique. Membranes were prepared from hippocampal synaptosomes subjected to relevant treatments, and they were assayed for the amount of [^3H]vesamicol binding sites. Saturation experiments indicated that [^3H]vesamicol binds with a K_d of $\sim 30 \text{ nM}$ (the results of two independent experiments with triplicate data points were 32 and 32.5 nM), similar to the results from rat brain membrane preparations (20 nM) [20,21]. This information allowed assay at near saturation.

Treatment of synaptosomes with ABV decreased the amount of specific binding greatly ($\sim 80\%$ inhibition, Fig. 1B). Therefore, as expected, ABV apparently remained bound to VACHT during preparation of the membranes and incubation with radiolabeled vesamicol [15,16]. Pretreatment of synaptosomes with PMA, but not with its inactive analog, blocked the decrease in binding of [^3H]vesamicol caused by ABV (Fig. 1B). This suggests that ABV binding itself was blocked, thus making VACHT available for subsequent binding to [^3H]vesamicol. In contrast, when the order of addition of PMA and ABV was reversed, the decrease in binding of [^3H]vesamicol caused by ABV was apparent (Fig. 1B). Prior exposure to PMA alone did not affect [^3H]vesamicol binding (Fig. 1B). This suggests that when PMA is removed during preparation of the membranes and activation of PKC ceases, VACHT may become desphosphorylated, perhaps due to endogenous protein phosphatase activity during the incubation with radiolabeled vesamicol.

Discussion

The present experiments tested whether PKC activation alters the interaction of vesamicol-like drugs with VACHT, by using a vesamicol analog, ABV. PKC activation prevented the interaction of ABV with VACHT, when the tissue was exposed to PMA before treatment with ABV, but not after the tissue was incubated with the vesamicol analog. This was reflected in a lack of inhibition of [3 H]ACh release in conditions in which binding of ABV to the transporter was decreased.

It is noteworthy that previous experiments with vesamicol have shown that PKC activation is effective even after exposure of the tissue to this drug [10]. The explanation for this difference probably resides in the characteristics of vesamicol and ABV binding to VACHT. Bound vesamicol and bound ABV dissociate with half-lives of a few minutes and about a day, respectively [15]. We do not know if only free VACHT can be phosphorylated or whether drug-bound VACHT can also be phosphorylated. In the former case, free VACHT susceptible to phosphorylation would form spontaneously for a brief period every several minutes by dissociation of the vesamicol complex, whereas it would not form significantly from the ABV complex. In the latter case, phosphorylated vesamicol complex presumably dissociates and does not reassociate, whereas phosphorylated ABV complex apparently does not dissociate. In either case, the experiments demonstrate that PKC must be activated before exposure to an irreversible VACHT inhibitor in order to protect VACHT from the drug.

The present experiments show with two complementary sets of data that PKC activation prevents the interaction of vesamicol-like drugs with VACHT. The simplest interpretation of the data is that phosphorylation of VACHT by PKC inhibits the binding of vesamicol analogs, although a causal relationship between VACHT phosphorylation and inhibition of binding has not been demonstrated directly. Other interpretations are possible, but they require more complicated circumstances. Therefore, based on the evidence that activation of PKC indeed causes VACHT phosphorylation [10] (see also discussion in [22]), we favor the simplest explanation.

If it is accepted that activation of PKC inhibits vesamicol binding as a consequence of VACHT phosphorylation, then one major question presents itself. What is the physiological role of VACHT phosphorylation? One possibility is that a protein or other endogenous factor interacts with VACHT at the vesamicol binding site to control its activity. Recent experiments on the pH dependence on both sides of the vesicular membrane suggest that

VACHT exchanges two protons for each ACh molecule taken up [23]. This stoichiometry provides a thermodynamic driving force much larger than required to account for the estimated concentration of vesicular ACh *in vivo* [23]. Hence, regulation of VACHT by a brake mechanism apparently operates, which might resemble a previous reported action of cAMP on monoamine transport [24].

This could allow vesicles to maintain a constant concentration of stored ACh in the presence of a declining concentration of cytoplasmic ACh during heavy nerve activity. Alternatively, such a mechanism might regulate the amount of stored transmitter in response to cellular signaling, as suggested by the pioneer experiments of Van der Kloot [6].

A somewhat similar regulatory mechanism has been proposed for the vesicular monoamine transporter (VMAT) in chromaffin cells. VMAT is homologous to VACHT, and a specific G-protein (G_{o2}) inhibits monoamine transport by VMAT [25]. The interaction of activated G-protein with VMAT seems to occur at the reserpine binding site to decrease transporter activity. Therefore, drugs that block the activity of this family of vesicular transporters might mimic a physiological mechanism of cellular signaling. We speculate that, in analogy with VMAT, ACh storage might be regulated by an endogenous vesamicol-like factor that binds to VACHT. Moreover, such regulation of VACHT might itself be controlled by PKC-mediated phosphorylation. Although the physiological role of VACHT phosphorylation on cholinergic transmission is not yet clear the results presented may be of importance for *in vivo* imaging of cholinergic neurons with vesamicol analogs. It thus should be taken into account that the pattern of phosphorylation of VACHT may alter the binding of such probes to the cholinergic system.

Conclusion

We suggest that activation of PKC, and perhaps phosphorylation of VACHT, can impair the binding of vesamicol-like drugs to the ACh transporter.

References

1. Parsons SM, Prior C, and Marshall IG. *Int Rev Neurobiol* **35**, 279–390 (1993).
2. Liu Y and Edwards RH. *Annu Rev Neurosci* **20**, 125–156 (1997).
3. Eiden LE. *J Neurochem* **70**, 2227–2240 (1998).
4. Collier B, Weiner SA, Ricny J, et al. *J Neurochem* **46**, 822–830 (1986).
5. Van der Kloot W and Branisteanu DD. *Pflugers Arch* **420**, 336–341 (1992).
6. Van der Kloot W. *Prog Neurobiol* **36**, 93–130 (1991).
7. Van der Kloot W and Van der Kloot TE. *Brain Res* **376**, 378–381 (1986).
8. Arenson MS and Gill DS. *Eur J Neurosci* **8**, 437–445 (1996).
9. Song H, Ming G, Fon E, et al. *Neuron* **18**, 815–826 (1997).
10. Barbosa J Jr, Clarizia AD, Gomez MV, et al. *J Neurochem* **69**, 2608–2611 (1997).
11. Enckson JD, Varoqui H, Schafel MK-H, et al. *J Biol Chem* **269**, 21929–21932 (1994).
12. Roghani A, Feldman J, Kohan SA, et al. *Proc Natl Acad Sci USA* **91**, 10620–10624 (1994).
13. Krantz DE, Peter D, Liu Y, et al. *J Biol Chem* **272**, 6752–6759 (1997).

14. Clarizia AD, Romano-Silva MA, Prado VF *et al. Neurosci Lett* **244**, 115–117 (1998).
15. Rogers GA, Kornreich WD, Hand K *et al. Mol Pharmacol* **44**, 633–641 (1993).
16. Leao RM, Gomez NW, Collier B *et al. Brain Res* **703**, 86–92 (1995).
17. Rogers GA, Parsons SM, Anderson DG *et al. J Med Chem* **32**, 1217–1230 (1989).
18. Dunkley PR, Heath JW, Harrison SM *et al. Brain Res* **441**, 59–71 (1988).
19. Prado MAM, Guatimosin C MV *et al. Biochem J* **314**, 145–150 (1996).
20. Marien MR, Parson SM and Altar CA. *Proc Natl Acad Sci USA* **84**, 876–880 (1987).
21. Meyer EM, Bryant SO, Wang RH *et al. Neurochem Res* **18**, 1067–1072 (1993).
22. Tan PK, Wates C, Liu Y *et al. J Biol Chem* **273**, 17351–17360 (1998).
23. Nguyen ML, Cox GD and Parson SM. *Biochemistry* **37**, 13400–13410 (1998).

24. Nakanishi N, Onozawa S, Matsumoto R *et al. J Neurochem* **64**, 600–607 (1995).
25. Ahnert-Hilger G, Numborg B, Exner T *et al. EMBO J* **17**, 406–413 (1998).

ACKNOWLEDGEMENTS: We are grateful for the suggestions of Dr F. G. de Mello and N. Loureiro from Universidade Federal do Rio de Janeiro. We also thank A. A. Guimardes and A. A. Pereira for technical help. This work was supported by grants from PRONEX (Center for Excellence Grant), PRPQ-UFMG, CNPq, FINEP, PADCT, FAPEMIG and the USA National Institutes of Health, NS15047.

Received 24 May 1999;

accepted 7 July 1999

Reprinted from

BRAIN RESEARCH

Brain Research 851 (1999) 39–45

Research report

Muscarinic regulation of Ca^{2+} oscillation frequency in GH_3 cells

Christopher Kushmerick *, Marco Aurélio Romano-Silva, Marcus Vinícius Gomez,
Marco Antônio Máximo Prado

*Departamento de Farmacologia, Instituto de Ciências Biológicas, Universidade Federal de Minas Gerais, Av. Antônio Carlos 6627, Pampulha, 31270-901
Belo Horizonte, MG, Brazil*



ELSEVIER

BRAIN RESEARCH

SCOPE AND PURPOSE

BRAIN RESEARCH provides a medium for the prompt publication of articles in the fields of neuroanatomy, neurochemistry, neurophysiology, neuroendocrinology, neuropharmacology, neurotoxicology, neurocommunications, behavioural sciences, molecular neurology and biocybernetics. Clinical studies that are of fundamental importance and have a direct bearing on the knowledge of the structure and function of the brain, the spinal cord, and the peripheral nerves will also be published.

TYPES OF PAPERS

1. **Interactive Reports** are papers describing original, high quality, fundamental research in any area of Neuroscience. These will first appear electronically on the WWW (<http://www.elsevier.com/locate/bres> or <http://www.elsevier.nl/locate/bres>) and published soon after in the relevant section of *Brain Research*. The on-line version may include additional data sets, 3-D/confocal images, animations, etc., and be linked to relevant on-line databases. Comments from readers may be appended later in a linked *Discussion Forum* at the discretion of an appointed Moderator.
2. **Research Reports** reporting results of original fundamental research in any branch in the brain sciences. It is expected that these papers will be published about three months after acceptance.
3. **Short Communications** reporting on research which has progressed to the stage when it is considered that the results should be made known quickly to other workers in the field. The maximum length allowed will be 1500 words or equivalent space in tables and illustrations. It is expected that Short Communications will be published about two months after acceptance.
4. **Protocols:** full-length protocols in any area of Neuroscience, to be published in the journal section *Brain Research Protocols*. Updates on published protocols submitted by the authors thereof, describing new developments which are of sufficient interest to the neuroscience community, but which do not warrant a completely new submission, will be published as **Protocol Updates**. The maximum length allowed will be 1500 words or equivalent space in tables and illustrations. Comments on published Protocols describing useful hints and "tricks" related to any aspect of the Protocol, such as timing, equipment, chemicals, troubleshooting, etc., will be published in the on-line version of the journal as linked **Technical Tips** at the discretion of the Editor.

SUBMISSION OF MANUSCRIPTS

Submission of a paper to *Brain Research* is understood to imply that it deals with original material not previously published (except in abstract form), and that it is not being considered for publication elsewhere. Manuscripts submitted under multiple authorship are reviewed on the assumption that all listed authors concur with the submission and that a copy of the final manuscript has been approved by all authors and tacitly or explicitly by the responsible authorities in the laboratories where the work was carried out. If accepted, the article shall not be published elsewhere in the same form, in either the same or another language, without the consent of the Editors and Publisher. The Publisher and Editor regret that they are unable to return copies of submitted articles except in the case of rejected articles, where only one set of manuscript plus figures will be returned to the author.

Manuscripts in English should be organised according to the *Brain Research Guidelines for the Submission of Manuscripts* and sent to the appropriate address shown below. Authors should state clearly the section of the journal for which the article/Interactive Report should be considered.

Research Reports & Short Communications:

Professor D.P. Purpura
Brain Research, Office of the Dean
Albert Einstein College of Medicine
Jack and Pearl Resnick Campus
1300 Morris Park Avenue
Bronx, NY 10461, USA
Tel.: (1) (718) 430-2387
Fax: (1) (718) 430-8980
E-mail: brain@aecom.yu.edu

Interactive Reports:

Professor F.E. Bloom
Brain Research Interactive
Dept. of Neuropharmacology
The Scripps Research Institute
10666 N. Torrey Pines Road
La Jolla, CA 92037, USA
Fax: (1) (858) 784-8851
E-mail: smart@scripps.edu
Website: <http://smart.scripps.edu>

Protocols & Protocol Updates:

Dr. Floris G. Wouterlood
Department of Anatomy
Faculty of Medicine
Free University
van der Boechorststraat 7
1081 BT Amsterdam
The Netherlands
Fax: (31) (20) 444-8054
E-mail: fg.wouterlood.anat@med.vu.nl

Correspondence regarding accepted manuscripts relating to proofs, publication and reprints should be sent to:

Brain Research, Elsevier Science B.V., P.O. Box 2759, 1000 CT Amsterdam, The Netherlands. Tel.: (31) (20) 485-3415; Fax: (31) (20) 485-2431; E-mail: a.brakel@elsevier.nl

EDITORIAL BOARD

Editor-in-Chief: Dominick P. Purpura (Bronx, NY, USA)

G.K. Aghajanian (New Haven, CT, USA)
B.W. Agranoff (Ann Arbor, MI, USA)
A.J. Aguayo (Montreal, Que., Canada)
P. Andersen (Oslo, Norway)
E.C. Azmitia (New York, NY, USA)
M.V.L. Bennett (Bronx, NY, USA)
L.I. Benowitz (Boston, MA, USA)
J.M. Besson (Paris, France)
A. Björklund (Lund, Sweden)
F.E. Bloom (La Jolla, CA, USA)
D. Choi (St. Louis, MO, USA)
R.E. Coggeshall (Galveston, TX, USA)
H. Collewijn (Rotterdam, The Netherlands)
W.M. Cowan (Bethesda, MD, USA)
A.C. Cuello (Montreal, Que., Canada)
M.S. Cynader (Vancouver, BC, Canada)
J.E. Dowling (Cambridge, MA, USA)
J.J. Dreifuss (Geneva, Switzerland)
R. Dubner (Baltimore, MD, USA)
S.B. Dunnett (Cambridge, UK)
P.C. Emson (Cambridge, UK)
S.J. Enna (Kansas City, KS, USA)
J. Feldman (Los Angeles, CA, USA)
H.L. Fields (San Francisco, CA, USA)
F.H. Gage (San Diego, CA, USA)
J. Glowinski (Paris, France)
P.S. Goldman-Rakic (New Haven, CT, USA)

S. Grillner (Stockholm, Sweden)
B. Gustafsson (Göteborg, Sweden)
A. Hamberger (Göteborg, Sweden)
U. Heinemann (Köln, Germany)
K.-P. Hoffmann (Bochum, Germany)
T.G.M. Hökfelt (Stockholm, Sweden)
R.L. Isaacson (Binghamton, NY, USA)
M. Ito (Saitama, Japan)
B.L. Jacobs (Princeton, NJ, USA)
E.G. Jones (Irvine, CA, USA)
P. Kalivas (Pullman, WA, USA)
K. Kogure (Saitama, Japan)
G.F. Koob (La Jolla, CA, USA)
L. Kruger (Los Angeles, CA, USA)
J. LaVail (San Francisco, CA, USA)
M. Le Moal (Bordeaux, France)
C.L. Masters (Parkville, Vic., Australia)
M. Mattson (Lexington, KY, USA)
B.S. McEwen (New York, NY, USA)
E.G. McGeer (Vancouver, BC, Canada)
R.Y. Moore (Pittsburgh, PA, USA)
P. Morell (Chapel Hill, NC, USA)
W.T. Norton (New York, NY, USA)
J.M. Palacios (Barcelona, Spain)
M. Palkovits (Budapest, Hungary)
R. Quirion (Verdun, Que., Canada)

C.S. Raine (Bronx, NY, USA)
G. Raisman (London, UK)
P. Rakic (New Haven, CT, USA)
H.J. Ralston III (San Francisco, CA, USA)
S.I. Rapoport (Bethesda, MD, USA)
C.E. Ribak (Irvine, CA, USA)
P. Rudomín (Mexico, DF, Mexico)
M. Schachner (Hamburg, Germany)
B.K. Siesjö (Honolulu, HI, USA)
E.J. Simon (New York, NY, USA)
R.S. Sloviter (Tucson, AZ, USA)
S.H. Snyder (Baltimore, MD, USA)
C. Sotelo (Paris, France)
J. Stone (Sydney, NSW, Australia)
D.F. Swaab (Amsterdam, The Netherlands)
L. Swanson (Los Angeles, CA, USA)
L. Terenius (Stockholm, Sweden)
M. Tohyama (Osaka, Japan)
S. Tucek (Prague, Czech Republic)
K. Unsicker (Heidelberg, Germany)
S.G. Waxman (New Haven, CT, USA)
F.G. Wouterlood (Amsterdam, The Netherlands)
R.J. Wurtman (Cambridge, MA, USA)
I.S. Zagon (Hershey, PA, USA)
W. Zieglgänsberger (Munich, Germany)
R.S. Zukin (Bronx, NY, USA)

GUIDELINES FOR THE SUBMISSION OF MANUSCRIPTS

These can be found on the *Brain Research Interactive* Website (<http://www.elsevier.com/locate/bres> or <http://www.elsevier.nl/locate/bres>) as well as in the "front matter" of every first issue of even-numbered volumes of the journal.

The preferred medium of submission is on disk with accompanying manuscript (see "Electronic manuscripts").

Research report

Muscarinic regulation of Ca^{2+} oscillation frequency in GH_3 cells

Christopher Kushmerick^{*}, Marco Aurélio Romano-Silva, Marcus Vinícius Gomez,
Marco Antônio Máximo Prado

*Departamento de Farmacologia, Instituto de Ciências Biológicas, Universidade Federal de Minas Gerais, Av. Antônio Carlos 6627, Pampulha, 31270-901
Belo Horizonte, MG, Brazil*

Accepted 7 September 1999

Abstract

The GH_3 anterior pituitary cell line has been used as a model to investigate diverse aspects of pituitary cell physiology including Ca^{2+} homeostasis and secretion. These cells possess muscarinic receptors which, by activating K^+ channels and inhibiting Ca^{2+} channels, should decrease electrical excitability. We measured the effect of carbachol (10 μM) on the frequency of Ca^{2+} oscillations caused by Ca^{2+} action potentials in the plasma membrane. Carbachol reduced oscillation frequency by $\approx 85\%$ ($p < 0.001$). This inhibition was reversed by atropine (1 μM), and was prevented by pre-incubation with pertussis toxin (200 ng/ml, 24 h). Since many anterior pituitary cell types secrete acetylcholine, the presence of muscarinic receptors coupled to cell excitability in these cells suggest that ACh could exert a paracrine- or autocrine-like action in GH_3 cell cultures. In experiments designed to test this idea, perfusion with 1 μM atropine caused a small but significant increase ($p < 0.05$) in oscillation frequency when the cells had previously been incubated for 30 min without perfusion. However, this effect was not blocked by either pre-treatment with pertussis toxin or by including atropine during the entire experiment (including the 30-min incubation without perfusion). We conclude that these cells respond to muscarinic agonists by decreasing oscillation frequency but find no evidence for feedback control by endogenous ACh under these conditions. © 1999 Elsevier Science B.V. All rights reserved.

Keywords: GH_3 cell; Muscarinic receptor; Ca^{2+} oscillation; Pertussis toxin; GTP binding protein

1. Introduction

The GH lines of clonal anterior pituitary cells present spontaneous action potentials in the plasma membrane which depend on Ca^{2+} and K^+ channels, but not on TTX-sensitive Na^+ channels [8]. During these action potentials, a depolarizing influx of Ca^{2+} through L-type channels rapidly increases intracellular Ca^{2+} from resting levels of ≈ 150 nM to peak levels approaching 1 μM [13]. These repetitive “ Ca^{2+} oscillations”, i.e., the rise in Ca^{2+} and its subsequent fall due to expulsion and intracellular buffering, can be monitored by following the fluorescence of an intracellular Ca^{2+} -sensitive dye, providing a way to monitor cellular excitability in large numbers of individual cells in real time. Recently, this method has been used in combination with K^+ channel antagonists to dissect the role of different K^+ channels in the control of excitability [4,10].

Acetylcholine (ACh), acting through muscarinic receptors, influences diverse aspects of GH_3 cellular physiology including the synthesis and liberation of hormones and the regulation of intracellular Ca^{2+} concentration. Some of these effects are mediated by decreases in the rate of synthesis and the level of cAMP [2,11,16]. In addition, G proteins activated by muscarinic receptors can act directly on K^+ and Ca^{2+} channels [1], and thus, these receptors should be able to change cellular excitability.

Despite the fact that Ca^{2+} oscillations in GH_3 cells are known to be highly variable from one cell to another, there is little data on the effects of cholinergic agonists on Ca^{2+} homeostasis or cell excitability studied at the level of individual cells. It has been shown that carbachol reduces average cytosolic $[\text{Ca}^{2+}]$ in GH_3 cells and also causes a membrane hyperpolarization [12]. These studies, however, were carried out on suspensions of cells, and thus report only average behavior of large number of cells. Cholinergic stimulation activates the “muscarinic” K^+ channel [1] and inhibits L-type Ca^{2+} channels [9] in these cells. Both of these activities might be expected to reduce electrical

^{*} Corresponding author. Fax: +55-31-499-2695; e-mail: chris@mono.icb.ufmg.br

excitability. However, one study conducted using whole cell current clamp in individual GH₃ cells suggests, to the contrary, that carbachol increases excitability by, among other effects, lowering the threshold for action potentials, perhaps by blocking a K⁺ channel [7]. Thus, the effect of cholinergic agonists on Ca²⁺ oscillation frequency in unstimulated individual cells is unsettled. In the present report, we use Ca²⁺ imaging to characterize the effect of muscarinic stimulation on Ca²⁺ oscillations in this pituitary model system. In addition, we investigated the possibility that endogenously released ACh or other secretions have a role in controlling Ca²⁺ oscillation frequency.

2. Materials and methods

2.1. Materials

All reagents were of analytic or tissue culture grade and were purchased from commercial suppliers. Pertussis toxin (PTX) was from List Biological Laboratories (Campbell, CA). Carbamylcholine chloride (carbachol) was from Sigma. Atropine sulfate (atropine) was from Merck. Cell culture reagents were from Sigma or Gibco.

2.2. Calcium measurements in cultured GH₃ cells

GH₃ cells were grown following standard tissue culture techniques as described previously [10]. Experiments were performed at room temperature (20°C–25°C). Cells grown on poly-lysine coated coverslips were incubated in Ringer (in mM: 140 NaCl, 5.4 KCl, 1.8 CaCl₂, 0.5 MgCl₂, 10 glucose, 5 HEPES, pH 7.4 adjusted with NaOH) containing 10 μM Fluo-3 AM for 1 h. After incubation with dye, the coverslips were washed with Ringer, then transferred to a custom holder in which the coverslip formed the bottom of a 400-μl bath. A gravity-fed perfusion system and a peristaltic pump drain allowed solution exchange with a time constant for solution turnover of ~20 s. When PTX was used, it was included at a concentration of 200 ng/ml in the tissue culture media and was also included in the dye-loading incubations as well as during the incubations without perfusion used for the experimental protocols (see text and figure legends).

Imaging was performed with a Bio-Rad MRC 1024 laser scanning confocal system running the software Time-course 1.0 coupled to a Zeiss microscope (Axiovert 100) with a water immersion objective (40×, 1.2 NA). Excitation was by the 488 nm line of an argon laser (Coherent) and emitted light passed through a 522/32 nm band-pass filter. Laser power was 0.3%–1%, and the detector iris was set to 8 (i.e., maximal open). Images were collected at 1.6 Hz. At the end of the experiment, a rectangular region was drawn within each cell, and average fluorescent intensity for each cell at each time point was recorded.

Statistical analysis of Ca²⁺ oscillation frequency was performed as previously described [10] with minor modification. In all of the experiments, each cell was analyzed individually. First, positions of the oscillations in the experimental record were determined for individual cells using a software peak detector. The detected oscillations for each cell were verified by visual inspection of the traces. Then, the number of oscillations that occurred before treatment (i.e., control) and during treatment were counted. The mean frequency of oscillations for each cell was calculated as the number of oscillations divided by the period of observation. To calculate the probability that the observed changes in oscillation frequency occurred by chance, we constructed cumulative frequency distributions and used the Kolmogorov–Smirnov statistic (D_{K-S}) [10].

To construct mean time courses of oscillation frequency, an array of dimensions $\{m \times n\}$ was formed, where m is the number of cells in the experiments and n is the number of time points. Values of the array were set to 1 if an oscillation peak occurred in the corresponding cell and time point or to 0 otherwise. Each row in the array was then passed through a 60-s running average software filter to obtain the time course for each cell. Finally, all the columns were averaged to form the mean time course for all cells in the experiment.

Each experiment consisted of Ca²⁺ measurements from 35 to 100 individual cells. Each result was reproduced in at least three independent experiments. Ca²⁺ traces from individual cells displayed in Section 3 were selected by numbering each cell sequentially and using a random number generator to choose the desired number of registers. Unless otherwise noted, results are stated as mean \pm 95% confidence limit and error bars are 95% confidence limits.

3. Results

3.1. Effect of cholinergic agonists on Ca²⁺ oscillation frequency

We characterized the effect of 10 μM carbachol on oscillation frequency in individual GH₃ cells (Fig. 1). Cells were loaded with Fluo-3, and intracellular Ca²⁺ was followed by recording images at 1.6 Hz. Each trace in Fig. 1A represents relative changes in intracellular Ca²⁺ recorded from an individual cell (shown are five cells chosen at random from 44 cells in the trial). The cells were perfused continuously and at the times indicated by the bars, 10 μM carbachol was included in the bath solution. Carbachol caused a dramatic reduction in Ca²⁺ oscillation frequency which recovered upon washout of the drug. Fig. 1B represents a 60-s moving average of oscillation frequency for all 44 cells studied in the experiment. In control conditions, the average oscillation frequency was 6–7 per min. Addition of carbachol rapidly reduced the average

frequency to ≈ 1 per min. This reduction in oscillation frequency reversed rapidly upon washout of the drug from the bath, and was reproducible during a second cycle of application and washout.

As is commonly observed in GH₃ cells, the frequency of Ca²⁺ oscillations varied greatly from cell to cell (see Fig. 1A). In order to compare oscillations from the population of cells in control conditions, during treatment with carbachol and after washout of the drug, we measured the oscillation frequency for each cell in each condition, and plotted the data as a cumulative distribution of oscillation frequencies (Fig. 1C). In the cumulative distributions shown in Fig. 1C and below, the value on the ordinate is the fraction of cells with oscillation frequency less than or equal to the corresponding value on the abscissa. Such a plot has the advantage that it shows all the data in the experiment and facilitates the calculation of the Kol-

mogorov–Smirnov statistic. As shown in Fig. 1C, in control conditions, 50% of the cells had an oscillation frequency greater than 6 per min. Treatment with carbachol significantly shifted this curve toward lower frequencies ($p < 0.001$). Upon washout, the distribution returned to control levels. The described effect of carbachol on oscillation frequency was verified in 150 cells in four independent experiments.

3.2. The effect of carbachol is mediated by muscarinic receptors

In order to determine what type of receptor mediated the effect of carbachol, we tested the effect of 1 μ M atropine, a muscarinic antagonist, and PTX (200 ng/ml, 24 h), which inactivates the G-proteins G_i and G_o. As shown in Figs. 2 and 3, both of these treatments completely antagonized the inhibition of oscillation frequency by carbachol.

Fig. 2A shows representative traces of the change in intracellular Ca²⁺ in control conditions, after application of 10 μ M carbachol, and after application of 1 μ M atropine in the continued presence of carbachol. Shown are data from five cells, chosen at random from 36 in the trial. Fig. 2B presents the time course of the average oscillation frequency for all 36 cells during the same conditions. In control conditions, the average oscillation frequency was 4–5 per min. Addition of carbachol reduced this average to ≈ 1 per min. In the continued presence of carbachol, atropine reversed this effect and brought the average back to control levels. Fig. 2C shows the cumulative distribution of oscillation frequency in the population of cells. Carbachol caused a significant ($p < 0.001$) shift in the distribution towards lower oscillation frequencies, and this shift was reversed by atropine in the continued presence of

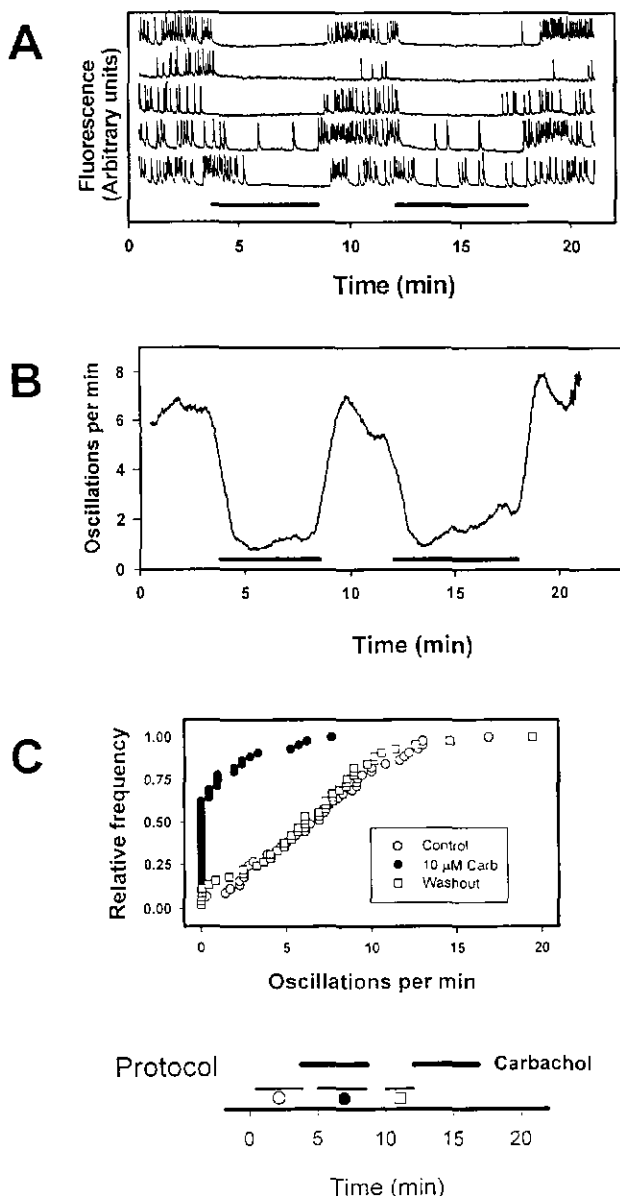


Fig. 1. Effect of 10 μ M carbachol on Ca²⁺ oscillation frequency. GH₃ cells were loaded with Fluo-3 and changes in intracellular Ca²⁺ followed in time by recording fluorescent images at 1.6 Hz. (A) Representative traces showing changes in intracellular Ca²⁺ in individual cells. Each trace represents data from one cell. The cells were perfused continuously and at the times indicated by the bars, 10 μ M carbachol was included in the bath. Shown are data for five cells chosen at random from 44 cells studied in the experiment. (B) Time course of the average oscillation frequency for all 44 cells in the experiments. Positions of all oscillations were determined for each cell, and a 60-s moving average was constructed. As in part A, the bars indicate the times during which 10 μ M carbachol was included in the bath. (C) Cumulative distribution of oscillation frequency. The average oscillation frequency was determined for each cell in control conditions (\circ), during exposure to 10 μ M carbachol (\bullet) and upon washout of the drug (\square). Plotted are the data for all 44 cells studied in one experiment typical of four. Each value on the ordinate is the fraction of cells with oscillation frequency less than or equal to the corresponding value on the abscissa. Protocol diagram: carbachol was included during the times indicated by the thick bars. The thin lines, with symbols underneath, indicate the times used for sampling oscillation frequency to construct the cumulative distributions of oscillation frequencies shown in panel C.

carbachol. After pre-treatment with PTX, Ca^{2+} oscillation frequency was 6.1 ± 0.92 per min (i.e., not different from control) but these cells were unresponsive to carbachol (Fig. 3). The effects of atropine and PTX were each verified in three independent experiments, each comprising 40–60 cells.

We have shown that carbachol, acting through muscarinic receptors, inhibits the frequency of Ca^{2+} oscillations in GH_3 cells. Since some anterior pituitary cells and cell lines are known to secrete ACh [3,6,15], this raises the possibility that released ACh from GH_3 cells in culture may provide a tonic inhibition of Ca^{2+} oscillations. To test this hypothesis, we recorded Ca^{2+} oscillations during control conditions (no drug added) and in the presence of atropine ($1 \mu\text{M}$). If endogenous ACh were providing tonic inhibition of oscillation frequency, application of atropine should antagonize this effect and result in an increase in oscillation frequency. Fig. 4A shows the cumulative distribution of oscillation frequencies before and during treatment with atropine. The results indicate that under these

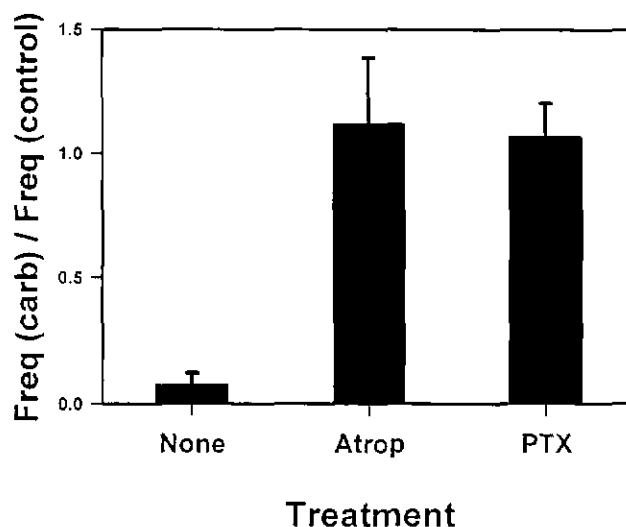


Fig. 3. Evidence that carbachol acts through a muscarinic receptor and a GTP-binding protein. Calcium oscillation frequency was measured in control Ringer and in the presence of $10 \mu\text{M}$ carbachol either with no treatment (None), with $1 \mu\text{M}$ atropine (Atrop), or after pre-treatment (24 h, 200 ng/ml) and in the continued presence of PTX. For each cell, the ratio of oscillation frequency in the presence of carbachol to control was calculated. Shown are the average ratios. Error bars are 95% confidence limits. $N = 30$ –60 cells.

conditions, atropine has no effect on Ca^{2+} oscillation frequency.

In the experiments described thus far, the cells were perfused continuously during the entire protocol. Since ACh might be released in very small amounts, the fast perfusion during the experiment shown in Fig. 4A may result in a very low concentration of the transmitter at the cell surface. Therefore, we modified the experimental protocol to include a 30-min period without perfusion, in an

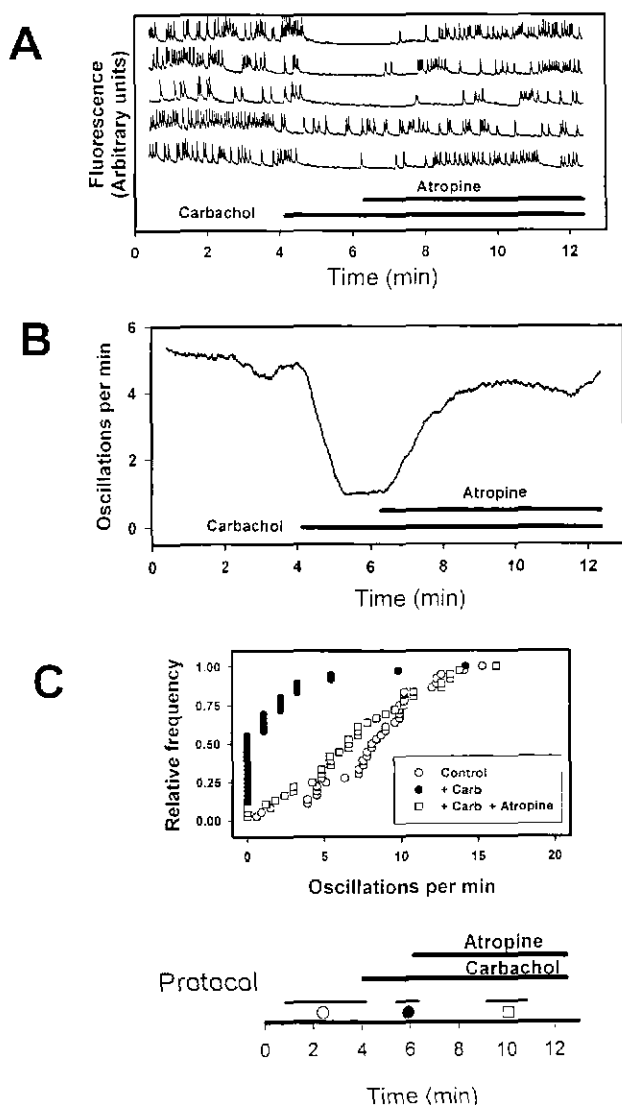


Fig. 2. Atropine reverses the effect of carbachol. GH_3 cells were loaded with Fluo-3 and changes in intracellular Ca^{2+} followed in time by recording fluorescent images at 1.6 Hz. (A) Representative traces showing changes in intracellular Ca^{2+} in individual cells. Each trace represents data from one cell. The cells were perfused continuously, and at the times indicated by the bars, $10 \mu\text{M}$ carbachol or $10 \mu\text{M}$ carbachol + $1 \mu\text{M}$ atropine were included in the bath. Shown are data from five cells chosen at random from 36 cells studied in the experiment. (B) Time course of the average oscillation frequency for all 36 cells in the experiments. Positions of all oscillations were determined for each cell, and a 60-s moving average was constructed. As in part A, the bars indicate the times during which $10 \mu\text{M}$ carbachol or $10 \mu\text{M}$ carbachol + $1 \mu\text{M}$ atropine were included in the bath. (C) Cumulative distribution of oscillation frequency. The average oscillation frequency was determined for each cell in control conditions (\circ), during exposure to $10 \mu\text{M}$ carbachol (\bullet) and during exposure to $10 \mu\text{M}$ carbachol + $1 \mu\text{M}$ atropine (\square). Plotted are the data for all 36 cells studied in one experiment typical of three. Each value on the ordinate is the fraction of cells with oscillation frequency less than or equal to the corresponding value on the abscissa. Protocol diagram: carbachol and atropine were included during the times indicated by the thick bars. The thin lines, with symbols underneath, indicate the times used for sampling oscillation frequency to construct the cumulative distributions of oscillation frequencies shown in panel C.

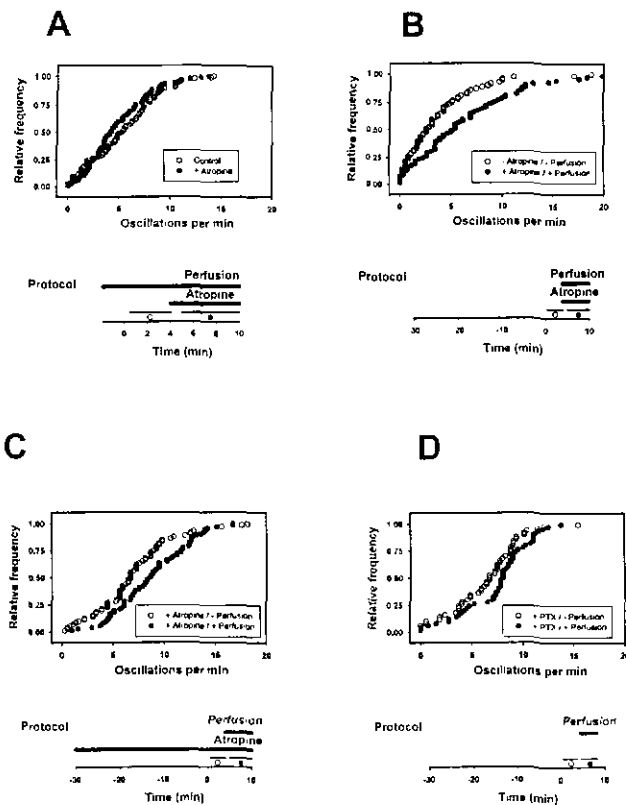


Fig. 4. Effects of atropine and perfusion on oscillation frequency. GH₃ cells were loaded with Fluo-3 and intracellular Ca²⁺ followed in time by recording fluorescent images at 1.6 Hz. The perfusion was off or on, and atropine (1 μ M) was included or not in the bath at the times indicated in the protocol diagrams. (A) Effect of atropine. Perfusion was on during the entire experiment. At the times indicated by the symbols in the protocol diagram, oscillation frequencies were measured in the absence (○) or presence (●) of atropine. (B) Effect of atropine after a 30-min rest period without perfusion. Cells were rested for 30 min without perfusion. At the times indicated by the symbols in the protocol diagram, oscillation frequencies were measured in control Ringer without perfusion (○) or during perfusion with atropine in the perfusate (●). (C) Effect of perfusion alone. Atropine was present during the entire experiment. At the times indicated by the symbols in the protocol diagram, oscillation frequencies were measured in the presence of atropine but without perfusion (○) or during perfusion in the continued presence of atropine (●). (D) Effect of perfusion on cells pre-treated with PTX. Cells were pre-treated with PTX as described in Section 2. At the times indicated by the symbols in the protocol diagram, oscillation frequencies were measured in the presence of PTX without perfusion (○) or during perfusion (●).

attempt to allow any released ACh to accumulate. We then recorded Ca²⁺ oscillations for 200 s without perfusion, turned on the perfusion with 1 μ M atropine and recorded oscillations for another 200 s. Fig. 4B shows the cumulative distribution of 69 cells in the study after the pre-incubation without perfusion, and during perfusion with atropine. In four of six experiments performed with this protocol, perfusion with atropine caused a significant ($p < 0.05$) shift in the distribution toward higher oscillation frequencies.

Since the act of perfusion alone could affect Ca²⁺ oscillations, we repeated the experiment of Fig. 4B with atropine in the bath for the entire period, including the 30-min pre-incubation, to prevent any released ACh from reaching its receptors. Fig. 4C indicates that when muscarinic receptors are blocked with atropine, perfusion alone is capable of significantly shifting the distribution to higher frequencies of oscillations ($p < 0.001$). This effect of perfusion on oscillation frequency was observed in three independent experiments.

Finally, we tried to antagonize the effect of perfusion with PTX (Fig. 4D). In three independent experiments, perfusion caused a significant increase in oscillation frequency ($p < 0.05$) in cells that had been pre-treated with PTX.

4. Discussion

We have characterized the effect of cholinergic stimulation (10 μ M carbachol) on Ca²⁺ oscillation frequency in individual GH₃ cells. Essentially, all cells responded by reducing their oscillation frequency dramatically. The effect was reversible upon washout of carbachol, by application of 1 μ M atropine in the continued presence of carbachol, or by pre-treatment with PTX, demonstrating the requirement for muscarinic receptors acting through a GTP-binding protein.

Our results are consistent with the observation that activation of muscarinic receptors activates G proteins which open K⁺ channels [1] and inhibits Ca²⁺ channels [9]. Either (or both) of these activities would tend to diminish electrical excitability in GH₃ cells; activation of K⁺ channels would make it more difficult for the cells to reach threshold, while inhibiting Ca²⁺ channels would tend to blunt the Ca²⁺ action potentials and the resulting Ca²⁺ oscillations. Recent reports have demonstrated the importance of K⁺ channels in determining Ca²⁺ oscillation frequency and that blocking K⁺ channels can increase the frequency of Ca²⁺ oscillations [4,10]. Our results also explain the observed decrease in average cellular Ca²⁺ observed in suspensions of cells treated with carbachol [12] and are consistent with the observed hyperpolarization of the cell membrane in the same report.

Our results differ from those obtained in a study using whole-cell current clamp to directly measure electrical excitability [7]. These authors found that carbachol actually increases electrical excitability and postulate that inhibition of a K⁺ channel may be involved. The differences between the two sets of results may relate to the fact that the whole-cell configuration causes the dialysis of intracellular components that may be crucial for normal receptor-effector interactions. In addition, normal Ca²⁺ levels are generally lost in the whole-cell configuration, and intracellular Ca²⁺, through its effects on Ca²⁺-sensitive K⁺ currents

and L-type Ca^{2+} channel inactivation, has a major role in regulating membrane electrical properties in these cells. Perforated-patch current clamp experiments may help to resolve these differences.

Hormone secretion in the pituitary is regulated mainly by specific hypothalamic releasing factors, but paracrine control of hormone release has also been demonstrated (for review see Ref. [14]). Although a number of peptides and amines have been found to regulate the synthesis and secretion of pituitary hormones, one intriguing idea is that ACh may function as a paracrine factor controlling the release of prolactin and growth hormone [3,6]. Since some types of anterior pituitary cells synthesize and release ACh upon depolarization [3,6,15], we asked whether endogenous ACh may affect Ca^{2+} oscillation frequency in GH_3 cell cultures.

To address this question, we looked for changes in Ca^{2+} oscillation frequency by addition of atropine (1 μM) to GH_3 cells being perfused with normal Ringer. We were unable to detect any significant effect of atropine alone. We modified the experiment to include a 30-min rest period (to allow any released ACh to accumulate), then measured oscillation frequency in normal Ringer without perfusion (to allow any accumulated ACh to stay in place), then turned on the perfusion with atropine. Under these conditions, we saw a small but significant increase in oscillation frequency during perfusion with atropine compared to in normal Ringer without perfusion. However, this increase can be explained by the effect of perfusion alone, because when we repeated the experiment in the presence of atropine during the entire experiment (including the "rest" period), so that the only variable was the presence or absence of perfusion, we again observed a significant increase in oscillation frequency. Furthermore, cells treated with PTX continued to respond to perfusion by increasing their oscillation frequency.

One explanation for the effect of perfusion is that GH_3 cells may continuously liberate some substance that inhibits oscillation frequency. Our data allow us to conclude that, if this is so, this substance is not acting on muscarinic receptors and probably not on a receptor coupled to G_i or G_o . An alternate explanation is that the mechanical stimulation generated by turning on the perfusion stimulates the cells. Indeed, mechanical effects have been observed when studying these cells with suction microelectrodes [8].

The idea of an endogenously secreted substance affecting electrical excitability has been suggested for chromaffin cells [5]. In these cells, ATP co-secreted with catecholamines acts on purinergic autoreceptors to inhibit Ca^{2+} channels. Similar to the results we have here, this effect was only seen when the cells were maintained without perfusion. However, since purinergic receptors inhibit Ca^{2+} channels through a PTX-sensitive pathway [5], such a mechanism is unlikely to explain the effect of perfusion on Ca^{2+} oscillation frequency that we present here, because PTX did not antagonize the effect of perfusion.

In conclusion, carbachol, acting through muscarinic receptors, reversibly decreased cellular excitability in intact GH_3 cells, measured as the frequency of spontaneous Ca^{2+} oscillations in individual, unstimulated cells. Initiation of perfusion, after a period of incubation without perfusion, appears capable of increasing oscillation frequency. While the mechanism behind this effect is unknown, it appears not to be due to a G_i - or G_o -coupled pathway. It could be that perfusion washes away some as yet unknown secretion, or the effect of perfusion could be due to mechanical stimulation. Finally, we found no evidence for feedback control by endogenous ACh in these cells, which agrees with other reports that although some pituitary cells synthesize and secrete ACh, the GH_3 cell line expresses little or no choline acetyltransferase [3], a key enzyme in ACh synthesis.

Acknowledgements

We are grateful to A.A. Guimarães and A.A. Pereira for technical assistance. Supported by Finep, FAPEMIG, CNPq, PADCT, PRPq-UFMG, and PRONEX.

References

- [1] L. Birnbaumer, J. Abramowitz, A. Yatani, K. Okabe, R. Mattera, R. Graf, J. Sanford, J. Codina, A.M. Brown, Roles of G proteins in coupling of receptors to ionic channels and other effector systems, *Crit. Rev. Biochem. Mol. Biol.* 25 (1990) 225–244.
- [2] B.L. Brown, R.J. Wojcikiewicz, P.R. Dobson, A. Robinson, L.I. Irons, Pertussis toxin blocks the inhibitory effect of muscarinic cholinergic agonists on cyclic AMP accumulation and prolactin secretion in GH_3 anterior-pituitary tumour cells, *Biochem. J.* 223 (1984) 145–149.
- [3] P. Carmeliet, C. Denef, Synthesis and release of acetylcholine by normal and tumoral pituitary corticotrophs, *Endocrinology* 124 (1989) 2218–2227.
- [4] A.C. Charles, E.T. Piro, C.J. Evans, T.G. Hales, L-type Ca^{2+} channels and K^+ channels specifically modulate the frequency and amplitude of spontaneous Ca^{2+} oscillations and have distinct roles in prolactin release in GH_3 cells, *J. Biol. Chem.* 274 (1999) 7508–7515.
- [5] K.P. Currie, A.P. Fox, ATP serves as a negative feedback inhibitor of voltage-gated Ca^{2+} channel currents in cultured bovine adrenal chromaffin cells, *Neuron* 16 (1996) 1027–1036.
- [6] Y. Egozi, Y. Kloog, G. Fleminger, M. Sokolovsky, Acetylcholine in the rat pituitary: a possible humoral factor, *Brain Res.* 475 (1988) 376–379.
- [7] B. Hedlund, J.L. Barker, Carbachol changes spike-generation properties of GH_3 pituitary cells, *Brain Res.* 402 (1987) 311–317.
- [8] Y. Kidokoro, Spontaneous calcium action potentials in a clonal pituitary cell line and their relationship to prolactin secretion, *Nature* 258 (1975) 741–742.
- [9] C. Kleuss, J. Hescheler, C. Ewel, W. Rosenthal, G. Schultz, B. Wittig, Assignment of G-protein subtypes to specific receptors inducing inhibition of calcium currents, *Nature* 353 (1991) 43–48.
- [10] C. Kushmerick, E. Kalapothakis, P.S. Beirao, C.L. Penaforte, V.F. Prado, J.S. Cruz, C.R. Diniz, M.N. Cordeiro, M.V. Gomez, M.A. Romano-Silva, M.A. Prado, Phosphatidylcholine transferase T×3-1

- blocks A-type K^+ currents controlling Ca^{2+} oscillation frequency in GH_3 cells, J. Neurochem. 72 (1999) 1472–1481.
- [11] P. Onali, C. Eva, M.C. Olanas, J.P. Schwartz, E. Costa, In GH_3 pituitary cells, acetylcholine and vasoactive intestinal peptide antagonistically modulate adenylate cyclase, cyclic AMP content, and prolactin secretion, Mol. Pharmacol. 24 (1983) 189–194.
- [12] W. Schlegel, F. Wuarin, C. Zbaren, C.B. Wollheim, G.R. Zahnd, Pertussis toxin selectively abolishes hormone induced lowering of cytosolic calcium in GH_3 cells, FEBS Lett. 189 (1985) 27–32.
- [13] W. Schlegel, B.P. Winiger, P. Mollard, P. Vacher, F. Wuarin, G.R. Zahnd, C.B. Wollheim, B. Dufy, Oscillations of cytosolic Ca^{2+} in pituitary cells due to action potentials, Nature 329 (1987) 719–721.
- [14] H. Vankelcom, C. Denef, Paracrine communication in the anterior pituitary as studied in reaggregate cell cultures, Microsc. Res. Tech. 39 (1997) 150–156.
- [15] F.J. Van Strien, E.W. Roubos, H. Vaudry, B.G. Jenks, Acetylcholine autoexcites the release of proopiomelanocortin-derived peptides from melanotrope cells of *Xenopus laevis* via an M1 muscarinic receptor, Endocrinology 137 (1996) 4298–4307.
- [16] R.J. Wojcikiewicz, P.R. Dobson, B.L. Brown, Muscarinic acetylcholine receptor activation causes inhibition of cyclic AMP accumulation, prolactin and growth hormone secretion in GH_3 rat anterior pituitary tumour cells, Biochim. Biophys. Acta 805 (1984) 25–29.

Elsevier Science

Fax: (31) (20) 485 2431

Phone: (31) (20) 485 3415

Postal Address:

Brain Research

Elsevier Science

P.O. Box 2759, 1000 CT Amsterdam

The Netherlands

Courier Service Address:

Brain Research

Elsevier Science

Sara Burgerhartstraat 25, 1055 KV Amsterdam

The Netherlands

* * *

If you need information about your accepted manuscript, proof, etc. then phone or FAX us at the above numbers, stating the journal name and article code number. We can FAX this journal's Instructions to Authors to you which can also be found on the World Wide Web: access under <http://www.elsevier.com>

ONLINE ACCESS OF BRAIN RESEARCH ARTICLES

on the *Brain Research Interactive* website

As of mid May 1999, online access to the **full text** of articles published in *Brain Research* or any of its sections has been **restricted to those individuals whose library subscribes to the corresponding print journal**. *There is no charge to either the libraries or their authorised users for this service*. Following an initial authorisation check, people logging into this website will be able to access this material simply if their IP domain/host site matches that of a subscribing library

Note: There are NO such subscription-related restrictions for accessing:

- the *Contents lists* of the print issues
- the *Abstracts* of articles published in the print journals
- the **interactive area** of the website, namely:
 - *Brain Research Interactive Reports* and linked Commentaries
 - *Brain Research Interactive Symposia* material: abstracts, papers, discussion fora
 - the general Discussion Forum

While the above information is accessible completely free of charge, users of this site must have registered once and log in in order to access the *Interactive Reports*.

Brain Research Interactive:

www.elsevier.com/locate/bres

www.elsevier.nl/locate/bres

www.elsevier.jp/locate/bres

SUBSCRIPTION AND PUBLICATION DATA 1999

Brain Research (including **Molecular Brain Research**, **Developmental Brain Research**, **Cognitive Brain Research**, **Brain Research Protocols** and **Brain Research Reviews**) will appear weekly and be contained in 61 volumes (129 issues): **Brain Research**, Volumes 815–850 (36 volumes in 72 issues), **Molecular Brain Research**, Volumes 62–73 (12 volumes in 24 issues), **Developmental Brain Research**, Volumes 112–118 (7 volumes in 14 issues), **Cognitive Brain Research**, Volume 7 (1 volume in 4 issues), **Brain Research Protocols**, Volumes 3 and 4 (2 volumes in 6 issues) and **Brain Research Reviews**, Volumes 29–31 (3 volumes in 9 issues). Please note that Volume 62 (Issues no. 1 and 2) and 63 (Issue no. 1) of **Molecular Brain Research**, Volume 7 (Issues no. 1 and 2) of **Cognitive Brain Research** and Volume 3 (Issues no. 1 and 2) of **Brain Research Protocols** were published ahead of schedule in 1998, in order to reduce publication time. The volumes remain part of the 1999 subscription year.

Separate subscriptions: **Molecular Brain Research**, Vols. 62–73, **Developmental Brain Research**, Vols. 112–118, **Cognitive Brain Research**, Vol. 7, **Brain Research Protocols**, Vols. 3 and 4 and **Brain Research Reviews**, Vols. 29–31, may also be ordered separately. Subscription prices are available upon request from the Publisher or from the Regional Sales Office nearest you or from this journal's website (<http://www.elsevier.nl/locate/bres>). Further information is available on this journal and other Elsevier Science products through Elsevier's website (<http://www.elsevier.nl>). Subscriptions are accepted on a prepaid basis only and are entered on a calendar year basis. Issues are sent by standard mail (surface within Europe, air delivery outside Europe). Priority rates are available upon request. Claims for missing issues should be made within six months of the date of dispatch.

Claims for missing issues must be made within six months of our publication (mailing) date, otherwise such claims cannot be honoured free of charge. **Orders, claims, and product enquiries:** please contact the Customer Support Department at the Regional Sales Office nearest you: **New York:** Elsevier Science, P.O. Box 945, New York, NY 10159-0945, USA; phone: (+1) (212) 633 3730, [toll free number for North American customers: 1-888-4ES-INFO (437-4636)]; fax: (+1) (212) 633 3680; e-mail: usinfo-f@elsevier.com. **Amsterdam:** Elsevier Science, P.O. Box 211, 1000 AE Amsterdam. The Netherlands; phone: (+31) 20 4853757; fax: (+31) 20 4853432; e-mail: nlinfo-f@elsevier.nl. **Tokyo:** Elsevier Science, 9-15 Higashi-Azabu 1-chome, Minato-ku, Tokyo 106-0044, Japan; phone: (+81) (3) 5561 5033; fax: (+81) (3) 5561 5047; e-mail: info@elsevier.co.jp. **Singapore:** Elsevier Science, No. 1 Temasek Avenue, #17-01 Millenia Tower, Singapore 039192; phone: (+65) 434 3727; fax: (+65) 337 2230; e-mail: asainfo@elsevier.com.sg. **Rio de Janeiro:** Elsevier Science, Rua Sete de Setembro 111/16 Andar, 20050-002 Centro, Rio de Janeiro - RJ, Brazil; phone: (+55) (21) 509 5340; fax: (+55) (21) 507 1991; e-mail: elsevier@campus.com.br [Note (Latin America): for orders, claims and help desk information, please contact the Regional Sales Office in New York as listed above].

Advertising information. Advertising orders and enquiries can be sent to: **USA, Canada and South America:** Mr Tino de Carlo, The Advertising Department, Elsevier Science Inc., 655 Avenue of the Americas, New York, NY 10010-5107, USA; phone: (+1) (212) 633 3815; fax: (+1) (212) 633 3820; e-mail: t.decarlo@elsevier.com. **Japan:** The Advertising Department, Elsevier Science K.K., 9-15 Higashi-Azabu 1-chome, Minato-ku, Tokyo 106-0044, Japan; phone: (+81) (3) 5561 5033; fax: (+81) (3) 5561 5047. **Europe and ROW:** Rachel Gresle-Farthing, The Advertising Department, Elsevier Science Ltd., The Boulevard, Langford Lane, Kidlington, Oxford OX5 1GB, UK; phone: (+44) (1865) 843565; fax: (+44) (1865) 843976; e-mail: r.gresle-farthing@elsevier.co.uk.

ADONIS Identifier. This Journal is in the ADONIS Service, whereby copies of individual articles can be printed out from CD-ROM on request. An explanatory leaflet can be obtained by writing to ADONIS B.V., P.O. Box 17005, 1001 JA Amsterdam, The Netherlands.

Inhibition of glutamate uptake by a polypeptide toxin (phoneutriatoxin 3-4) from the spider *Phoneutria nigriventer*

Helton J. REIS*, Marco A. M. PRADO*, Evanguedes KALAPOTHAKIS*, Marta N. CORDEIRO†, Carlos R. DINIZ†, Luiz A. DE MARCO*, Marcus V. GOMEZ* and Marco A. ROMANO-SILVA^{†1}

*Divisão de Biologia Celular, Departamento de Farmacologia, ICB, Universidade Federal de Minas Gerais, Av. Antonio Carlos 6627 Pampulha, 31270-901 Belo Horizonte, MG, Brasil, and †Fundação Ezequiel Dias, Rua Conde Pereira Carneiro 80, 30550-010 Belo Horizonte, MG, Brasil

Glutamate concentration increases significantly in the extra-cellular compartment during brain ischaemia and anoxia. This increase has an important Ca^{2+} -independent component, which is due in part to the reversal of glutamate transporters of the plasma membrane of neurons and glia. The toxin phoneutriatoxin 3-4 (Tx3-4) from the spider *Phoneutria nigriventer* has been reported to decrease the evoked glutamate release from synaptosomes by inhibiting Ca^{2+} entry via voltage-dependent Ca^{2+} channels. However, we report here that Tx3-4 is also able to inhibit the uptake of glutamate by synaptosomes in a time-

dependent manner and that this inhibition in turn leads to a decrease in the Ca^{2+} -independent release of glutamate. No other polypeptide toxin so far described has this effect. Our results suggest that Tx3-4 can be a valuable tool in the investigation of function and dysfunction of glutamatergic neurotransmission in diseases such as ischaemia.

Key words: brain ischaemia, calcium, glutamate transport, synaptosomes.

INTRODUCTION

Glutamate, the major excitatory neurotransmitter in the central nervous system, has key roles in brain function and dysfunction. The release and homeostasis of glutamate involve synthesis, packaging into synaptic vesicles, release via exocytosis, and subsequent reuptake of glutamate by specialized transporters in the plasma membrane of neurons and glial cells. There is no evidence for an enzyme that inactivates glutamate at the synaptic cleft; termination of its action therefore relies on reuptake by neurons and glia [1]. Prolonged contact of neurons with glutamate results in neurotoxicity and cell death [2].

Several isoforms of amino acid transporters, named EAAT1 (GLAST), EAAT2 (GLT-1), EAAT3 (EAAC1), EAAT4 and EAAT5, have been identified in the central and peripheral nervous systems of different species [3–8]. Their function relies on the Na^+ gradient across the plasma membrane and on the countertransport of K^+ and OH^- [1]. Therefore changes in the concentration of these ions can alter transport function up to the point of reversing its activity, resulting in net glutamate release [9]. This release is distinguished from exocytotic release by the fact that it is independent of Ca^{2+} influx via selective voltage-dependent channels. In brain cortical synaptosomes depolarized with KCl, approx. 50% of measured glutamate release is Ca^{2+} -independent and is mediated by reversal of the glutamate carrier [10,11]. The transporter can be inhibited by several glutamate analogues such as dihydrokainate and β -D,L-threo-hydroxy-aspartate. A polyamine from spider venom was shown to inhibit glutamate uptake [12] but no further investigation has been reported since.

The venom of the spider *Phoneutria nigriventer* contains several neurotoxic peptides with actions such as inhibition of the inactivation of Na^+ channels [13], blockage of K^+ channels [14]

and blockage of Ca^{2+} channels [15,16]. Among these peptides, the toxin phoneutriatoxin 3-3 has been shown to inhibit the evoked Ca^{2+} -dependent release of glutamate from synaptosomes [17]. Further studies showed that another toxin, phoneutriatoxin 3-4 (Tx3-4), had an inhibitory effect on Ca^{2+} uptake in synaptosomes [18]. Here we report that synaptosomes preincubated with Tx3-4 for 30 min and then depolarized with KCl have a decreased Ca^{2+} -independent release of glutamate, probably owing to inhibition of the activity of glutamate transporters. This opens interesting perspectives in the study of protein–protein interactions to shed more light on the transporter function and to allow the development of new drugs with therapeutic value in ischaemia and anoxia.

EXPERIMENTAL

Materials

Tx3-4 was purified as described by Cordeiro et al. [19], dissolved in water (80 μM) and stored in aliquots at -20°C . L-[^3H]Glutamate was purchased from Amersham International (Little Chalfont, Bucks., U.K.). Glutamate dehydrogenase (EC 1.4.1.3), β -NADP $^+$ (1 mM stock solution in deionized water) and all other chemicals, unless stated otherwise, were purchased from Sigma Chemical Co. (St. Louis, MO, U.S.A.).

Preparation of synaptosomes

Adult Wistar rats were killed by decapitation without the use of anaesthetics. Approval for this procedure was given by the local ethics committee for animal research. The brains were extracted, the hippocampi were dissected and the tissue was kept on ice throughout subsequent processing. Tissue was homogenized

Abbreviations used: GPVs, glial plasmalemmal vesicles; Tx3-4, phoneutriatoxin 3-4.

¹ To whom correspondence should be addressed (e-mail mromano@icb.ufmg.br).

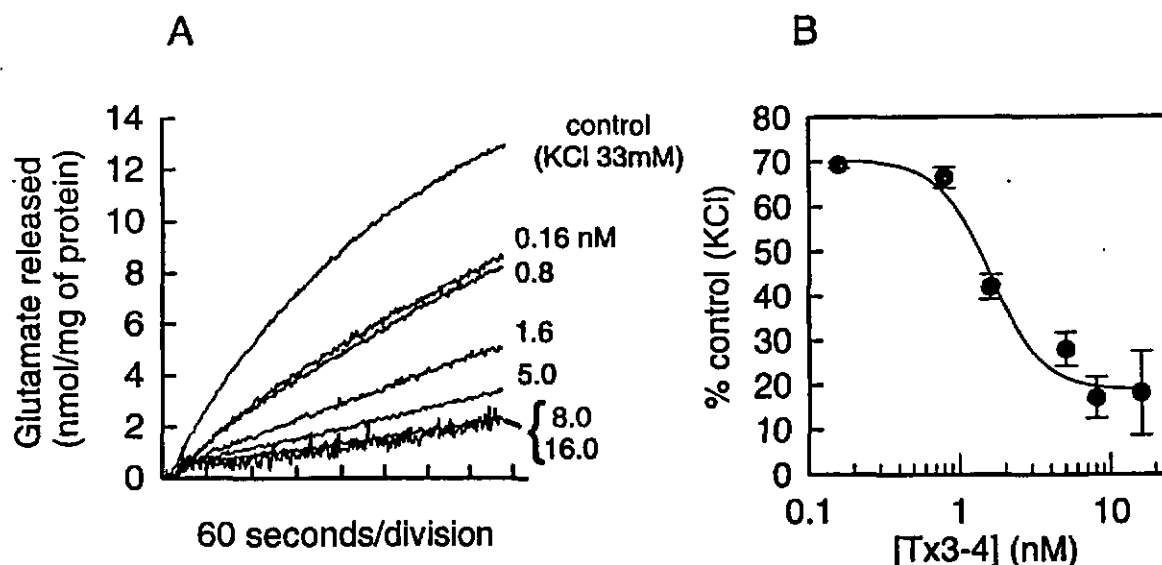


Figure 1 Effect of the toxin Tx3-4 on glutamate release in hippocampal synaptosomes

Synaptosomes prepared as described in the Experimental section were incubated with Tx3-4 at various concentrations indicated for 30 min before depolarization with 33 mM KCl. (A) Time course of glutamate release. After preincubation with Tx3-4 at the concentrations shown (0.16–16 nM) or positive control. (B) Dose–response curve generated from the data in (A) after 6 min of stimulation and expressed as percentages of inhibition of the control. Data are means \pm S.D. for at least three separate experiments.

(0.1 g of tissue/ml) in gradient solution (0.32 M sucrose/1 mM EDTA/0.25 mM dithiothreitol, adjusted to pH 7.4 with 1 M NaOH). Synaptosomes were isolated by Percoll® gradient centrifugation [20] and resuspended in HBSS (124 mM NaCl/4 mM KCl/1.2 mM $MgSO_4$ /10 mM glucose/25 mM Hepes, adjusted to pH 7.4 with 5 M NaOH) at approx. 5.0 mg/ml protein, as described previously [11].

Preparation of glial plasmalemmal vesicles (GPVs)

GPVs were prepared as described in [21]. In brief, the hippocampi of Wistar rats were dissected and the tissue was kept on ice throughout subsequent processing. Tissue was homogenized (0.1 g of tissue/ml) in modified gradient solution (0.32 M sucrose/1 mM EDTA/0.25 mM dithiothreitol/20 mM Hepes, adjusted to pH 7.4 with 1 M NaOH) and centrifuged at 1000 g for 10 min. The supernatant was layered on a discontinuous gradient composed of 20%, 10%, 6% and 2% (v/v) Percoll in gradient solution. The tubes were centrifuged at 33 500 g for 5 min. The layer between 2% and 6% (v/v) Percoll was diluted (to 10 ml) and centrifuged at 1000 g for 20 min; the supernatant was centrifuged at 33 500 g for 40 min. The precipitate was washed twice with gradient solution and used as the GPV-fraction.

Continuous glutamate release assay

Glutamate release was assayed by monitoring the increase in fluorescence due to the production of NADPH in the presence of NADP⁺ and glutamate dehydrogenase [10,11]. In experiments designed to assess the Ca²⁺-independent release of glutamate under different conditions, we omitted CaCl₂ from the assay buffer and added 2.0 mM EGTA.

Glutamate content of synaptosomes

Glutamate content was assayed as described above in samples of the supernatant of centrifuged synaptosomes incubated in the

presence of Tx3-4; the pellet was treated with Triton X-100 [0.05% (v/v) final concentration] before measurement of the glutamate remaining.

Assay for lactate dehydrogenase release

Synaptosomes were incubated for 1 or 30 min with Tx3-4 (8 nM) followed by centrifugation at 10 000 g for 15 s at room temperature. The supernatant was assayed for lactate dehydrogenase as described [22].

Uptake of L-[³H]glutamate

Synaptosomes or GPVs were diluted to a concentration of 0.8 mg/ml protein in HBSS without CaCl₂. Samples (500 μ l) were pipetted into tubes and incubated for 15 min at 35 °C. CaCl₂ (1 mM final concentration) was added to synaptosomes or GPVs and incubated with 0.35 μ Ci of L-[³H]glutamate for 30 s after preincubation with toxins (Tx3-4 or ω -conotoxin MVIIC) or control experiments. To stop the uptake, 5 ml of ice-cold HBSS was added; the synaptosomal or GPV suspension was then vacuum-filtered (2.3 μ m filter pore size). The filters were washed twice with 5 ml of HBSS containing 5 μ M non-radioactive glutamate. The washed filters were then transferred to scintillation vials containing 5 ml of scintillation cocktail [30% (v/v) ethanol/30% (v/v) dioxane/30% (v/v) toluene/1% (v/v) Triton X-100/7% (w/v) naphthalene/0.02% 1,4-bis-(5-phenyloxazol-2-yl)benzene ('POPOP')/0.5% 2,5-diphenyloxazole ('PPO')] and the radioactivity was quantified in a liquid-scintillation spectrophotometer (TR 1600 Tri Carb; Packard). Data in c.p.m. were converted to d.p.m. after correction for sample quenching and background subtraction.

Statistics

The statistical analysis for comparison between means (\pm S.D.) was performed by analysis of variance (Sigma-Stat, Jandel

Corporation). Differences were considered significant at $P < 0.05$.

RESULTS

Concentration compared with effect of Tx3-4 on glutamate release

Figure 1 shows the dose-dependent effect of Tx3-4 on glutamate release evoked by 33 mM KCl. Concentrations of Tx3-4, ranging from 0.16 to 16 nM, progressively decreased the KCl-evoked release of glutamate from hippocampal synaptosomes, achieving a maximal effect (approx. 75% inhibition) at 8.0 nM (Figure 1A). Up to 32 nM Tx3-4 was tested, with results identical with those obtained for 8 and 16 nM, but for clarity these results are not shown. The amount of accumulated glutamate release, as a percentage of the control level, measured after 6 min of incubation with 33 mM KCl, was used to construct the concentration-effect plot (Figure 1B). An IC_{50} of 1.6 nM was calculated from the data shown in Figure 1(B), which corresponds to the inflexion point of the curve.

Time-dependence of the effect of Tx3-4

In the experiments shown in Figure 1, Tx3-4 (8 nM) was added 30 min before stimulation with 33 mM KCl. To characterize the time dependence of the toxin effect, preincubations of 1, 5, 15, 30 and 45 min with Tx3-4 were performed, followed by depolarization with KCl (Figure 2A). The addition of Tx3-4 (8 nM) at 1, 5 or 15 min before KCl caused approx. 50% inhibition of induced glutamate release. However, further inhibition (up to 75%) was observed only at incubations of 30 min or longer with Tx3-4. The KCl-induced release of glutamate from rat cortical synaptosomes has Ca^{2+} -dependent and Ca^{2+} -independent components [10]. The latter can be measured in the presence of the Ca^{2+} chelator EGTA. The Ca^{2+} -independent release evoked by 33 mM KCl is shown in Figure 2(A), as indicated (EGTA), and corresponds to approx. 47% of the total release. This is not different from the KCl-evoked release in the presence of 8 nM Tx3-4 ($P > 0.5$) added up to 15 min before KCl. However, when synaptosomes were preincubated for 30 or 45 min with Tx3-4, the KCl-evoked release was significantly smaller than that in the presence of EGTA alone, suggesting an inhibition of the Ca^{2+} -independent component.

Ca^{2+} -channel blocker ω -conotoxin MVIIC does not inhibit Ca^{2+} -independent glutamate release

Short-term incubation with Tx3-4 seems to block Ca^{2+} channels [18]; for comparative purposes we therefore tested the Ca^{2+} channel blocker ω -conotoxin MVIIC in the same experimental conditions as used for Tx3-4. ω -Conotoxin MVIIC is able to inhibit completely the Ca^{2+} -dependent release of glutamate evoked by KCl in synaptosomes [17,23]. Hippocampal synaptosomes were incubated for 1 or 30 min with ω -conotoxin MVIIC (1 μ M) followed by the addition of 33 mM KCl (Figure 2A). ω -Conotoxin MVIIC was able to inhibit KCl-evoked release after 1 min of incubation. The inhibition was not different from that in nominal Ca^{2+} -free medium (EGTA column; $P > 0.05$), however, no enhancement of the effect was observed when the preincubation period was extended to 30 min (Figure 2A).

Effect of Tx3-4 on glutamate uptake

Many lines of evidence suggest that the Ca^{2+} -independent release of glutamate is due to the reversal of the glutamate carrier of the plasma membrane [10,11,24]. Tx3-4 inhibited Ca^{2+} -independent

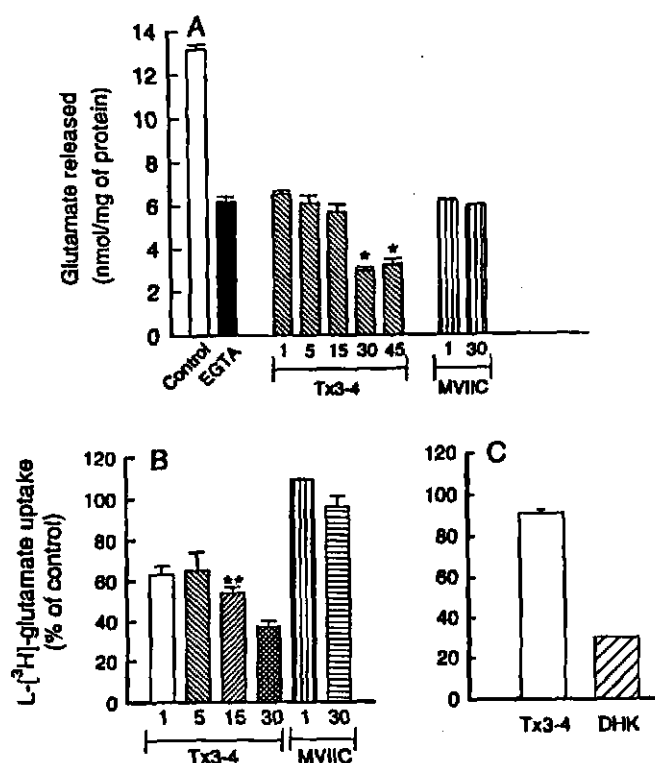


Figure 2 Time-dependence of the effect of Tx3-4 on release and uptake of glutamate

Synaptosomes and GPVs were prepared as described in the Experimental section. (A) The release of glutamate from synaptosomes preincubated with Tx3-4 for different periods (1, 5, 15, 30 or 45 min) before depolarization with KCl (33 mM) was compared with control and against synaptosomes preincubated with ω -conotoxin MVIIC (1 μ M) for 1 or 30 min. Ca^{2+} -independent glutamate release was measured in the presence of 2 mM EGTA, as indicated. *Significant difference ($P < 0.001$) from EGTA. (B) Synaptosomes were left to take up L-[3 H]glutamate for 30 s after being treated with 8 nM Tx3-4 for different periods (1, 5, 15 or 30 min) or with ω -conotoxin MVIIC (MVIIC) for 1 or 30 min. **Significant difference ($P < 0.05$) from Tx3-4 at 30 min. (C) GPVs were allowed to uptake L-[3 H]glutamate for 30 s after being treated with 8 nM Tx3-4 for 30 min. Data are means \pm S.D. for at least three separate experiments. Abbreviation: DHK, dihydrokainate.

glutamate release; we therefore tested whether Tx3-4 could inhibit the activity of the glutamate transporter in hippocampal synaptosomes. Preincubation with Tx3-4 (8 nM) was able to inhibit L-[3 H]glutamate uptake by $36.9 \pm 12.5\%$ at 1 min and $34.9 \pm 15.7\%$ at 5 min of preincubation, and by $45 \pm 7.4\%$ and $63 \pm 9.4\%$ when the incubation was extended to 15 and 30 min respectively (Figure 2B). Under the same conditions, ω -conotoxin MVIIC (1 μ M) did not have any effect on uptake at 1 or 30 min of preincubation (Figure 2B).

GPVs possess a high capacity of glutamate uptake via GLT-1 and GLAST glutamate transporters [21,25]. We therefore investigated the effect of Tx3-4 on glutamate uptake in that preparation. Figure 2(C) shows that Tx3-4 (8 nM) was able to inhibit glutamate uptake in GPVs by only 9.5% after 30 min of preincubation with the toxin. Dihydrokainate was able to decrease uptake by 70% under the same conditions, showing that the uptake was due to glial glutamate transporters [21,26].

Additive effects of Tx3-4 and EGTA on glutamate release

To test whether Tx3-4 was able to affect the component of release that is independent of Ca^{2+} , synaptosomes were preincubated

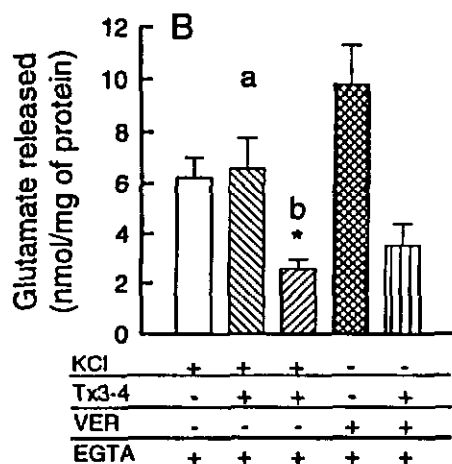
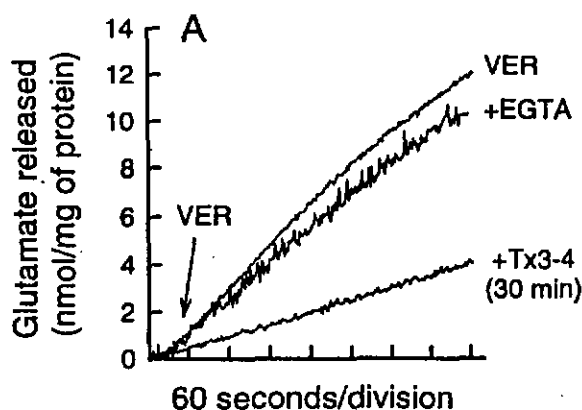


Figure 3 Tx3-4 inhibition of the glutamate release from the Ca^{2+} -independent (cytoplasmic) pool

(A) Veratridine (VER; 10 μM) was incubated with synaptosomes in the presence or absence of EGTA (2 mM) to show that veratridine-evoked release was mainly Ca^{2+} -independent and sensitive to Tx3-4 (8 nM). (B) KCl- or veratridine-evoked glutamate release in the presence of EGTA (Ca^{2+} -independent release) was measured in synaptosomes preincubated with 8 nM Tx3-4 for 1 min (column labelled a) or for 30 minutes (column labelled b). *Significant difference ($P < 0.05$) from KCl + EGTA. Data are means \pm S.D. for at least three separate experiments.

with Tx3-4 (8 nM) for 1 or 30 min, followed by the addition of EGTA (2 mM) and then KCl (33 mM) or veratridine (10 μM).

Veratridine is an alkaloid that binds to toxin site 2 of Na^+ channels and induces the release of glutamate from synaptosomes [27]. However, the release evoked by veratridine is predominantly Ca^{2+} -independent. Veratridine-evoked glutamate release was slightly inhibited (approx. 15%) in nominally Ca^{2+} -free medium. In contrast, it was inhibited by more than 60% when synaptosomes were preincubated with 8 nM Tx3-4 for 30 min (Figure 3A). Tx3-4 (8 nM) inhibited KCl- or veratridine-evoked Ca^{2+} -independent glutamate release by 59% and 64% respectively (Figure 3). As a control, synaptosomes were preincubated with Tx3-4 for 1 min before the addition of EGTA and KCl; the result was not different from that with EGTA plus KCl alone (Figure 3B).

Tx3-4 is not a competitive inhibitor of glutamate uptake

To characterize the inhibition of glutamate transport by Tx3-4, we analysed the transport kinetics in relation to the concentration of glutamate. L-[^3H]Glutamate uptake was measured as described above but in the presence of increasing concentrations of

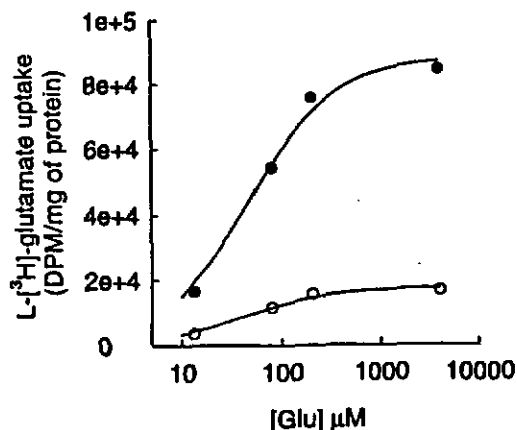


Figure 4 The effect of Tx3-4 on glutamate uptake in the presence of increasing glutamate concentrations

Synaptosomes were left to take up L-[^3H]glutamate for 30 s in the presence (○) or absence (●) of Tx3-4. Tx3-4 (8 nM) markedly decreased the uptake of L-[^3H]glutamate independently of the glutamate concentration in the incubation medium. Data are means for at least three separate experiments.

glutamate, from 14 μM (basal free glutamate) to 4 mM. Glutamate uptake was plotted against increasing glutamate concentrations, in the presence (○) or absence (●) of Tx3-4 (Figure 4). In the presence of Tx3-4, glutamate uptake was markedly inhibited, as represented by the lower curve, independently of the glutamate concentration in the incubation medium. That suggests a non-competitive relationship. The values obtained for K_m were 47.6 μM (control) and 40.0 μM (Tx3-4); those for V_{max} were 1.33×10^7 molecules/s (control) and 3.36×10^6 molecules/s (Tx3-4). Thus the V_{max} was decreased but the K_m was essentially unchanged, suggesting that the inhibition of glutamate uptake by Tx3-4 does not rely on competition.

As a last control, to discard possible damage to the membrane by Tx3-4, which could have resulted in a glutamate leakage, we tested the integrity of synaptosomes by assaying the release of lactate dehydrogenase in the presence of Tx3-4. There was no difference between control and synaptosomes incubated with 8 nM Tx3-4 for 1 or 30 min (results not shown).

DISCUSSION

During brain ischaemia, the Ca^{2+} -independent accumulation of glutamate occurs extracellularly in nerve tissue [28–31]. A better comprehension of the mechanisms involved in this process is important in establishing the therapeutic window and prospective treatment procedures. Specific inhibitors of the glutamate carrier could aid these studies.

Our investigation started with the observation that the inhibitory effect of Tx3-4 on KCl-evoked glutamate release from synaptosomes was enhanced when preincubation with the toxin was prolonged from 1 to 30 min. This finding suggested that when Tx3-4 was preincubated for 30 min with synaptosomes, the Ca^{2+} -independent component of release was inhibited. This observation extends previous reports that Tx3-4 can decrease the KCl-evoked Ca^{2+} -dependent (exocytotic) release after a 1 min preincubation [17] and is reinforced by our finding that after 1 min of preincubation Tx3-4 had no effect on Ca^{2+} -independent glutamate release (Figure 3B).

The Ca^{2+} -independent release of glutamate is thought to occur via the reversal of the glutamate transporter of the plasma membrane [10]. It was shown in astrocytes that the Ca^{2+} -

independent release has a fast and a slow phase, when cells were depolarized with 100 mM KCl [32], the first and transient release being due to transporter reversal, and the second via an as-yet uncharacterized anion channel. Concentrations of KCl lower than 70 mM elicited the transient transporter-mediated release preferentially [32,33]. Because the anion channel involved in this phenomenon has not yet been demonstrated in neurons, and the concentration of KCl used in our experiments was 33 mM, we assume that the Ca^{2+} -independent release observed in our conditions, and clearly inhibited by Tx3-4, was mediated by the glutamate transporter.

Ca^{2+} -channel blockers are used as tools to investigate neurotransmitter release mechanisms. ω -Conotoxin MVIIC inhibits the elevation of intracellular $[\text{Ca}^{2+}]$ and the Ca^{2+} -dependent glutamate release evoked by KCl [15,17,23]. However, there are no reports of an effect of ω -conotoxin MVIIC on the Ca^{2+} -independent release of glutamate. We demonstrated, as expected, that ω -conotoxin MVIIC had no effect on L-[^3H]glutamate uptake measured in hippocampal synaptosomes after 1 or 30 min of incubation. Thus the impairment of glutamate uptake mediated by Tx3-4 could not be related to its action on Ca^{2+} channels.

Veratridine is a potent inducer of neurotransmitter release that also evokes Ca^{2+} -independent glutamate release owing to an increase in intracellular $[\text{Na}^+]$ [34]. Veratridine was therefore used as a positive control to compare with the depolarization evoked by 33 mM KCl. Tx3-4 (8 nM) inhibited veratridine-evoked release by approx. 65%, in comparison with the 15% inhibition in Ca^{2+} -free medium (Figure 3A). Thus, because veratridine depolarizes the membrane via a mechanism distinct from that of KCl, an artifact related to the conditions produced by depolarization with KCl, such as swelling [35], was less probable.

Our analysis of the kinetic of glutamate transport in hippocampal synaptosomes yielded an apparent K_m of 40 μM (Figure 4). This value is somewhat higher than that reported for synaptosomes from other brain regions. In cortex slices the apparent K_m is 3 μM [36], whereas in cerebellar synaptosomes from GLAST-gene-inactivated mice the affinity is 10 μM [37]. The glutamate transporter EAAC1 was reported to be the major subtype found in hippocampal neurons [38]. In cultured cells, this transporter has an apparent K_m of 17 μM for glutamate [39,40]. Again, this is a somewhat higher affinity than we measured, but within the same order of magnitude. The IC_{50} value obtained for the effect of Tx3-4 on KCl-evoked glutamate release was 1.6 nM, whereas the IC_{50} calculated for the inhibition of Ca^{2+} influx in cerebrocortical synaptosomes was 7.9 nM [18]. Despite the fact that the experiments were performed in different preparations, the calculated constants fall within a narrow range, in agreement with our results, in which the effect of toxin on the Ca^{2+} -dependent and Ca^{2+} -independent release occurs within the same concentration range.

Although it was shown that 1 min of preincubation with Tx3-4 was enough to decrease L-[^3H]glutamate uptake by approx. 40%, the effect on Ca^{2+} -independent release was detected only after preincubation for 30 min or more. This delay could be required to decrease the synaptosomal glutamate content to a critical level so as to impair release. In control conditions, after 1 min of preincubation, synaptosomes are loaded with glutamate to the same level as occurs at 30 min (approx. 80 nmol/mg of protein; results not shown). If basal release is considered, the glutamate content must be in a dynamic steady state in which uptake equals spontaneous release. When uptake is blocked, basal release continues, depleting the terminal of its glutamate. The effect of Tx3-4 on Ca^{2+} -independent release was therefore probably linked to a decrease in synaptosomal glutamate content.

In addition, owing to the high activity of glutamate transporters [41,42], an inhibition of uptake greater than 60% might be required to produce a significant impairment in the overall function. That would explain why no inhibition of Ca^{2+} -independent release was observed after 1 min of preincubation with Tx3-4, at a point at which uptake is already inhibited by 40%.

These observations could reflect the heterogeneity and distinct pharmacological sensitivity of glutamate transporters present in synaptosomes [43,44] and cultured cells [45,46]. In fact, the experiments performed with GPVs, which is a preparation rich in GLAST and GLT-1, reinforce this view, because a much smaller effect of Tx3-4 was observed in comparison with synaptosomes; this suggests that the toxin might have some specificity towards one or more neuronal types of glutamate transporter, such as EAAC1. To shed more light on these questions, further investigation of the effect of Tx3-4 on isolated systems is necessary. The toxin has been cloned by our group (L. Grossi, M. A. Romano-Silva, M. A. M. Prado, M. V. Gomez and E. Kalapothakis, unpublished work); future experiments are therefore aimed at expressing Tx3-4 *in vitro* and at producing variants of the peptide to gain a better understanding of its mechanism of interaction and to identify its binding site.

In conclusion, the toxin Tx3-4 could be the starting point for the development of more selective inhibitors of the glutamate transport, which would have immediate application to research and to potential therapeutic use in conditions in which decreasing the activity of glutamate transporters could be beneficial.

We thank Dr. Michael J. Brammer and Dr. Christopher Kushmerick for critical and English reviews, and Ms. A. Pereira, Ms. A. Guimarães and Mr. A. C. Gomes for technical assistance. This work was supported by FAPEMIG, FINEP, PADCT, PRONEX and PRPq-UFMG. M.A.R.-S., M.V.G., E.K., M.A.M.P. and L.A.D.M. are CNPq research fellows. H.J.R. is the recipient of a CAPES Ph.D. fellowship.

REFERENCES

- Robinson, M. B. and Dowd, L. A. (1997) *Adv. Pharmacol.* **37**, 69–115
- Choi, D. W., Maulucci-Gedde, M. and Kriegstein, A. R. (1987) *J. Neurosci.* **7**, 357–368
- Kanai, Y. and Hediger, M. (1992) *Nature (London)* **360**, 467–471
- Pines, G., Danbolt, N. C., Bjoras, M., Zhang, Y., Bendahan, A., Eide, L., Koepsell, H., Storm-Mathisen, J., Seeborg, E. and Kanner, B. I. (1992) *Nature (London)* **360**, 464–467
- Storck, T., Schulte, S., Hofmann, K. and Stoffel, W. (1992) *Proc. Natl. Acad. Sci. U.S.A.* **89**, 10955–10959
- Kanai, Y., Smith, C. P. and Hediger, M. A. (1993) *Trends Neurosci.* **16**, 365–370
- Arriza, J. L., Fairman, W. A., Wadiche, J. I., Murdoch, G. H., Kavanaugh, M. P. and Amara, S. G. (1994) *J. Neurosci.* **14**, 5559–5569
- Arriza, J. L., Eliasof, S., Kavanaugh, M. P. and Amara, S. G. (1997) *Proc. Natl. Acad. Sci. U.S.A.* **94**, 4155–4160
- Attwell, D., Barbour, B. and Szatkowski, M. (1993) *Neuron* **11**, 401–440
- Nicholls, D. G., Sihra, T. S. and Sanchez-Prieto, J. (1987) *J. Neurochem.* **49**, 50–57
- Romano-Silva, M. A., Ribeiro-Santos, R., Ribeiro, A. M., Gomez, M. V., Diniz, C. R., Cordeiro, M. N. and Brammer, M. J. (1993) *Biochem. J.* **296**, 313–319
- Pan-Hou, H., Suda, Y., Sumi, M., Yoshioka, M. and Kawai, N. (1989) *Brain Res.* **478**, 354–357
- Araujo, D. A., Cordeiro, M. N., Diniz, C. R. and Beirao, P. S. (1993) *Naunyn-Schmiedeberg's Arch. Pharmacol.* **347**, 205–208
- Kushmerick, C., Kalapothakis, E., Beirao, P. S. L., Penaforte, C. L., Prado, V. F., Cruz, J. S., Diniz, C. R., Cordeiro, M. N., Gomez, M. V., Romano-Silva, M. A. and Prado, M. A. M. (1999) *J. Neurochem.* **72**, 1472–1481
- Guatimosim, C., Romano-Silva, M. A., Cruz, J. S., Beirao, P. S., Kalapothakis, E., Moraes-Santos, T., Cordeiro, M. N., Diniz, C. R., Gomez, M. V. and Prado, M. A. M. (1997) *Br. J. Pharmacol.* **122**, 591–597
- Cassola, A. C., Jaffe, H., Fales, H. M., Aleche, S. C., Magnoli, F. and Cipolla-Neto, J. (1998) *Pflügers Arch. Eur. J. Physiol.* **436**, 545–552
- Prado, M. A. M., Guatimosim, C., Gomez, M. V., Diniz, C. R., Cordeiro, M. N. and Romano-Silva, M. A. (1996) *Biochem. J.* **314**, 145–150
- Miranda, D. M., Romano-Silva, M. A., Kalapothakis, E., Diniz, C. R., Cordeiro, M. N., Santos, T. M., Prado, M. A. and Gomez, M. V. (1998) *Neuroreport* **9**, 1371–1373

- 19 Cordeiro, M. N., Figueiredo, S. G., Valentim, A. C., Diniz, C. R., von Eickstedt, V. R. D., Gilroy, J. and Richardson, M. (1993) *Toxicon* **31**, 35–42
- 20 Dunkley, P. R., Heath, J. W., Harrison, S. M., Jarvie, P. E., Glenfield, P. J. and Rostas, J. A. P. (1988) *Brain Res.* **441**, 59–71
- 21 Nakamura, Y., Iga, K., Shibata, T., Shudo, M. and Katoaka, K. (1993) *Glia* **9**, 48–56
- 22 Henriques, M. C. and Gomez, M. V. (1975) *Brain Res.* **93**, 182–187
- 23 Turner, T. J. and Dunlap, K. (1995) *Neuropharmacology* **34**, 1469–1478
- 24 Romano-Silva, M. A., Gomez, M. V. and Brammer, M. J. (1994) *Biochem. J.* **304**, 353–357
- 25 Nakamura, Y., Kubo, H. and Katoaka, K. (1994) *Neurochem. Res.* **19**, 1145–1150
- 26 Levy, M., Warr, O. and Altwell, D. (1998) *J. Neurosci.* **18**, 9620–9628
- 27 Sanchez-Prieto, J., Sihra, T. S. and Nicholls, D. G. (1987) *J. Neurochem.* **49**, 58–64
- 28 Benveniste, H., Drejer, J., Schousboe, A. and Diemer, N. H. (1984) *J. Neurochem.* **43**, 1369–1374
- 29 Kauppinen, R. A., McMahon, H. T. and Nicholls, D. G. (1988) *Neuroscience* **27**, 175–182
- 30 Neal, M. J., Cunningham, J. R., Hutson, P. H. and Hogg, J. (1994) *J. Neurochem.* **62**, 1025–1033
- 31 Rego, A. C., Santos, M. S. and Oliveira, C. R. (1996) *J. Neurochem.* **68**, 2506–2516
- 32 Rutledge, E. M. and Kimelberg, H. K. (1996) *J. Neurosci.* **16**, 7803–7811
- 33 Rutledge, E. M., Aschner, M. and Kimelberg, H. K. (1998) *Am. J. Physiol.* **274**, C1511–C1520
- 34 Jacques, Y., Fosset, M. and Lazdunski, M. (1978) *J. Biol. Chem.* **253**, 7383–7391
- 35 Kimelberg, H. K., Rutledge, E., Goderie, S. and Charniga, C. (1995) *J. Cereb. Blood. Flow Metab.* **15**, 409–416
- 36 Dixon, J. F. and Hokin, L. E. (1998) *Proc. Natl. Acad. Sci. U.S.A.* **95**, 8363–8368
- 37 Watanabe, K., Hashimoto, K., Kano, M., Yamada, K., Watanabe, M., Inoue, Y., Okuyama, S., Sakagawa, T., Ogawa, S., Kawashima, N. et al. (1998) *Eur. J. Neurosci.* **10**, 976–988
- 38 Rothstein, J. D., Martin, L., Levey, A. L., Dykes-Hoberg, M., Jin, L., Wu, D., Nash, N. and Kuncl, R. W. (1994) *Neuron* **13**, 713–725
- 39 Ptakidou-Dymock, S. and McGivan, J. D. (1993) *Biochem. J.* **295**, 749–755
- 40 Wang, G. J., Chung, H. J., Schnuer, J., Prall, K., Zable, A. C., Kavanaugh, M. P. and Rosenberg, P. A. (1998) *Mol. Pharmacol.* **53**, 88–96
- 41 Wadiche, J. I., Amara, J. L., Amara, S. G. and Kavanaugh, M. P. (1995) *Neuron* **14**, 1019–1027
- 42 Bergles, D. E., Dzuby, J. A. and Jahr, C. E. (1997) *Proc. Natl. Acad. Sci. U.S.A.* **94**, 14821–14825
- 43 Ferkany, J. and Coyle, J. T. (1986) *J. Neurosci. Res.* **18**, 491–503
- 44 Robinson, M. B., Hunter-Ensor, M. and Sinor, J. D. (1991) *Brain Res.* **544**, 196–202
- 45 Garlin, A. B., Sinor, J. D., Jee, S. H., Grinspan, J. B. and Robinson, M. B. (1995) *J. Neurochem.* **64**, 2572–2580
- 46 Dowd, L. A., Coyle, A. J., Rothstein, J. D., Pritchett, D. B. and Robinson, M. B. (1996) *Mol. Pharmacol.* **49**, 465–473

Received 10 May 1999/21 July 1999; accepted 13 August 1999

TOXICON

Editor-in-Chief: Professor Alan Harvey
Department of Physiology and Pharmacology
University of Strathclyde
27 Taylor Street
Glasgow
G4 0NR, UK

October 21, 1999

Dr E. Kalapothakis
Departamento de Farmacologia ICB
Divisao de Biologia Celular
Universidade Federal de Minas Gerais
Av Antonio Carlos 6627
Belo Horizonte, MG 31270-901
BRAZIL

Tel: 0141-553 4155
Fax: 0141-552 8376
Email: toxicon@strath.ac.uk

Dear Dr Kalapothakis

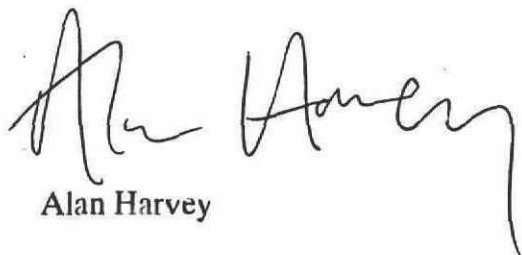
Manuscript number **99 154**

C.L. Penaforte, V.F. Prado, M.A.M. Prado, M.A. Romano-Silva, P.M. Guimaraes, L. De Marco,
M.V. Gomez and E. Kalapothakis

**MOLECULAR CLONING OF cDNAs ENCODING INSECTICIDAL NEUROTOXIC
PEPTIDES FROM THE SPIDER PHONEUTRIA NIGRIVENTER**

I am pleased to tell you that your paper has been accepted for *Toxicon*. I have sent it to the publishers, and you should get proofs in due course.

Yours sincerely



Alan Harvey



PII S0361-9230(00)00259-8

AUTHOR'S
PROOF

Brain Research Bulletin, Vol. 52, No. 4, pp. 000–000, 2000
Copyright © 2000 Elsevier Science Inc.
Printed in the USA. All rights reserved.
0361-9230/00/\$-see front matter

The effect of isoflurane on the release of [³H]-acetylcholine from rat brain cortical slices

R. S. Gomez,^{1*} M. V. Gomez² and M. A. M. Prado²

¹Departamento de Cirurgia, Faculdade de Medicina da UFMG, Belo Horizonte-Minas Gerais, Brasil; and

²Laboratório de Neurofarmacologia, Departamento de Farmacologia, Belo Horizonte-Minas Gerais, Brasil

[Received 22 November 1999; Revised 21 February 2000; Accepted 21 February 2000]

ABSTRACT: Volatile general anaesthetics are believed to affect synaptic transmission, but their actions in the central nervous system (CNS) remains unclear. Acetylcholine (ACh) is one of the most important neurotransmitter in the CNS and thus, it is possible that its release could be one of the targets for volatile anaesthetic action. However, the effects of these agents on the release of ACh are not yet fully understood. Rat brain cortical slices were loaded with [3 H]-choline in order to study the effect of isoflurane on the release of [3 H]-ACh from this preparation. Isoflurane (28, 43, 54, 95 and 182 nM) significantly increased the basal release of [3 H]-ACh. This effect was independent of the extracellular sodium and calcium concentration but was decreased by tetracaine and dantrolene, inhibitors of Ca^{2+} -release from intracellular stores. These findings indicate that isoflurane may cause a Ca^{2+} -release from internal stores that increases [3 H]-ACh release in rat brain cortical slices. © 2000 Elsevier Science Inc.

KEY WORDS: Anaesthetics volatile, Isoflurane, ACh release, Neurotransmitter, Brain cortical slices, Calcium intracellular release, Calcium internal stores, Rat.

INTRODUCTION

An important component of volatile anaesthetic action appears to be an alteration of synaptic transmission in the central nervous-system (CNS) through presynaptic and postsynaptic mechanisms [14,18,29]. Therefore, one possible mechanism for an anaesthetic-induced alteration of transmission is through a change in the concentration of neurotransmitter in the synaptic cleft [14]. Thus, the investigation of the effects of anaesthetics on the release of neurotransmitters may provide information on the mechanisms that contribute to the effects of these agents during anaesthesia.

Acetylcholine (ACh) is one of the most studied neurotransmitters and some *in vivo* observations have suggested that cholinergic transmission may be a target for anaesthetic action [3,32]. However, conflicting results have been obtained in *in vitro* studies. Thus, a significant inhibition of potassium-stimulated release of ACh by halothane from rat brain synaptosomes [16] and cortical slices [13] has been reported. On the other hand, no effect on the release of ACh induced by high concentration of potassium was observed in the presence of halothane, enflurane and methoxyflurane in a rat brain slice preparation [1,2]. In addition, little effort

has been made to evaluate the effects of isoflurane, one of the most widely used volatile anaesthetics, on the ACh release from an *in vitro* preparation.

In a recent investigation we observed that halothane increased the basal release of [^3H]-ACh from rat brain cortical slices and this appeared to be related to release of calcium from intracellular stores [12]. Therefore, the aim of the present work was to investigate the potential effect of isoflurane on the basal release of [^3H]-ACh from rat brain cortical slices.

MATERIALS AND METHODS

Drugs and Solutions

The incubation medium used contained 136 mM NaCl, 2.7 mM KCl, 1.8 mM CaCl_2 , 5.5 mM glucose, 10 mM Tris base, and 20 μM diethyl β -nitrophenyl phosphate (Paraoxon; Sigma Chemical Co., St. Louis, MO, USA) was added to prevent hydrolysis of $[^3\text{H}]\text{-ACh}$. The final pH was adjusted to 7.4. The Ca^{2+} free solution was prepared by removing CaCl_2 and adding 2.0 mM ethyleneglycol-bis-(β -aminoethyl ether) N,N,N',N' -tetraacetic acid (EGTA). Isoflurane was obtained from Rhone Poulenc Chemicals LTD. (England). Tetracaine, tetrodotoxin, cadmium and dantrolene were obtained from Sigma Chemical. The n-heptane chromatography grade was obtained from Merck Darmstadt (Darmstadt, Germany). All other chemicals and reagents were of analytical grade.

[³H]-ACh Release

Adult Wistar rats (200–250 g) of either sex, treated according to a local ethics committee, were decapitated and had their brains removed. Slices of cerebral cortex (0.5 mm) were obtained using a McIlwain Tissue Slicer (Brinkman Instruments Inc., UK). The brain cortical slices were weighted (40 mg) and then placed into the incubating medium.

The release of [^3H]-ACh into the incubating fluid was studied after labelling the tissue ACh with [methyl- ^3H]choline chloride (78 Ci/mmol; Amersham Searle), as previously described [5,10]. Briefly, endogenous ACh stores were first depleted by incubation at 37°C for 15 min in high- K^+ (50 mM) salt medium (3.0 ml) and the slices were separated from the incubating medium by centrif-

* Address for correspondence: R. S. Gomez, Departamento de Cirurgia, Sala 4000-Faculdade de Medicina da UFMG, Avenida Alfredo Balena, 190 CEP: 30130-100, Belo Horizonte-Minas Gerais, Brasil. Fax: 55-31-499-2695; E-mail: gomez@mono.icb.ufmg.br

ugation ($5000 \times g$ for 10 min). To load the brain cortical slices with [^3H]-ACh, they were incubated in salt medium for 30 min (37°C) with $0.11 \mu\text{Ci ml}^{-1}$ of [methyl- ^3H]-choline (free of choline carrier). The slices were then separated from the incubating fluid by centrifugation ($5000 \times g$ for 10 min) followed by two washes with a medium containing $1.0 \mu\text{M}$ choline.

Administration of Isoflurane

Isoflurane was administered as previously described [12]. Briefly, 10 ml of incubating medium was equilibrated with liquid anaesthetic (100, 200, 300, 400, 800 or 1600 μl) at 37°C in Teflon-capped glass vials for 30 min. Subsequently, 500 μl of stock, anaesthetic-saturated solution was added to 1.0 ml of the incubation medium with a glass syringe. The vial was immediately capped, mixed and incubated for 5 min.

Measurement of [^3H]-ACh Release

Aliquots (300 μl) of the samples were counted for radioactivity by liquid scintillation spectrophotometry using a Packard spectrophotometer. On each group of experiments, [^3H]-ACh and [^3H]-choline were separated from the supernatants by the choline kinase method [9,28]. [^3H]-ACh represented about 65% of the total radioactivity released in all set of experiments. Confirming this data, the same magnitude of ^3H efflux induced by isoflurane was also obtained when paraoxan was replaced by $10 \mu\text{M}$ hemicholinium-3 (HC-3), suggesting that accumulation of ACh due to cholinesterase inhibition was not altering the release of transmitter (data not shown).

Measurement of Aqueous Isoflurane Concentrations

The saturation of the stock solution and the aqueous concentration of isoflurane in the incubating medium after a 5-min incubation were confirmed by n-heptane extraction and measurement by gas chromatography using a Hewlett Packard Series II-5890 gas chromatograph [31].

Statistical Analysis

Results are presented as mean \pm SEM. Differences between means were determined by analysis of variance and multiple comparison tests. A value of $p < 0.05$ was considered significant. The IC_{50} value was obtained by using the Sigma Plot software (Jandel Scientific).

RESULTS

In the first set of experiments, the effect of isoflurane on the basal release of [^3H]-ACh from rat brain cortical slices was investigated. Figure 1 shows that isoflurane (28, 43, 54, 95 and 182 nM) increased significantly the basal release of [^3H]-ACh ($p < 0.05$). The release of [^3H]-ACh was linear up to the concentration of 54 nM (Fig. 1) and 5 min of incubation (data not shown). Thus, we used 54 nM isoflurane during 5 min of incubation for the next group of experiments.

In the second set of experiments, we investigated the mechanism(s) by which isoflurane could change the basal release of [^3H]-ACh. Thus, we evaluated whether the release of [^3H]-ACh in brain cortical slices induced by isoflurane is dependent on the presence of extracellular Na^+ or Ca^{2+} and did involve the entry of Ca^{2+} by calcium channels. To test this possibility, the slices were incubated for 15 min in the absence or presence of $0.5 \mu\text{M}$ tetrodotoxin (a sodium channel blocker) [24], 2.0 mM EGTA (no calcium added to the medium) or $100 \mu\text{M}$ Cd^{2+} (nonspecific blocker of calcium channels) [8]. Thereafter, the slices were incu-

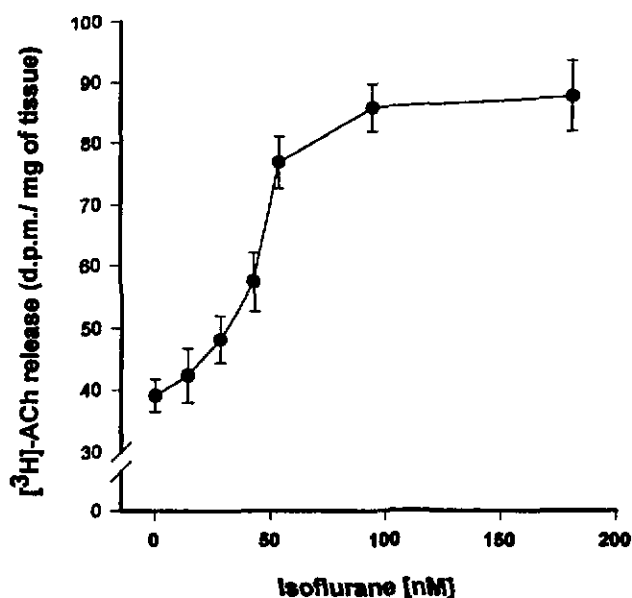


FIG. 1. Effect of isoflurane on the release of [^3H]-acetylcholine (ACh) in rat brain cortical slices. Brain cortical slices (40 mg) loaded with [^3H]-choline were preincubated for 5 min in salt medium in the absence (control) or in the presence of isoflurane at a concentration of 14, 28, 43, 54, 95 or 182 nM, respectively. Values are mean \pm SEM, from five experiments performed in duplicate. For other details, see text.

bated for 5 min in the absence or presence of 54 nM isoflurane. Figure 2 shows that these agents failed to affect the release of [^3H]-ACh evoked by isoflurane.

We also examined whether the isoflurane-induced release of [^3H]-ACh in brain cortical slices was sensitive to drugs that affect

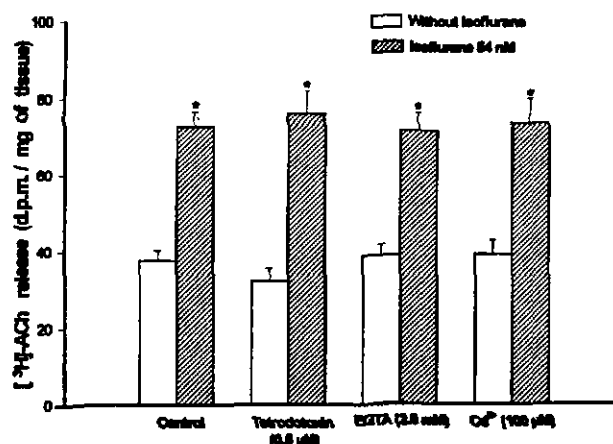


FIG. 2. Effect of tetrodotoxin, EGTA or Cd^{2+} on the release of [^3H]-acetylcholine (ACh) in rat brain cortical slices. Brain cortical slices (40 mg) loaded with [^3H]-choline were preincubated for 15 min in salt medium in the absence or in the presence of tetrodotoxin ($0.5 \mu\text{M}$), EGTA (2.0 mM) or Cd^{2+} ($100 \mu\text{M}$) and then incubated for 5 min in the absence or presence of isoflurane (54 nM). The experiments with EGTA were performed in a calcium free medium. Values are mean \pm SEM, from five experiments performed in duplicate. For other details, see text. * $p < 0.05$ vs. the value without isoflurane.

ISOFLURANE AND RELEASE OF [³H]-ACETYLCHOLINE

3

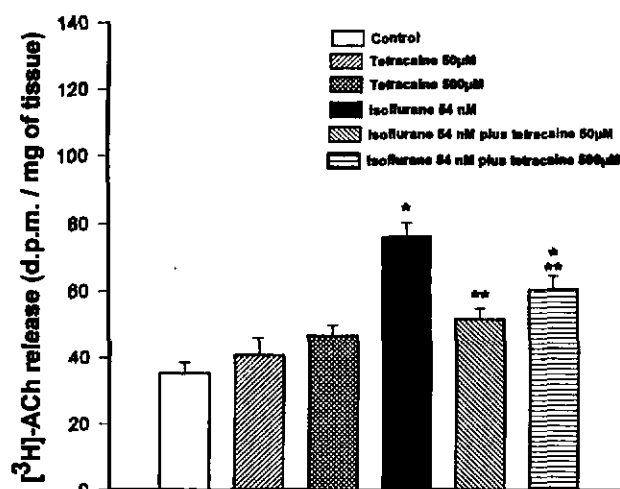


FIG. 3. Effects of tetracaine on the release of [³H]-acetylcholine (ACh) in rat brain cortical slices. Brain cortical slices (40 mg) loaded with [³H]-choline were preincubated for 15 min in salt medium in the absence (control) or in the presence of tetracaine (50 or 500 µM). They were then incubated for 5 min in the absence (control) or presence of isoflurane (54 nM). Values are mean ± SEM, from five experiments performed in duplicate. For other details, see text. **p* < 0.05 vs. control. ***p* < 0.05 vs. isoflurane value.

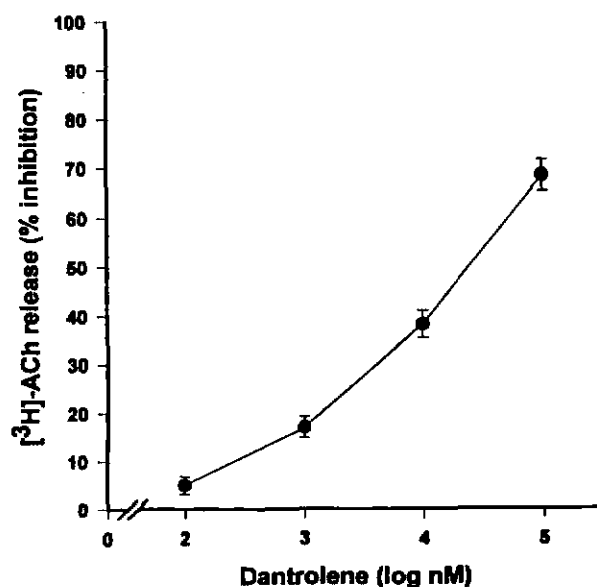


FIG. 4. Effects of dantrolene concentration on the release of [³H]-acetylcholine (ACh) in rat brain cortical slices. Brain cortical slices (40 mg) loaded with [³H]-choline were preincubated for 15 min in salt medium in the absence (control) or in the presence of dantrolene at the indicated concentrations in abscissa. They were then incubated for 5 min in the presence of isoflurane (54 nM). The release of [³H]-ACh induced by isoflurane (54 nM) in the absence of dantrolene (0% inhibition) was 76.3 ± 5.2 dpm/mg of tissue. Values are mean ± SEM, from five experiments performed in duplicate. For other details, see text.

intracellular calcium homeostasis. Thus, brain cortical slices were preincubated for 15 min in the absence or presence of 50 and 500 µM tetracaine, a blocker of calcium release from intracellular stores [15,25,27], or dantrolene (0.1–100 µM), a blocker of Ca²⁺ release from ryanodine-sensitive stores [21,26,34]. Thereafter, the slices were incubated for 5 min in the absence or presence of 54 nM isoflurane. Figure 3 shows that 50 and 500 µM tetracaine decreased by 73.45 ± 3.7% and 66.4 ± 4.5%, respectively, the isoflurane evoked release of [³H]-ACh (stimulated minus basal release) (*p* < 0.05). Dantrolene did not affect the basal release of [³H]-ACh (data not shown) but caused a dose-dependent reduction in volatile anaesthetic evoked ACh release (Fig. 4, *p* < 0.05). The IC₅₀ for dantrolene to inhibit [³H]-ACh evoked release by isoflurane was 6.7 µM (Fig. 4).

DISCUSSION

We have demonstrated that the volatile general anaesthetic isoflurane produced a dose-dependent increase on the basal release of [³H]-ACh from rat cerebral cortex due to an interference with intracellular calcium homeostasis. This observation strengthens the assumption that these agents increase the release of calcium from internal stores.

There have been extensive efforts to characterize the mechanism of action of volatile anaesthetics, but their molecular and cellular actions are still a matter of debate. One possible consequence of volatile anaesthetic action is to alter presynaptic activity and the release of neurotransmitters [14]. ACh is one of the most important neurotransmitters in the CNS, however, few studies of the effects of volatile anaesthetics on the release of this transmitter have been performed. Moreover, there is little agreement between the studies observed in the literature. Thus, there are some studies showing that the volatile anaesthetic halothane decreases the potassium-evoked ACh from rat cortical synaptosomes and rat cortical slices [13,16]. In addition, isoflurane and sevoflurane have been shown to suppress, *in vivo*, ACh release from rat cerebral

cortex [32]. However, halothane, enflurane and methoxyflurane, at concentrations of 1.25%, 3% and 0.2%, respectively, were reported to have no effect on ACh release from a rat brain slice preparation [1,2]. It was recently demonstrated that halothane did not alter the electrical-stimulated release of [³H]-ACh from rat brain cortical slices, but it increases the basal release of [³H]-ACh [12]. In addition, Taguchi and colleagues demonstrated that halothane increases ACh release from the midbrain interpeduncular nucleus of rats during anaesthesia [33].

In the present study we observed that 14 nM isoflurane had no effect on the basal release of [³H]-ACh. However, higher concentrations of isoflurane (28, 43, 54, 95 and 182 nM) significantly increased the basal release of [³H]-ACh. Relating these concentrations to those that might be achieved *in vivo* we observed that they were lower (0.046 MAC, 0.093 MAC, 0.143 MAC, 0.186 MAC, 0.316 MAC and 0.606 MAC) than that used clinically and in the experiments with isoflurane *in vivo* (0.5 MAC, 1.0 MAC and 1.5 MAC) [32]. However, as discussed by Eckenhoof and Johansson, although clinically relevant concentrations of anaesthetic are important to examine the integrated responses in the intact animal, their relevance to *in vitro* studies should be taken with care due to our lack of understanding how to integrate *in vitro* systems into the anaesthesia model [7].

There is a distinct dependence of sodium and calcium ions on the release of ACh induced by different stimuli. In fact, the release of ACh evoked by high concentrations of potassium is decreased in the absence of calcium [30,37]. On the contrary, the electrical-stimulated release of ACh is Na⁺ and Ca²⁺ dependent and is inhibited by tetrodotoxin and the absence of calcium [22,30,37]. We demonstrated that EGTA, Cd²⁺ or tetrodotoxin did not significantly affect the basal or isoflurane-induced ACh release. Thus,

the release of [3 H]-ACh in rat brain cortical slices induced by isoflurane is independent of the presence of extracellular Na^+ or Ca^{2+} and did not involve the entry of Ca^{2+} by calcium channels.

Volatile anaesthetic agents have been shown to increase intracellular Ca^{2+} concentration ($[\text{Ca}^{2+}]_i$) due a release of calcium from internal stores in many cell types [6,20,36]. In addition, this increase in $[\text{Ca}^{2+}]_i$ in neurons may alter signalling pathways that influence neurotransmission. Kindler and colleagues demonstrated that isoflurane increases basal $[\text{Ca}^{2+}]_i$ in rat cortical brain slices in a dose-dependent manner [17]. They also showed that this effect of isoflurane occurred due a release of calcium from intracellular stores since that it was not altered by calcium channel blockers or a calcium-free medium, but was significantly reduced by azumolene, a calcium-release inhibitor from internal stores. In addition, it has been demonstrated that the volatile anaesthetic halothane increases $[\text{Ca}^{2+}]_i$ in SN56 cells (a cholinergic cell line) [4] by increasing the release of Ca^{2+} from an intracellular storage site [11]. Our results showing a significant inhibition of isoflurane induced release of [3 H]-ACh by tetracaine and dantrolene also suggests the involvement of intracellular calcium stores in cholinergic neurons that are able to supply calcium for transmitter release independently of the presence of extracellular calcium or influx of this ion by calcium channels.

Presynaptic nicotinic receptors are believed to play a major role in cholinergic neurotransmission [35]. The activation of nicotinic receptors mediates ACh basal outflow; however, these receptors easily desensitize on exposure to agonists. It was also demonstrated that this desensitization was prevented by lowering the extracellular calcium or chelation of internal Ca^{2+} [19]. Furthermore, it has also been demonstrated that ethanol modulates the neuronal nicotinic ACh receptor [23]. Although this was not the aim of the present study, we can not ruled out a possible action of isoflurane on nicotinic receptor. In fact, we can speculate that the increase of [3 H]-ACh release induced by isoflurane, which was rapidly saturable occurs due to a desensitization of the nicotinic receptor by the release of calcium from internal stores. However, further investigations are necessary to explore this point.

In summary, we have demonstrated that isoflurane alters intracellular calcium homeostasis in cholinergic neurons accounting for the ACh release induced by this volatile anaesthetic from rat brain cortical slices.

ACKNOWLEDGEMENTS

This work was supported by grants of FAPEMIG, FINEP, PADCT-PRONEX and CNPq. We thank Miss A. A. Pereira and Miss A. G. Alves for technical assistance and Dr. L. A. de Marco for reading and suggestions in this manuscript.

REFERENCES

- Bazil, C. W.; Minneman, K. P. Effects of clinically effective concentrations of halothane on adrenergic and cholinergic synapses in rat brain in vitro. *J. Pharmacol. Exp. Ther.* 248:143-148; 1989.
- Bazil, C. W.; Minneman, K. P. Clinical concentrations of volatile anesthetics reduce depolarization-evoked release of [3 H]-norepinephrine, but not [3 H]acetylcholine, from rat cerebral cortex. *J. Neurochem.* 53:962-965; 1989.
- Bertorelli, R.; Hallström, Å.; Hurd, Y. L.; Karlsson, A.; Consolo, S.; Ungerstedt, U. Anaesthesia effects on in vivo acetylcholine transmission: Comparisons of radioenzymatic and HPLC assays. *Eur. J. Pharmacol.* 175:79-83; 1990.
- Blusztajn, J. K.; Venturini, A.; Jackson, D. A.; Lee, H. J.; Wainer, B. H. Acetylcholine synthesis and release is enhanced by dibutyl cyclic AMP in a neuronal cell line derived from mouse septum. *J. Neurosci.* 12:93-99; 1992.
- Casali, T. A. A.; Gomez, R. S.; Moraes-Santos, T.; Romano-Silva, M.; Prado, M. A. M.; Gomez, M. V. Different effects of reducing agents on ω -conotoxin GVIA inhibition of [3 H]-acetylcholine release from cortical slices and guinea-pig myenteric plexus. *Br. J. Pharmacol.* 120: 88-92; 1997.
- Daniell, L. C.; Harris, R. A. Neuronal intracellular calcium concentrations are altered by anesthetics: Relationship to membrane fluidization. *J. Pharmacol. Exp. Ther.* 245:1-7; 1988.
- Eckenhoff, R. G.; Johansson, J. S. On the relevance of "clinically relevant concentrations" of inhaled anesthetics in *in vitro* experiments. *Anesthesiology* 91:856-860; 1999.
- Fox, A. P.; Nowicky, M. C.; Tsien, R. W. Kinetic and pharmacological properties distinguishing three types of calcium currents in chick sensory neurons. *J. Physiol. (Lond.)* 394:149-172; 1987.
- Goldberg, A. M.; McCaman, R. E. The determination of picomole amounts of acetylcholine in mammalian brain. *J. Neurochem.* 20:1-8; 1973.
- Gomez, R. S.; Gomez, M. V.; Prado, M. A. M. Inhibition of Na^+ , K^+ -ATPase by ouabain opens calcium channels coupled to acetylcholine release in guinea pig myenteric plexus. *J. Neurochem.* 66:1440-1447; 1996.
- Gomez, R. S.; Guatimosim, C.; Massensini, A.; Gomez, M. V.; Prado, M. A. M. The effect of halothane on cytosolic free calcium concentration of SN56 cells. *Br. J. Anaesth.* 82:91-92; 1999.
- Gomez, R. S.; Prado, M. A. M.; Carazza, F.; Gomez, M. V. Halothane enhances exocytosis of [3 H]-acetylcholine without increasing calcium influx in rat brain cortical slices. *Br. J. Pharmacol.* 127:679-684; 1999.
- Griffiths, R.; Greiff, J. M. C.; Haycock, J.; Elton, C. D.; Rowbotham, D. J.; Norman, R. I. Inhibition by halothane of potassium-stimulated acetylcholine release from rat cortical slices. *Br. J. Pharmacol.* 116: 2310-2314; 1995.
- Griffiths, R.; Norman, R. I. Effects of anaesthetics on uptake, synthesis and release of transmitters. *Br. J. Anaesth.* 71:96-107; 1993.
- Györke, S.; Lukyanenko, V.; Györke, I. Dual effects of tetracaine on spontaneous calcium release in rat ventricular myocytes. *J. Physiol. (Lond.)* 500:297-309; 1997.
- Johnson, G. V. W.; Hartzell, C. R. Choline uptake, acetylcholine synthesis and release, and halothane effects in synaptosomes. *Anesth. Analg.* 64: 395-399; 1985.
- Kindler, C. H.; Eilers, H.; Donohoe, P.; Ozer, S.; Bickler, P. E. Volatile anesthetics increase intracellular calcium in cerebrocortical and hippocampal neurons. *Anesthesiology* 90:1137-1145; 1999.
- Larrabee, M. G.; Posternak, J. M. Selective action of anesthetic on synapses and axons in mammalian sympathetic ganglia. *J. Neurophysiol.* 15:92-114; 1952.
- Marchi, M.; Lupinacci, M.; Bernero, E.; Bergaglia, F.; Raiteri, M. Nicotinic receptors modulating ACh release in rat cortical synaptosomes: Role of Ca^{2+} ions in their function and desensitization. *Neurochem. Int.* 34:319-328; 1999.
- Mody, I.; Tanelian, D. L.; MacIver, M. B. Halothane enhances tonic neuronal inhibition by elevating intracellular calcium. *Brain Res.* 538: 319-323; 1991.
- Morgan, K. C.; Bryant, S. H. The mechanism of action of dantrolene sodium. *J. Pharmacol. Exp. Ther.* 201:138-147; 1977.
- Nakashima, Y.; Sugiyama, S.; Shindoh, J.; Taki, F.; Takagi, K.; Satake, T.; Ozawa, T. Effects of sodium channel blockers on electrical field stimulation-induced guinea-pig tracheal smooth muscle contraction. *Arch. Int. Pharmacodyn. Ther.* 306:130-138; 1990.
- Narahashi, T.; Aistrup, G. L.; Marszalec, W.; Nagata, K. Neuronal nicotinic acetylcholine receptors: A new target site of ethanol. *Neurochem. Int.* 35:131-141; 1999.
- Narahashi, T.; Moore, J.; Scott, W. R. Tetrodotoxin blockage of sodium conductance increase in lobster giant axon. *J. Gen. Physiol.* 147:965-974; 1964.
- Ohnishi, S. T. Calcium-induced calcium release from fragmented sarcoplasmic reticulum. *J. Biochem.* 86:1147-1150; 1979.
- Ohta, T.; Ito, S.; Ohga, A. Inhibitory action of dantrolene on Ca^{2+} release from sarcoplasmic reticulum in guinea pig skeletal muscle. *Eur. J. Pharmacol.* 178:11-19; 1990.
- Pike, G. K.; Abramson, J. J.; Salama, G. Effects of tetracaine and procaine on skinned muscle fibres depend on free calcium. *J. Musc. Res. Cell. Motil.* 10:337-349; 1989.

ISOFLURANE AND RELEASE OF [³H]-ACETYLCHOLINE

5

28. Prado, M. A. M.; Gomez, M. V.; Collier, B. Mobilization of a vesamicol-insensitive pool of acetylcholine from a sympathetic ganglion by ouabain. *J. Neurochem.* 61:45–56; 1993.
29. Richards, C. D. Actions of general anaesthetics on synaptic transmission in the CNS. *Br. J. Anaesth.* 55:201–207; 1983.
30. Richardson, C. M.; Dowdall, M. J.; Bowman, D. Inhibition of acetylcholine release from presynaptic terminals of skate electric organ by calcium channel antagonists: A detailed pharmacology study. *Neuropharmacology* 25:537–546; 1996.
31. Rutledge, C. O.; Seifen, E.; Alper, M. H.; Flacke, W. Analysis of halothane in gas and blood by gas chromatography. *Anesthesiology* 24:862–867; 1963.
32. Shichino, T.; Murakawa, M.; Adachi, T.; Arai, T.; Miyazaki, Y.; Moris, K. Effects of inhalation anaesthetics on the release of acetylcholine in the rat cerebral cortex *in vivo*. *Br. J. Anaesth.* 80:365–370; 1998.
33. Taguchi, K.; Andresen, M. J.; Hentall, I. D. Acetylcholine release from the midbrain interpeduncular nucleus during anesthesia. *Neuroreport* 2:789–792; 1991.
34. Van Winkle, W. B. Calcium release from skeletal muscle sarcoplasmic reticulum: Site of action of dantrolene sodium? *Science* 193:1130–1131; 1976.
35. Vizi, E. S.; Sershen, H.; Balla, A.; Mike, A.; Windisch, K.; Juranyi, Z.; Lajtha, A. Neurochemical evidence of heterogeneity of presynaptic and somatodendritic nicotinic acetylcholine receptors. *Ann. NY Acad. Sci.* 757:84–99; 1995.
36. Wheeler, D. M.; Rice, R. T.; Hansford, R. G.; Lakatta, E. G. The effect of halothane on the free intracellular calcium concentration of isolated rat heart cells. *Anesthesiology* 69:578–583; 1988.
37. Yokoyama, K.; Yagasaki, O. Effects of Ca²⁺ blockers on the various types of stimuli-induced acetylcholine release from guinea-pig ileum myenteric plexus. *Jpn. J. Pharmacol.* 52:109–114; 1990.

AQ—1 msp. 5. Au: please provide location of supplier/manufacturer.

Subject: Paper do Jones

Date: Fri, 28 Apr 2000 08:52:34 -0300

From: "Marco Romano-Silva" <mromano@icb.ufmg.br>

Organization: UFMG

To: "Evanguedes Kalapothakis" <ekalapo@icb.ufmg.br>,

"Marco Prado" <mprado@icb.ufmg.br>,

"Marcus Vinicius Gomez" <gomez@icb.ufmg.br>

Inhibition of glutamate uptake by Tx3-4 is dependent on

the redox state of cysteine residues Helton J. Reis*, Marcus V. Gomez*, Evanguedes Kalapothakis*,

Carlos R. Diniz[‡], Marta N. Cordeiro[‡], Marco A.M. Prado* and Marco A. Romano-Silva*
<?import namespace = o urn = "urn:schemas-microsoft-com:office:office" declareNamespace />

Scheduled p/ Neuroreport, volume 11 issue 10 (14 July 2000).

Casali, R.S. Gomez, T. Moraes-Santos, M.A. Romano-Silva, **M.A.M. Prado**, M.V. Gomez. **British Journal of Pharmacology 120: 88-92 (1997).**

Tityustoxin-Induced Release of ATP from Rat Brain Cortical Synaptosomes. A.H. Salgado, **M.A.M. Prado**, T. Moraes-Santos, M.A. Romano-Silva, M.V. Gomez. **Neuroscience Letters 229: 113-116 (1997).**

Sinalização Celular. C.R.S. Machado, E. Kalapothakis, L.F.L. Reis, P.S.L. Beirão, **M.A.M. Prado**. **Anais da 49 reunião anual da SBPC, Vol 49: 100-102 (1997)**

A Toxin from the Spider *Phoneutria nigriventer* that Blocks Calcium Channels Coupled to Exocytosis. C. Guatimosim, M.A. Romano-Silva, J.S. Cruz, P.S.L. Beirão, E. Kalapothakis, M.N. Cordeiro, C.R. Diniz, M.V. Gomez, **M.A.M. Prado**. **British Journal of Pharmacology 122: 591-597 (1997).**

Effect of Protein Kinase C Activation on the Release of [³H] Acetylcholine in the Presence of Vesamicol. J. Barbosa-Júnior, A.D. Clarizia; M.V. Gomez; M.A. Romano-Silva, V.F. Prado, **M.A.M. Prado**. **Journal of Neurochemistry 69: 2608-2611 (1997).**

Recycling of Synaptic Vesicles at the Frog Neuromuscular Junction in the Presence of Strontium. C. Guatimosim, M.A. Romano-Silva, M.V. Gomez, **M.A.M. Prado**. **Journal of Neurochemistry 70: 2477-2483 (1998).**

Role of Protein Kinase C on the Release of [³H]Acetylcholine from Myenteric Plexus Treated with Vesamicol. A.D. Clarizia, M.A. Romano-Silva, V.F. Prado, M.V. Gomez, **M.A.M. Prado**. **Neuroscience Letters 244: 115-117 (1998)**

Investigation of the Effect of PhTx2 from the Venom of the Spider *Phoneutria nigriventer*, on the Release of [³H]acetylcholine from Rat Cerebrocortical Synaptosomes J.R. Moura, **M.A.M. Prado**, M.V. Gomez, E. Kalapothakis, C.R. Diniz, M.N. Cordeiro, M.A. Romano-Silva. **Toxicon 36: 1189-1192 (1998)**

Relatório Técnico final relativo ao projeto CBS 931/97

Coordenador Marco Antonio Maximo Prado

Esse projeto estuda a modulação da transmissão sináptica por canais iônicos, armazenagem do neurotransmissor, e o tráfego de proteínas e membranas em células nervosas.

Como ponto positivo em relação ao projeto considero a compra do material permanente, principalmente câmera CCD e software para aquisição e análise de imagens. Esse material já se encontra em uso constante no laboratório de Neurofarmacologia.

O uso desse equipamento permitiu a obtenção de imagens ao mesmo tempo em que células foram estudadas com a técnica de whole-cell patch-clamp. Essa técnica foi portanto fundamental para a realização de vários experimentos pois permite obter dados eletrofisiológicos ao mesmo tempo que obtemos imagens.

Como principal ponto negativo do mesmo considero o corte pela FAPEMIG de recursos na ordem de R\$ 2.300,00 (Em projeto de US\$ 54.000,00) para a compra de material de consumo nacional, dinheiro que seria utilizado em grande parte para a compra de ^{32}P . Esse corte inviabilizou todos os experimentos de fosforilação do transportador vesicular de acetilcolina, pois não tivemos outros recursos aprovados para a compra deste material em tempo hábil. Sendo essa área de pesquisa extremamente competitiva, e levando-se em conta que nós fomos os primeiros a demonstrar que o transportador é fosforilado (Barbosa Jr. et al., 1997), foi com grande pesar que tivemos de parar com esses experimentos. É grave o fato pois vários dos experimentos programados foram feitos pelo grupo do Prof. R. Edwards e portanto atualmente não temos mais condição de competir com o mesmo para publicação sobre fosforilação do transportador vesicular de acetilcolina. Portanto, recentemente dois trabalhos foram publicados estudando a fosforilação do transportador vesicular de acetilcolina, no Journal of Cell Biology, e Journal of Biological Chemistry, por Krantz et al., 2000; e Cho et al., 2000 confirmando as observações originais feitas pelo meu grupo (Barbosa Jr. et al., 1997) e complementado vários aspectos que tínhamos a intenção de ter estudado.

Portanto, considero-me descompromissado em relação aos aspectos de fosforilação do transportador vesicular de acetilcolina contidos originalmente no projeto aprovado pela FAPEMIG.

Vale salientar que embora o número de publicações não tenha tido um aumento expressivo, o índice de impacto dos periódicos que publicamos nossos trabalhos em 1999-2000 tem sido na sua maioria entre 3 e 4. Portanto, a qualidade das publicações foi acentuadamente aumentada graças ao auxílio FAPEMIG.

Produção científica 1997-2000

Different Effects of Reducing Agents on w-conotoxin GVIA Inhibition of $[\text{Ca}^{2+}]_i$ -Acetylcholine Release from Rat Cortical Slices and Guinea-Pig Myenteric Plexus. T.A.A.

